Gas chromatography-mass spectrometry analyses of fatty acid methyl esters from marine algae

Rawan Khalil Alfahmawi

Master thesis in Chemistry

Department of chemistry

University of Bergen

2019

Page intentionally left blank

Acknowledgments

This study was completed in the Department of chemistry, University of Bergen.

I would first like to thank my thesis supervisor, Associate Professor Svein Are Mjøs for providing me with this project and for his patience, advices and always helping me when I have any question.

I would also like to thank Pia Stenrücken at Department of Biological Sciences for providing the algae samples and associated data, and senior executive officer Unni Lange Buanes for her help in matters related to registration.

I am deeply grateful to my husband Dr. Ammar Mahamid for his helps, supports and always being beside me. I owe a great debt of gratitude to my parents who have been and still to be the main motivation for my success. In addition, I would like to thank my friend Andrea E. Carpinteyro Diaz.

Finally, I want to thank every person who help me in my project.

Rawan Khalil Alfahmawi

Abstract:

In this study it was attempted to identify the fatty acids that are common in marine algae and investigate how these behave on different chromatographic columns when derivatized to fatty acid methyl esters (FAME).

The capillary columns BPX70 and DB20 are commonly applied for FAME analyses. In the first part of the work, GC-MS was used to study the retention patterns of FAME on ten different commercial GC columns (BPX70, BP20, DB225, DB5, DB23, SLB-IL61, SLB-IL82, SLB-IL100, RTX50, RTX200, RXI1). It was decided to continue with DB5 and DB225 in addition to BPX70 and DB20 for analyses of the algae.

These four columns were applied in the analysis of 38 samples from 19 algal strains. Two samples (both exponential and stationary growth phase) from each strain were selected. The strains were from two different kingdoms and four phyla. *Chlorophyta* phylum from the *Plantae* kingdom and *Haptophyte*, *Ochrophyta* and *Bacillariophyta* phyla from the *Chromista* kingdom.

The GC-MS data were analyzed in Chrombox Q 16-05 (www.chrombox.org) using both mass spectra and retention indices for compound identification. Two-dimensional scatter plots of equivalent chain lengths (ECL) were applied to get information about the analyte properties by combining information from more than two columns.

In total 114 compounds were found to have an area percent above 0.2% in at least one sample. It was necessary to do further work with the identification of 58 compounds, either because they had tentative identification or because they were unknowns. All the tentative identifications seemed correct. Of the unknowns, 21 are expected not to be FAME. More information could be gained on the structure of several of the remaining unknowns that were regarded as FAME.

However, there are still compounds that are not identified. The largest peak that remains unknown constituted 1.5% of the chromatographic area in one of the samples, but this compound is not expected to be a FAME. The largest unknown peak expected to be FAME constituted 0.9%. There are also several monoenes with unknown double bond position. The largest of these constituted 1.4 % of the area in one of the samples.

Table of Contents

List of abbreviations

AA	Arachidonic acid
CNP	Cyanopropyl
DHA	Docosahexaenoic acid
DUFA	Diunsaturated fatty acid
ECL	Equivalent chain length
EI	Electron impact
EPA	Eicosapentaenoic acid
FA	Fatty acid
FAME	Fatty acid methyl ester
FID	Flame ionization detector
GC	Gas chromatography / Gas chromatograph
IL	Ionic liquid
k	Retention factor
MS	Mass spectrometry
m/z	Mass-to-charge ratio
M^+	Molecular ion
MI	Methylene interrupted
MUFA	Monounsaturated fatty acid
N	Plate number
NMI	Non-methylene interrupted

PEG	Pollyethylene glycol
PCA	Principal component analysis
PUFA	Polyunsaturated fatty acid
R_s	Chromatographic resolution
SCOT	Support-coated open tubular
SN	Separation number
TCD	Thermal conductivity detector
t_M	Minimum time of components to stay in in the system
t_R	Retention time
$t_{R'}$	Adjusted retention time (t_R-t_M)
w_b	Peak width at baseline
w_h	Peak width measured at half height
WCOT	Wall-coated open tubular
α	Chromatographic selectivity

1 Introduction

1.1 Aims of the study

Long chain omega-3 fatty acids, particularly eicosapentaenoic acid (EPA) and docosahexaenoic acid, are important both for human nutrition and as ingredients in fish feed. Due to high pressure on global fish resources, there is an increasing demand for alternative sources of omega-3 fatty acids. Direct utilization of marine algae that is grown under controlled conditions is an alternative to traditional fisheries with great potential as source of omega-3 fatty acids.

Currently, there is work in progress at Department of Biology that investigates the feasibility of local alga strains for production of omega-3 fatty acids. Small scale production facilities for algae have recently been installed at department of Biology and a pilot plant (CO2Bio) for production in larger scale has been built on Mongstad outside Bergen.

Department of Chemistry currently performs fatty acid analyses for Department of Biology. With the increasing demand for algal fatty acid analyses that can be expected, there is a need to gain data and knowledge about which fatty acids that may be present in these samples, and how they can be separated and identified. Compared to fish oil, algae have special fatty acid patterns. They often contain relatively high amounts of polyunsaturated fatty acids with chain lengths of 16 and 18 carbons and may also contain other compounds that are less abundant in other organisms. This requires special focus and may require specific mass spectral libraries for compound identification and adjustments to the chromatographic methods that are developed for other sample types.

The major goals for the project are to identify the fatty acids that are common in marine algae and investigate how these behave on different chromatographic columns when derivatized to fatty acid methyl esters (FAME). The aim for this task is to identify compounds that constitute 0.2% or more of the total fatty acids in at least one of the analyzed samples.

In addition to the two gas chromatographic columns that are commonly in use for FAME analyses at Department of Chemistry (BPX70 and BP20), two one new columns (DB-225 and

DB5) was evaluated for analysis of algal FAME. A more theoretical study of FAME retention on a larger number of columns was also carried out.

1.2 Fatty acids

Fatty acids are carboxylic acids that have a long carbon chain, typically from 4 to 28 carbons. Generally, fatty acids have an unbranched chain and even carbon number with one or more double bonds, usually with cis configurational isomerism. Commonly, more than 40 fatty acids are found in food[1, 2].

A fatty acid has a distinctive carboxyl end group (COOH) and methyl group (CH3) named Omega (ω) at the other end of the molecule. The carbon close to methyl group is called α and the next carbon atom it is called β [3] (Figure 1.1).

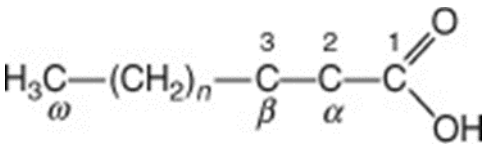

Figure 1.1. Nomenclature for fatty acids. One way to name Fatty acids is by the systematic or trivial nomenclature. Using methyl (omega) end group is a to title the fatty acid. This way describes the location of the double bonds from the end of the fatty acid. Also, the letter n is also usually used to locate double bond [4].

When all bonds between carbon atoms are single, the fatty acid is called a saturated fatty acid (SAFA), and when there are one or more double bonds between the carbon atoms, then its termed an unsaturated fatty acid. The number of unsaturated bonds in a fatty acid typically varies between one (Monounsaturated fatty acid) and six (polyunsaturated fatty acid, PUFA) [5].

There is different nomenclature that are used to describe fatty acids. The most common systems that are used are, the common name, the systemic name, and the omega classification. One system uses the number of carbon atoms together with the number of double bonds. For example, Myristic acid, a C14:0 saturated fatty acid, has 14 carbon atoms with no double bond. The end methyl group, named Omega (ω), can be used to label the location of the double bond from the methyl end of the molecule. The letter "n" minus double bond position is also used for this purpose. For example, the C18:3 ω3 fatty acid is a polyunsaturated fatty acid that has 18 carbon atoms with three double bonds, and the first double bond is located at the third carbon

atom from the methyl group. Alternatively, it can be written as 18:3 n-3. Another way to name the location of the double bond is to begin from the carboxyl group and the symbol delta (Δ) is then used to designate the positions of all double bonds, for example $\Delta^{9,12,15}$ C18:3[6, 7].

Several studies have mentioned that an increased nutritive consumption of long-chain omega 3 PUFA has positive health effects. These positive results have been described for different disorders, like cardiovascular [8, 9] , and neurodegenerative disease [10] , inflammation [11], diabetes [12] and a number of cancer forms [13]. A diet high in fatty fish or fish oils is considered to be a good source of essential fatty acids. Other food sources are plants like flaxseed and flaxseed oil, walnuts and walnut oil, and canola oil. Lately it is found that algae are a good alternative source of essential fatty acids [14-18].

When the two hydrogen atoms next to the double bond are positioned at the same side of the chain, this gives the fatty acid a cis configuration. On the other hand, when the hydrogen atoms are on opposite sides, it gives the double bond a trans- configuration (Figure 1.2) [19].

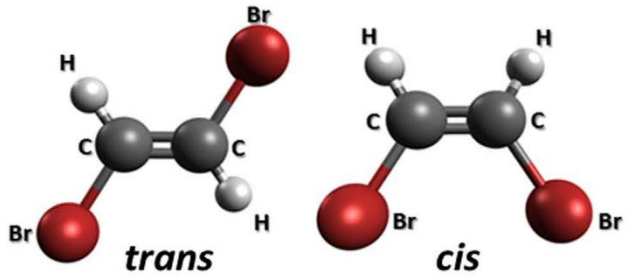

Figure 1.2. Cis-trans configuration [19].

When two or more double bonds are separated with single methylene group in PUFA, the PUFA is termed methylene interrupted (MI) double bonds PUFA or homoallylic double bonds [20]. On the other hand, when there are two or more methylene groups between the double bonds, the molecule is termed non-methylene interrupted (NMI) FA, In such cases its common to locate the double bond from the carboxyl group [21, 22].

The adipose tissue of our body and vegetable oils are mainly composed of triacylglycerols (Triglycerides, TG). A TG molecule is an ester of three fatty acids and a one glycerol. Fatty acid methyl esters (FAME) are made by a process called transesterification (Figure 1.3) where the R″ group in the TG ester molecule is replaced with the R′ group of an alcohol (usually methanol). This reaction is catalyzed by adding of an acid or base reagent [23, 24].

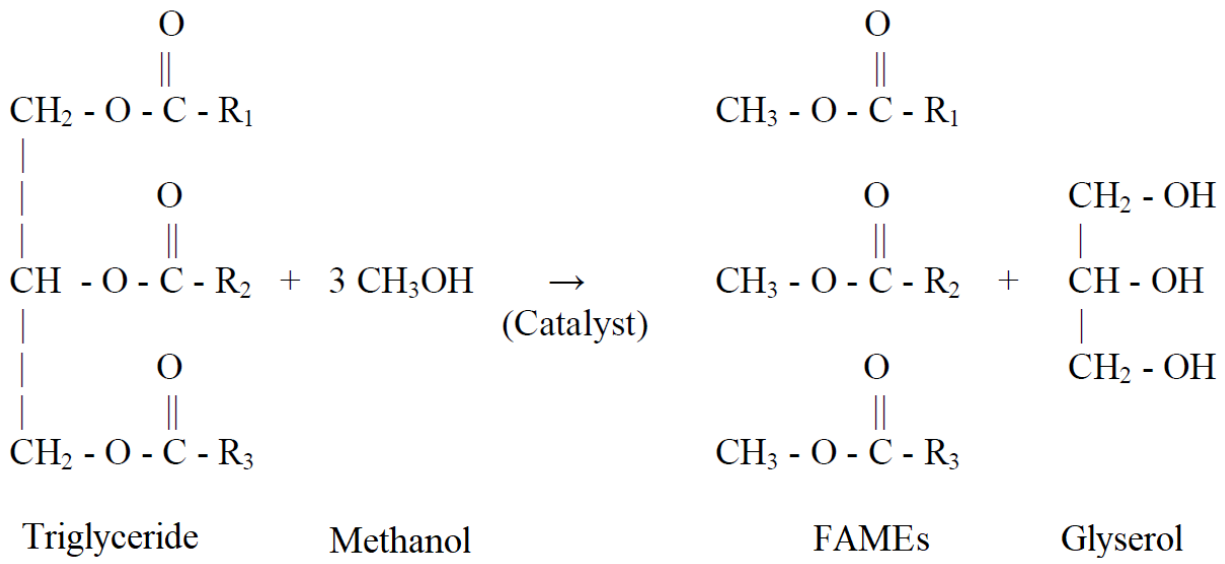

Figure 1.3. Transesterification process. The R″ group in the TG is replaced with the R′ group of an methanol. This reaction is catalyzed by adding of an acid or base reagent [25].

Fatty fish like Salmon is considered to be one of the important sources to obtain omega-3 long-chain polyunsaturated fatty acids (LC-PUFA), Eicosapentaenoic (EPA) and Docosahexaenoic (DHA) acids. However, this source has its limitation when it comes to the supply of omega-3 from traditional fisheries. Lately, some studies show that algae can be a replacement source of omega 3 fatty acids. Hamilton et al. have stated that heterotrophic microalga can yield enhanced amounts of both Long-chain omega-3 Eicosapentaenoic acid (EPA) and Docosahexaenoic acid (DHA) fatty acids [26]. Also Ahlgren et al have shown relatively high amounts of Omega-3 LC-PUFC in algae, especially in Cryptomonas, Rhodomons and Peridinium [27].

1.3 Algae and the biosynthesis of fatty acids

The biosynthetic pathway of fatty acids (EPA and DHA) in microalgae occurs in the chloroplasts. The process typically begins by synthesis of stearic acid (18:0) in the chloroplast, then a sequence of changes by desaturation and chain elongation processes at the endoplasmic reticulum, enhanced by a different step of desaturation and elongation of highly specific fatty acids. The desaturation step adds a double bond to the molecule, on the other hand two new carbon atoms are added to the molecule by elongation.

Stearic acid is desaturated to oleic acid (18:1 n-9) and linoleic acid (LA, 18:2 n-6). Desaturation of fatty acids can lead into two different metabolic pathways, either n-6 or the n-3 fatty acids. From linoleic acid, α-linolenic acid (ALA, 18:3 n-3) can be formed by adding the next double bond toward the methyl-end of the molecule.

Fatty acid desaturation can go in two different metabolic directions, either the n-6 or the n-3 route. Within the n-3 route, desaturation of LA produces α-linolenic acid (ALA, 18:3 n-3) by introducing the next double bond toward the methyl-end of the molecule. Additional chain elongation and desaturation reactions produce EPA and DHA. On the other hand, in the n-6 route, the LA is desaturated leading to produce ɤ-linolenic acid (18:3 n-6) by adding a double bond to the carboxyl-end of the molecule. This will lead to arachidonic acid (AA 20:4 n-6), which can be further desaturated to EPA. Those were the conventional ways of the biosynthesis of EPA and DHA, however the are other alternative ways to produce them [28].

2 Theory

2.1 Chromatography

Chromatography is an effective and common technique used in analytical chemistry for separation and analyzing mixtures, like separation of fatty acid derivatives. Chromatography separates materials based on their difference in velocities in two-phase systems. This system is made to maximize the rate of mass transfers between the two phases [29]. There are several types of chromatography, like liquid chromatography, gas chromatography, supercritical chromatography, and planar (thin layer) chromatography.

Chromatographic techniques are based on three components. The first one is the stationary phase which is a solid phase or can be a liquid adsorbed to a surface of a solid layer. The second is the mobile phase, which can be a liquid or a gas, and the last component is the molecules that are separated [30].

2.1.1 Gas Chromatography

Gas chromatography uses the gas as the mobile phase. Stationary phases in gas chromatography can be solid adsorbents (gas-adsorption chromatography) or high degree boiling viscous and immobilized liquids on a solid carrier (gas-liquid chromatography) [31].

GC has different elements. The inlet is attached to the column head where the sample is injected into a constant flow of the carrier gas (Figure 2.1).

The carrier gas has to be chemically inert. The commonly used gases are, nitrogen, hydrogen, argon and helium. The carrier gas is often chosen depending on the selected detector type. A molecular filter can also be used in the carrier gas system to get rid of water and other impurities.

Separation of the sample into different components take place in the column. Columns differ in inner diameter and length depending the usage type, which can be capillary (open tubular) or packed. Packed columns contain a finely divided, inert, solid support material (commonly based on diatomaceous earth) coated with liquid stationary phase. Usually packed columns are 1.5 - 10 m in length and the internal diameter of 2 - 4 mm.

Capillary columns have a small internal diameter (typical dimension 10-60 m x 0.1-0.5 mm x 0.1-1 µ m film thickness). There are two types of Capillary columns, wall-coated open tubular (WCOT) or support-coated open tubular (SCOT). The wall of the capillary tube in the WCOT are coated with liquid stationary phase, while in SCOT, the inner wall of the capillary is coated with a thin layer of supporting material, such as diatomite (also known as diatomaceous earth), where the stationary phase is adsorbed. Capillary columns are more common because of higher efficiency than packed columns.

The temperature in GC is controlled using an oven that heats quickly has good thermal control. A suitable column temperature depends on the boiling point of the sample and is precisely controlled in modern equipment. Higher temperature decrease elution times, but often at the cost of the separation. When the sample has a large boiling point range, temperature programmed GC (pTGC) is usually be advantageous. The injector and detector are also partly within the GC oven.

The data system gets the signal from the detector and digitizes it to produce the chromatogram, which is usually a plot of signal intensity versus retention time. Moreover, the data system can do several quantitative and qualitative processes on the chromatogram.

This detector can determine the mass and estimate the concentration of the components. The time that molecules uses in the carrier to pass through the stationary phase is known as retention time (t_R). The value of t_R will depend on degree of solubility the component has in the stationary phase.

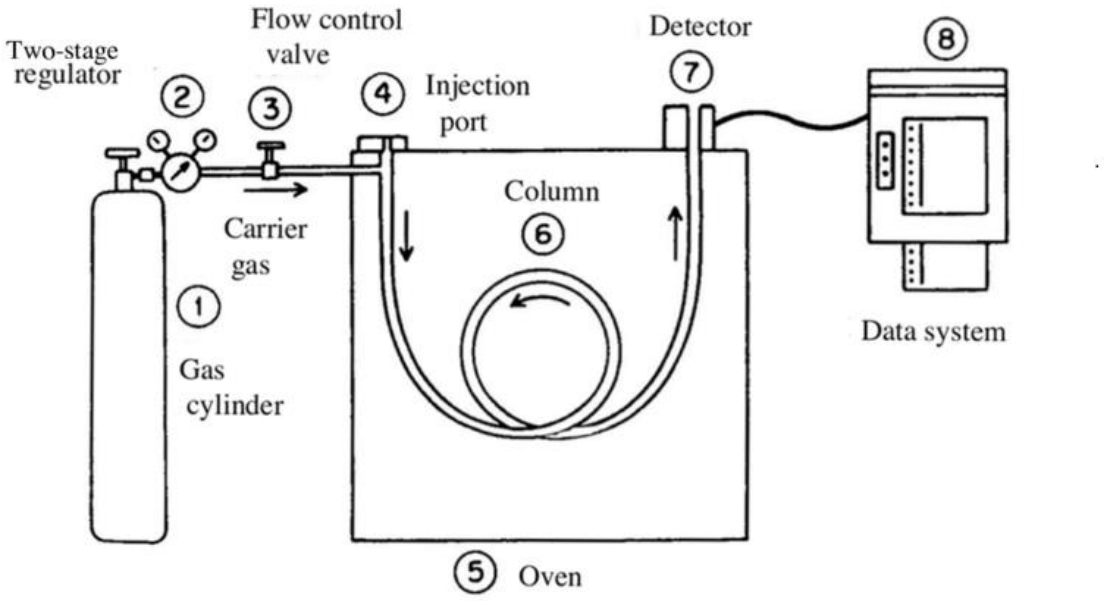

Figure 2.1. Basic components of a gas chromatograph [32].

There are different detector types that can be used in gas chromatography depending on sample type and required specificity or selectivity of detectors. The non-selective detector is used for all materials except the carrier gas, while a selective detector responds to a range of materials with a shared property. A specific detector is used typically for a single chemical class. The most common detectors that are used are the thermal conductivity detector (TCD), the flame ionization detector (FID) and mass spectrometers (MS).

The chromatographic process is summarized in Figure 2.2. The column is represented by the horizontal lines; each line is like a part of the process at a different time, where time increase from top bottom. The sample, which is a mix of components A and B, is injected onto the column in a narrow area, it is then carried through the column (in the figure from left to right) in the mobile phase. Each partition of the component between the two phases, as displayed by the distributions of peaks above and below the line, contributes to the separation. Peaks above the

line act for the amount of a certain component in the mobile phase, and peaks below the line account for the amount in the stationary phase. Component A has a larger distribution in the mobile phase and because of that it is passed down the column faster than component B, which uses more time in the stationary phase. In this way, separation of A from B happens as they both pass through the column. These components leave the column (elute) and move through the detector as demonstrated in the figure. The resulting signal from the detector produces a chromatogram as displayed in the figure.

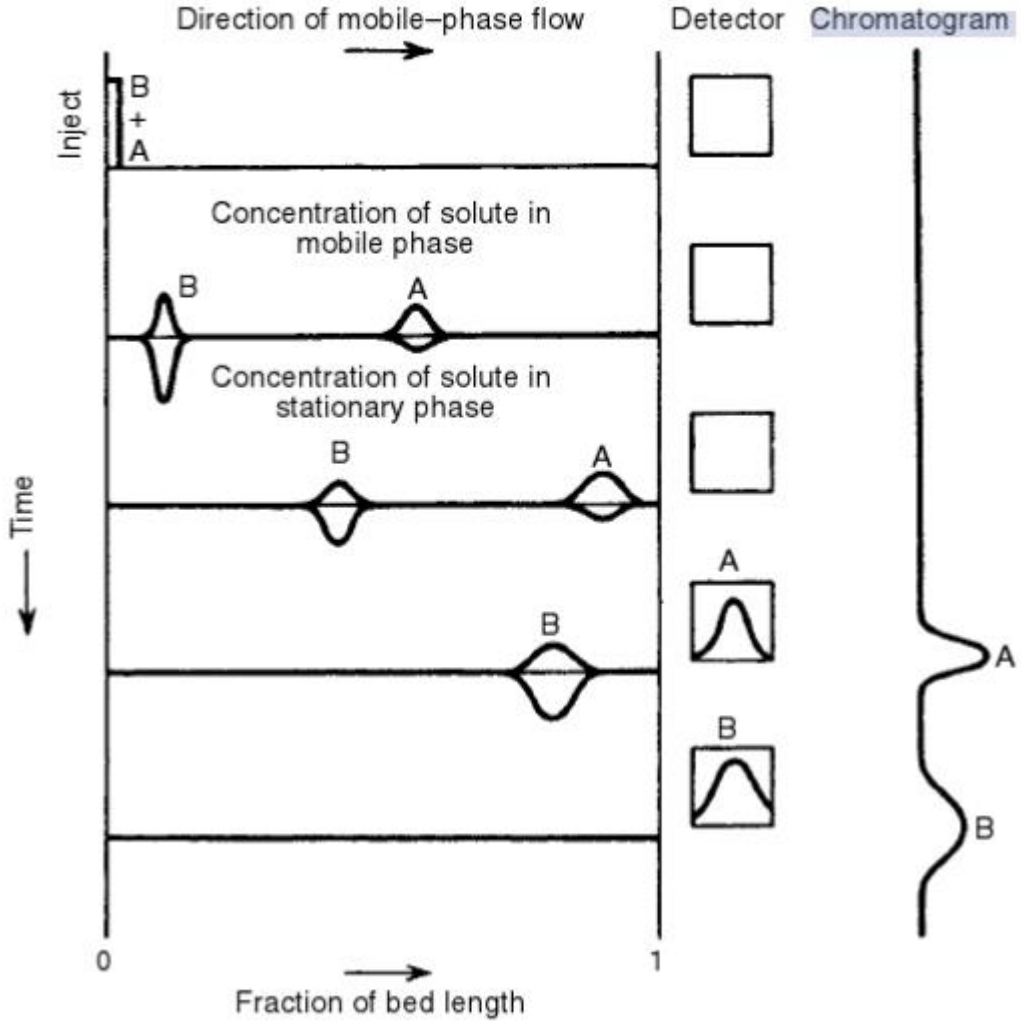

Figure 2.2. Chromatography process [33].

Figure 2.3 shows small chromatogram with two main peaks, A and B. Retention time (t_R) is the time it takes from the analyte is injected into the column until it is eluted out of the system. The small peak to the left side of Figure 2.3 shows analyte that is not absorbed by the stationary phase and moved through the column within the speed of the mobile phase, this peak is represented by t_M, which is the time the mobile phase takes to traverse the column, often referred to as holdup time or dead time. A net retention time (t'_R), usually referred to as adjusted retention time, can be determined by subtracting the retention time of the mobile phase (t_M) from the peak's retention time (t_R). This is equivalent to the time the compounds spend in the stationary phase before they elute. From Figure 2.3, it can be noticed that component B has more affinity than compound A to the stationary phase because it stays longer in the column [34, 35].

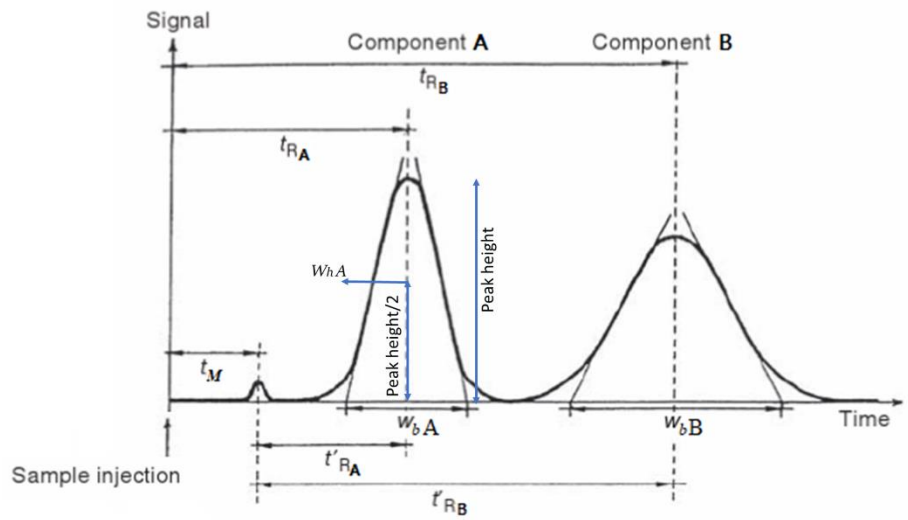

Figure 2.3. Typical chromatogram. tM the minimum time that a non-retained chemical species will remain in the system. tR is retention time. . tR'A equal tRA minus tM. Wb is the peak width at baseline (Wb also can be defined as 4σ). Wh is the peak width at half of peak height (Wh can be defined as 2.355σ). σ is the standard deviation of the normal distribution curves [34, 36].

The chromatographic separation between the two chromatographic peaks, A and B. Separation can be measured quantitatively by the Resolution (R_s) by Equation (1):

$$R_s = \frac{2\left(t_{R(B)} - t_{R(A)}\right)}{w_{b(A)} + w_{b(B)}} = \frac{\Delta t_R}{(\overline{w}_b)} \quad (1)$$

where R_s the peak resolution, t_R is retention time, w_b (4σ assuming that the shape of the peak follows the normal distribution curve) is the width of the peak at the base line, w_h is the peak width at the half height of the peak.

Separation depends on the following important factors, chromatographic retention (or capacity) factor (*k*), chromatographic efficiency (*N*) and chromatographic selectivity (α).

Retention factor, *k*, is defined as the distribution of the analytes between the stationary phase and the mobile phase as in Equation (2):

$$k = \frac{amount\ of\ analyte\ in\ stationary\ phase}{amount\ of\ analyte\ in\ mobile\ phase} \quad (2)$$

A high *k* value indicates that the sample is highly retained and has spent a long time interacting with the stationary phase. *k* depends on the solubility of the analyte in the stationary phase (k increases with increased thickness), column diameter (*k* decreases with increased diameter), and the temperature (*k* decreases with increased temperature).

Chromatographic efficiency, or plate number (*N*) is the ratio of retention time to the width of a peak as in Equation (3):

$$N = 16\left(\frac{t_R}{w_b}\right)^2 \quad (3)$$

Chromatographic selectivity (α) is the ratio between the adjusted retention times (t'_R)

or between the retention factors (*k*) of the two components as in Equation (4):

$$\alpha = \frac{t'_{R(B)}}{t'_{R(A)}} = \frac{k_{(B)}}{k_{(A)}} \quad (4)$$

The resolution R_s between two peaks in a chromatogram can be determined by Purnell equation as Equation (5).

$$R_s = \frac{\sqrt{N_{(B)}}}{4}\left(\frac{\alpha - 1}{\alpha}\right)\left(\frac{k_{(B)}}{1 + k_{(B)}}\right) \quad (5)$$

where R_s is the resolution between the two peaks. N_B is the plate number of the second peak. α is the separation factor between the two peaks. $k_{(B)}$ is the retention factor of the second peak.

The Purnell equation shows that presence of all three factors, retention, selectivity and efficiency, is necessary to achieve separation, where *N* and *k* should be above 0, and α should be above 1.

It is important to note that the Purnell equation and plate numbers (*N*) are only valid for isothermal chromatography. Because retention factors gradually decrease in temperature-programmed GC efficiency and selectivity must be described differently when temperature programming is applied [36, 37].

2.1.2 Equivalent Chain Length (ECL) values

Retention indices was introduced by Kováts in 1963 [38]. The principle is that retention is described relative to the chain length of a reference series instead of in retention time units. In the Kováts retention index system, n-alkanes are used as the reference series and the Kováts indexes of the references are by definition 100 times the chain length. The principle is illustrated in Figure 2.4, where the green peaks of n-alkanes defines the retention index scale.

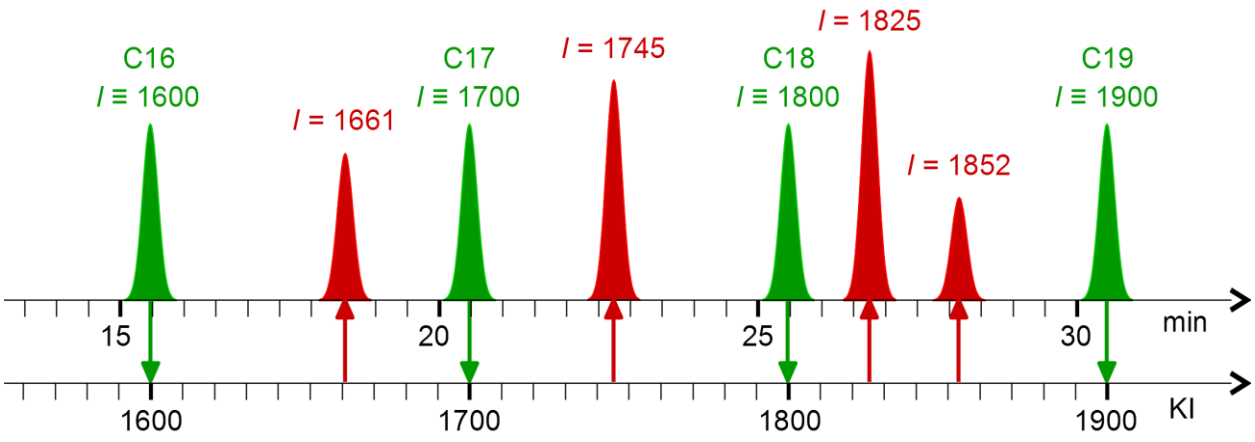

Figure 2.4. Principle of the Kováts retention index system. Green peaks are reference compounds that define the secondary retention index scale (KI). Red peaks are other compounds.

Equivalent chain lengths (ECL) is a retention index system that is commonly applied for fatty acid methyl esters. Here the normal saturated FAMEs define the scale, and the ECL value of these are equal to the number of carbon atoms in the fatty acid chain. Equation (6) can be used to calculate ECL values at isothermal conditions:

$$ECL_{(x)} = n\frac{\log t'_{R(x)} - \log t'_{R(z)}}{\log t'_{R(z+n)} - \log t'_{R(z)}} + z \quad (6)$$

where t'_R is adjusted retention times of the compound of interest, *x*, and two saturated FAMEs eluting on each side of the compound. *z* signifies the number of carbon atoms in the carbon chain of the saturated FAME eluting before *x*, and *n* is the difference in the number of carbon atoms between the two references. To calculate the ECL values at temperature programmed conditions, Equation (7) can be used.

$$ECL_{(x)} = n\frac{t_{R(x)} - t_{R(z)}}{t_{R(z+n)} - t_{R(z)}} + z \quad (7)$$

where *n*, *x* and *z* are the same as in Eq. (6) [39].

2.1.3 Temperature programmed gas chromatography

In Temperature programmed gas chromatography, the temperature is maintained at low level for a short period of time, then the temperature is increased to help luting the heavier compounds.

This process causes in varied solute-stationary phase and solute-mobile phase interactions over the time of analysis, and though the retention factor (*k*) will have different values. Based on that the equations that are directly or indirectly dependent on *k* are not viable. This includes Equations 3, 4, 5 and 6 above and means that both selectivity and efficiency for temperature programmed GC must be defined by other means. Although the Purnell equation is not applicable to temperature-programmed GC, it still the same three factors (retention, efficiency and selectivity) that result into separation. The efficiency in temperature programmed GC can be defined by the separation number (*SN*) and selectivity can be defined by retention indexes. The separation number is almost equal to the number of peaks that theoretically can be solved with R_s equal to 1 in the area between two members of a homologous series and is calculated by Equation (8)

$$SN = \frac{t_{R(z+1)} - t_{R(z)}}{w_{h(z)} - w_{h(z+1)}} - 1 \quad (8)$$

where z represents the shortest of the two homologues and $z + 1$ represents the longest of the two homologues, t_R is retention time and w_h is the peak width measured at half height [40-42]. The principle is illustrated in Figure 2.5.

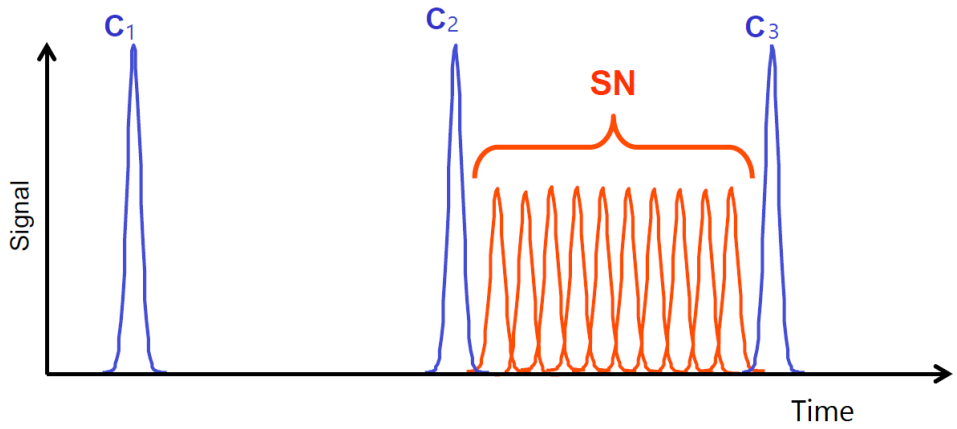

Figure 2.5. The separation number (SN) shows the approximate number of peaks that can be placed with Rs≈1 between two alkanes with z and z + 1 carbon atoms [42].

2.1.4 Gas chromatography for fatty acids

GC is used broadly to analyze fatty acid methyl esters (FAMEs). Before FAs are derivatized, it is hard to analyze them because of high polarity that have a tendency to form hydrogen bonds, causing high boiling points and adsorption problems in the column. Though, reducing the polarity of the FAs by derivatization make them more suitable for analysis by GC. When polar carboxyl functional groups are neutralized, this allows column separation by several factors, such as by the degree and location of unsaturation, the cis/trans configuration of unsaturation, and chain length.

Polar columns are commonly used for separation of complex fatty acid mixtures. There are two types of polar phases that are frequently used. the polyethylene glycol (PEG) columns where the polar functional group is the hydroxy (-OH) group and the cyanopropyl (CNP) columns where the polar functional group is the cyano (-CN) group [34].

In polar phases, the compounds will usually elute depending firstly on the number of carbons and secondly on the number of double bonds. For those compounds with the same number of carbon and double bonds, mainly the compounds with the double bonds located closest to the carboxyl

group will elute first, for example an n-6 fatty acid will elute before the n-3 isomer, However, there are some exceptions.

2.1.5 Stationary phases for GC

The separation pattern of a FAME reference mixture was evaluated on 11 different stationary phases (BP20, DB225, DB23, DB5, IL100, IL61, 1L82, RTX200, RTX50, RTX11 and BPX70) in this work.

These stationary phases have different functional groups. Stationary phases structures are shown in Table 2.1. There are three main phase types: polysiloxane polymers, polyethylene glycol and ionic liquids.

Polysiloxan polymers were first applied in the beginning 1950s. Examples of popular commercial columns for fatty acid analyses are: DB-225 (Agilent), CP-Sil 88 (Agilent), SP-2330 (Supelco), SP-2560 (Supelco) and BPX-70 (SGE). The polysiloxane phases consist of silicon, oxygen and functional groups (R) and they have the chemical formula $[R_2SiO]_{n.}$ The functional groups can be methyl, phenyl, cyanopropyl and trifluoropropyl. The thermal limits depend on the R-groups and typically vary between 260 and 325ºC.

In 1950s the polyethylene glycol (PEG) phase were also introduced. Typically, the name of the commercial columns contains wax and the columns are often referred to as wax columns. The chemical formula for PEG is $H{-}(O{-}CH_2{-}CH_2)_n{-}OH$. The (PEG) phases have thermal limit of around 280 ºC.

Ionic liquid stationary phases were introduced in 2008. Some examples of the IL commercial columns are IL59, IL60, IL76, IL100. Ionic liquid columns are unique because of their distinctive properties. The IL phases are available with other functional groups than traditional stationary phases, and they can be applied for both polar and apolar analytes.

The non-polar columns such as RXI1 and DB5 are effective for non-polar compounds. RTX200 and RTX50 are intermediate polarity columns, therefore they are best for intermediate polarity compounds. DB225, BP20, DB23, BPX70, IL61, IL82 and IL100 are high polarity stationary phases [43].

Table 2.1. Stationary phase structure and properties

Phase	Type	Description
RXI1	Dimethyl polysiloxane	Polysiloxane based. Apolar, will be found near the intersection between the three lines in Figure 2.7
DB5	5% diphenyl polysiloxane,95% dimethyl polysiloxane	Polysiloxane based. Apolar with some phenyl groups, along line 2, but near the intersection of the three lines in Figure 2.7
RTX200	Trifluoropropylmethyl polysiloxane	Polysiloxane based. 50% of the R-gropups are trifluoropropyl. 50% are methyl, will be a long line 1 in Figure 2.7
RTX50	Phenyl methyl polysiloxane	Polysiloxane based. 50% of the R-gropups are phenyl. 50% are methyl, will be a long line 2 Figure 2.7
DB225	50% cyanopropylphenyl 50% dimethylpolysiloxane	Polysiloxane based. 25% of the R-groups are cyanopropyl, 25% are phenyl, 50% are methyl. Should be found between line 2 and line 3 in Figure 2.7
IL61	1,12-Di(tripropylphosphonium)dodecane bis(trifluoromethylsulfonyl)imide trifluoromethylsulfonate	Ionic liquid. Unique selectivity, not in the plot but expected to be between IL59 and IL76 in Figure 2.7
BP20	Polyethyleneglycol (PEG)	Polyethylene glycol. In cluster I in Figure 2.7
DB23	50% cyanopropylpolysiloxane, 50% methylpolysiloxane	Polysiloxane based. 50% of the R-gropups are cyanopropyl. 50% are methyl, will be a long line 3 in Figure 2.7
BPX70	70% cyanopropyl 30% polysilphenylene-siloxane	Polysiloxane based, but with phenyl groups in the backbone. 70% of the R-gropups are cyanopropyl, 30% are methyl. Should be found along line 3, but with possible influence from the phenyl groups (line 2 in Figure 2.7)
IL82	1,12-di(2,3-dimethylimidazolium)dodecane bis(trifluoromethanesulfonyl)imide	Ionic liquid. Unique selectivity, shown in Figure 2.7
IL100	1,9-di(3-vinylimidazolium)nonane bis(trifluoromethanesulfonyl)imide	Ionic liquid. Unique selectivity, shown in Figure 2.7

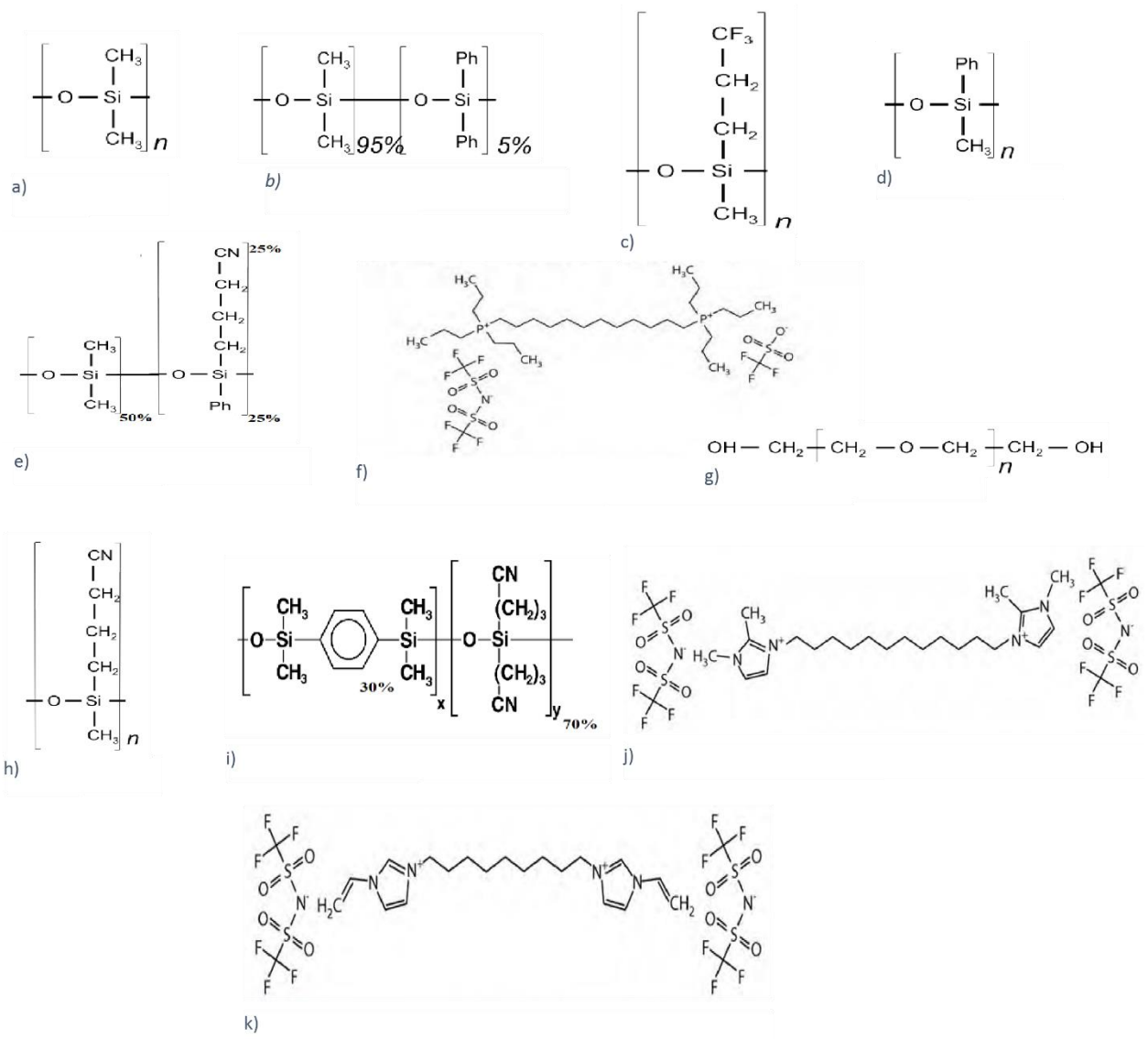

Figure 2.6. Stationary phases chemical structures for the columns which were used to evaluation the columns. a) RXI1 b) DB5, c) RTX200, d) RTX50, e) DB225, f) IL61, g) BP20, h)DB23, i) BPX70, j) IL82, k) IL100.

Principal component analysis has been used to evaluate the selectivity of a large number of stationary phases for GC [44]. The score plots in Figure 2.7 shows that stationary phases are divided to three lines and two clusters. The hydrogen-bond basicity of the stationary phases and the ability of the stationary phases for dipole-type interactions are linked respectively to the principal components 1 and 2, while the ability of the stationary phases for Π-Π and n-Π interactions and the hydrogen-bond acidity are linked to principal component 3.

Line 1 displays trifluoropropyl substituted phases, line 2 displays phenyl substituted, and line 3 displays cyanopropyl substituted. Cluster I show polyethyleneglycol phases and cluster II shows ionic liquid phases.

By looking to the PCA score plot it can by seen that the values of PC1 and PC3 are high at the same time only for ionic liquids columns, that mean the other columns do not have the same separation characteristics as the ionic liquid columns, which simultaneously have strong hydrogen-bond basicity, hydrogen-bond acidity and capability for Π-Π and n-Π interactions.

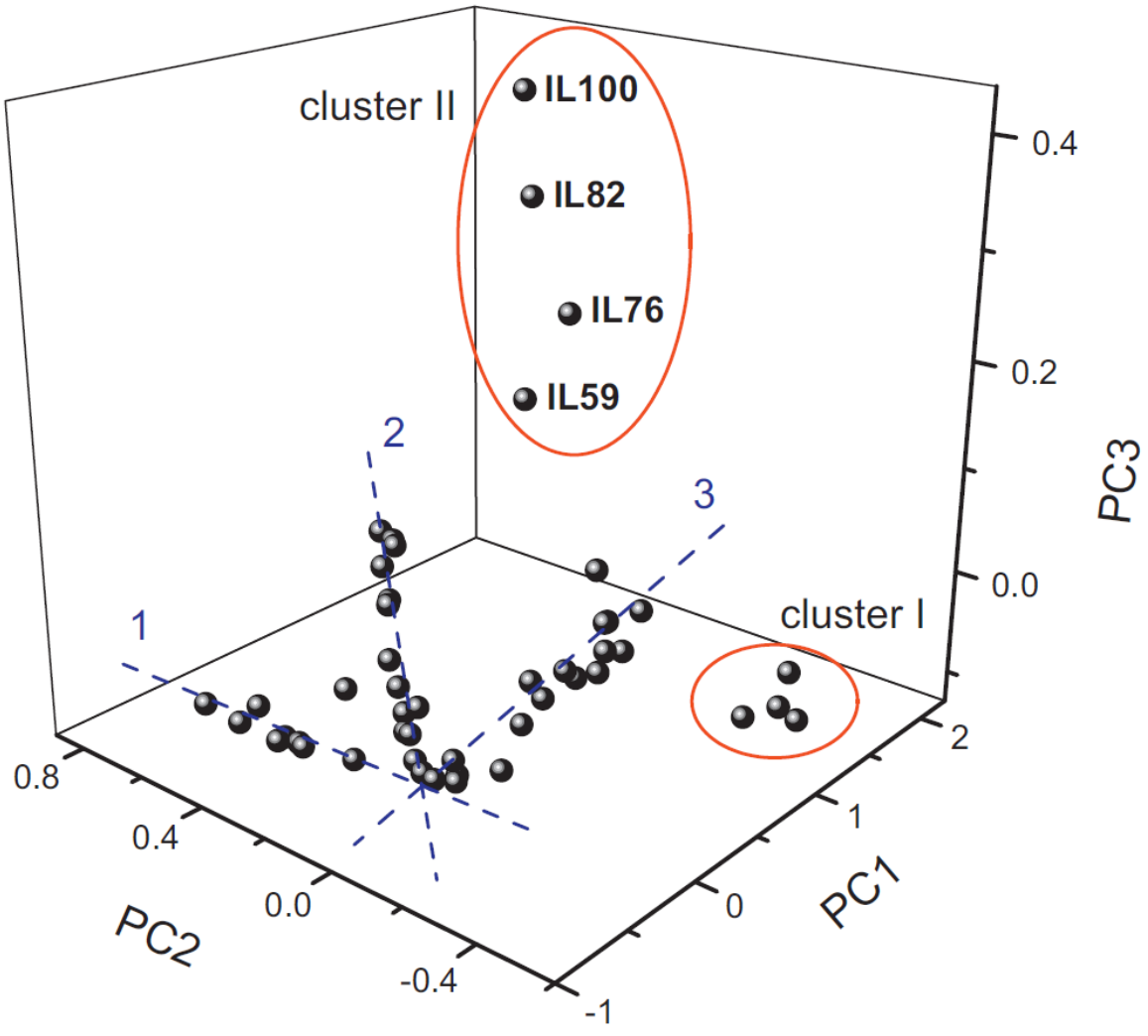

Figure 2.7. PCA of system constants for 49 stationary phases. line 1 shows trifluoropropyl-substituted polysiloxanes, line 2 shows phenyl substituted polysiloxanes, and line 3 shows cyanopropyl substituted polysiloxanes. Cluster 1 is polyethyleneglycol (PEG) phases and cluster 2 is ionic liquid phases. From [44].

2.2 Mass spectrometry

Mass spectrometry (MS) is an analytical technique used to identify compounds. The main principle of mass spectrometry is separating the ions in a sample according to their mass to charge ratio (m/z). Mass spectrometry differs from other methods of analysis. Mass spectrometry is highly sensitive and therefore do not require a large quantity of sample. Whereas the MS is a destructive analysis technique, the sample cannot be used again after analysis. The mass spectrometer has three main parts: ion source, mass analyzer and detector [45].

In chromatography–mass spectrometry system the molecules enter the mass spectrometer after being separated by the chromatograph. In this system the molecules can be directly moved from capillary column into the ion source. Hydrogen (H2) and helium (He) have very low atomic and molecular masses, therefore they are mostly used as carrier gasses for GC/MS, where they can be easily removed from mass spectrometer by the vacuum system [45].

After introducing the sample, the molecules must be ionized. There are several ionization methods, but the electron ionization (EI) was used in this work. In the electron source, a ray of highly energetic electrons interrelates with the molecules. Because of the ionization the molecules become positively charged (cations). The ionization process provides energy that are enough to form fragments. Fragmentation formation depends on the ability of the molecule to stabilize the positive charge. After that, the mass to charge ratios (m/z) are recorded by the detector. The mass of fragments can be determined if the charge of the detected fragments is known, and it can usually be assumed to be +1. The molecular ion (M^+) can determine the molecular mass [34, 45].

2.2.1 Mass spectrometry of fatty acid methyl esters

In EI-MS a two- dimensional graph is usually used to describe the Spectra. The X-axis signifies the m/z values of the ions and the Y-axis signifies the relative amount of the ions. The mass spectrum can be used to determine the number of carbons and number of double bonds, as well as other features of the molecules. It can be noticed that the strongest signal is referred to as the base peak, while the highest mass may represent the molecular ion mass M^+ [46]. Further details and example spectra of FAMEs are given below. The spectra are acquired from www.chrombox.org/data

2.2.1.1 Saturated FAME

Figure 2.8 shows three examples of saturated FAMEs. For short-chain FAMEs (Figure 2.8a) the molecular ion (M^+) can be absent and the strong ion $[M-43]^+$ must be used to confirm the molecular mass. The spectra in Figure 2.8b and c are simple and characteristic spectra with little fragmentation and a relatively strong molecular ion. The McLafferty ion (m/z 74) is base peak, and m/z 87 is also strong [47].

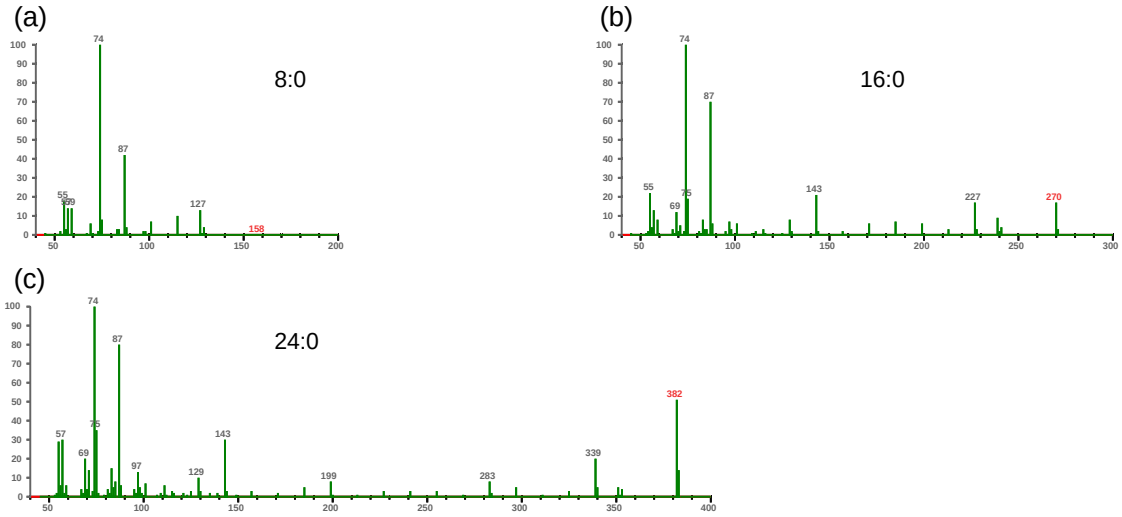

Figure 2.8. Examples of saturated FAME

2.2.1.2 Branched saturated FAME

Branched saturated FAME examples are compared with their unbranched isomer in Figure 2.9. The most common branched series, iso (i) and ante-iso (ai) isomers are very difficult to distinguish from the corresponding unbranched isomers, but there are some minor differences in the relative abundance of $[M-31]^+$ and $[M-29]^+$. For 15:0 these correspond to m/z 225 and 227, and for 17:0 the ions are m/z 253 and 255. For the unbranched isomers $[M-31]^+$ is higher than $[M-29]^+$. In the iso-isomers $[M-31]^+$ is lower compared to the unbranched isomers, and the two ions are of approximately equal size, both with very low abundance. In the ante-iso isomers $[M-29]^+$ is more abundant than $[M-31]^+$. There are also additional ions that can distinguish between the isomers, but these are often so weak that they can be difficult to separate from noise [48].

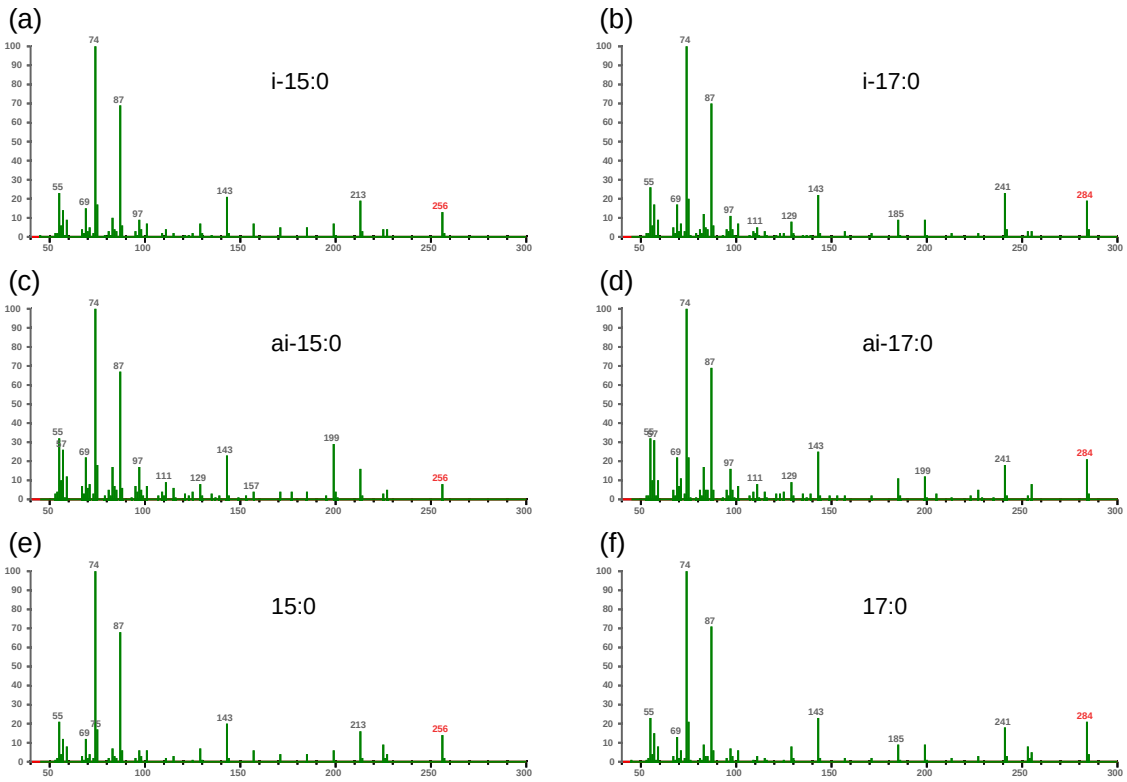

Figure 2.9. Examples of branched saturated FAME

Figure 2.10 shows the spectra of branched FAMEs with a methyl group near the carboxyl chain. The difference is very clear in this case. With methyl-substitution in 2-position in pristanic acid ME the McLafferty ion will be m/z 88. While for methyl branch in the 3-position in phytanic acid ME the McLafferty ion will be m/z 101 [49, 50].

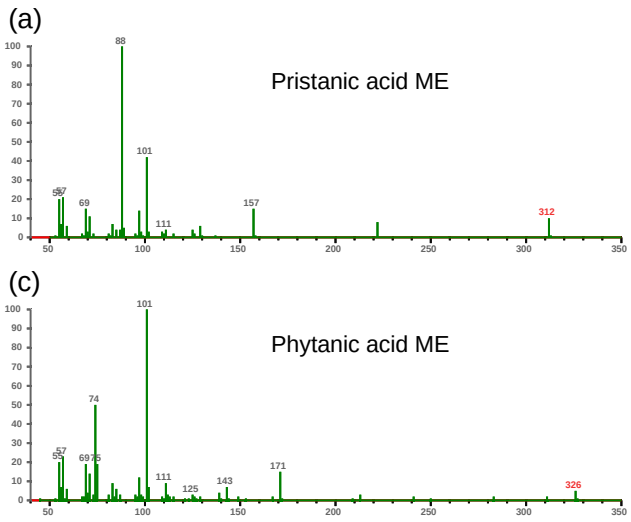

Figure 2.10. Branched FAME with methyl groups near the carboxyl chain. (a) pristanic acid ME. (c) phytanic acid ME.

2.2.1.3 Monounsaturated FAME

In monounsaturated FAMEs the base peak is usually m/z 55, but the strength of this ion decreases when the distance between the double bond and the carboxyl group is reduced. Figure 2.11 show examples of monounsaturated FAMEs. The strength of the ion m/z 74 is weakest for 16:1 n-5 figure 8d where is the double bond is far from the carboxyl group, while the strength of the same ion is highest for 16:1 n-11 Figure 2.11a. Except from this, there is no diagnostic ions that will indicate the position of the double bond. The ions $[M-32^{+}]$, $[M-74]^{+}$ and $[M-166]^{+}$ are often stronger than M^{+} and can be used to confirm the molecular mass in spectra of low quality[51].

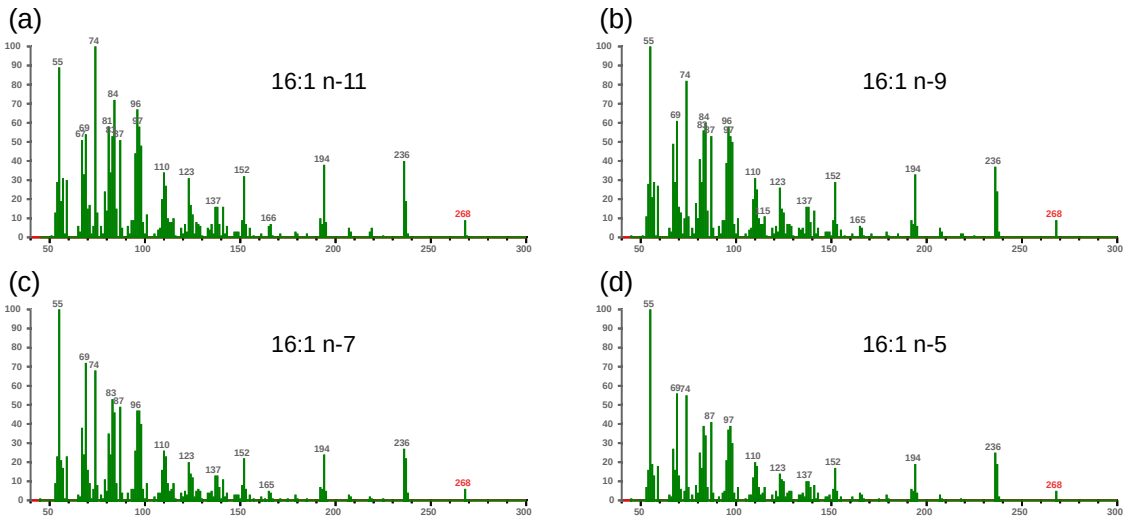

Figure 2.11. Examples of monounsaturated FAME

2.2.1.4 Cyclic FAME

Cyclopropane fatty acids are isomers of normal unsaturated FAME and have the same fragmentation mechanisms. They can therefore not be clearly distinguished from the normal mono-unsaturated FAMEs as shown in Figure 2.12 [52].

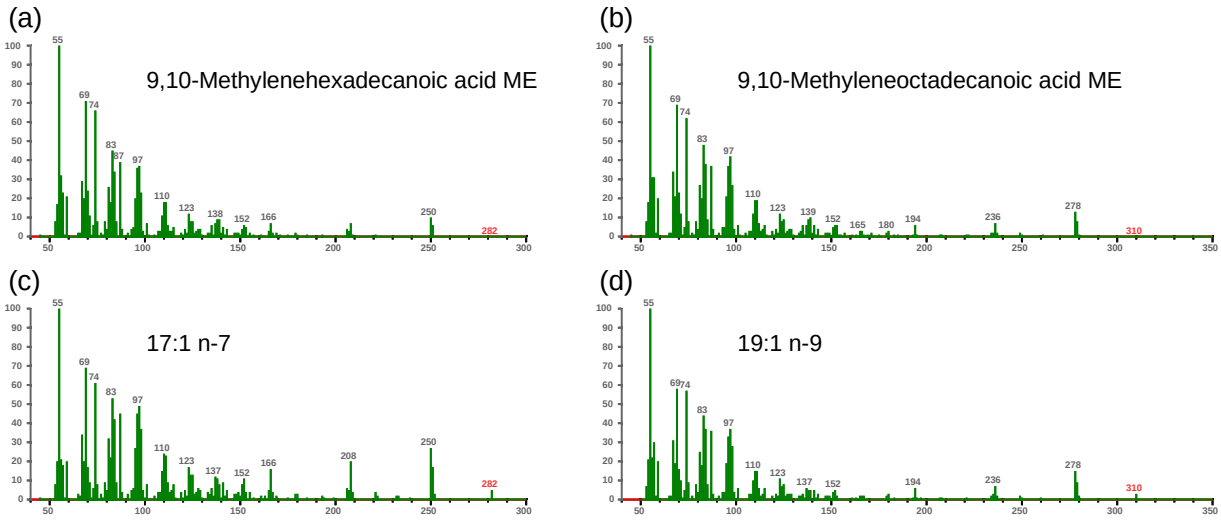

Figure 2.12. Cyclopropane fatty acids (a and b) compared to monounsaturated isomers (c and c).

2.2.1.5 Diunsaturated FAME

The spectrum of 18:2 n-6 is shown in Figure 2.13a. The m/z 67 is the base peak and it is the most common base peak in methylene-interrupted diunsaturated FAMEs, but 79, 81 and 95 can be equally strong or stronger[53]. Isomers of normal methylene-interrupted diunsaturated FAMEs

have almost identical spectra and there are no ions that tell the double bond positions. Therefore, it is difficult to differentiate between 18:2 n-6 and 18:2 n-4 (Figure 2.13a and b)[36].

Dienes with conjugated double bond systems Figure 2.13c have very similar spectra to methylene-interrupted dienes, but the molecular ion tends to be stronger. Spectra of compounds with non-methylene interrupted double bonds (NMI) Figure 2.13d show more variation and differ significantly from the normal dienes. There are cases where the double bond position in NMI dienes can be found from diagnostic ions [53] [54]

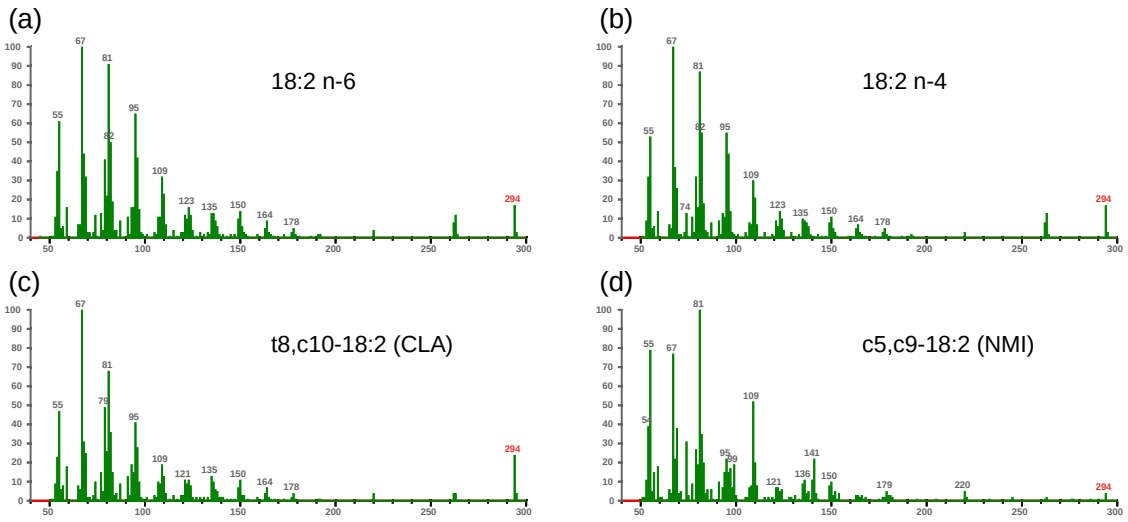

Figure 2.13. Examples of diunsaturated FAMEs.

2.2.1.6 Polyunsaturated FAME

For methylene-interrupted polyunsaturated FAMEs there are diagnostic ions that tells the double bond position from the methyl end (omega-ion) and carboxyl end (alpha-ion)[37, 55].

Figure 2.14 shows examples of polyunsaturated FAME. M/z 79 is usually base peak, but m/z 91 increases with number of double bonds and it can be the base peak in highly unsaturated PUFA. Figure 2.14(a-c) show 18:3 FAME belonging to the n-6, n-4 and n-3 series, respectively. As the number of double bonds increase in Figure 2.14(c-e), the diagnostic ions, as well as the molecular ion will be weaker, which can make it difficult to identify highly unsaturated FAMEs from their spectra[37]. Spectra of NMI PUFAs can be similar to spectra of NMI dienes [56].

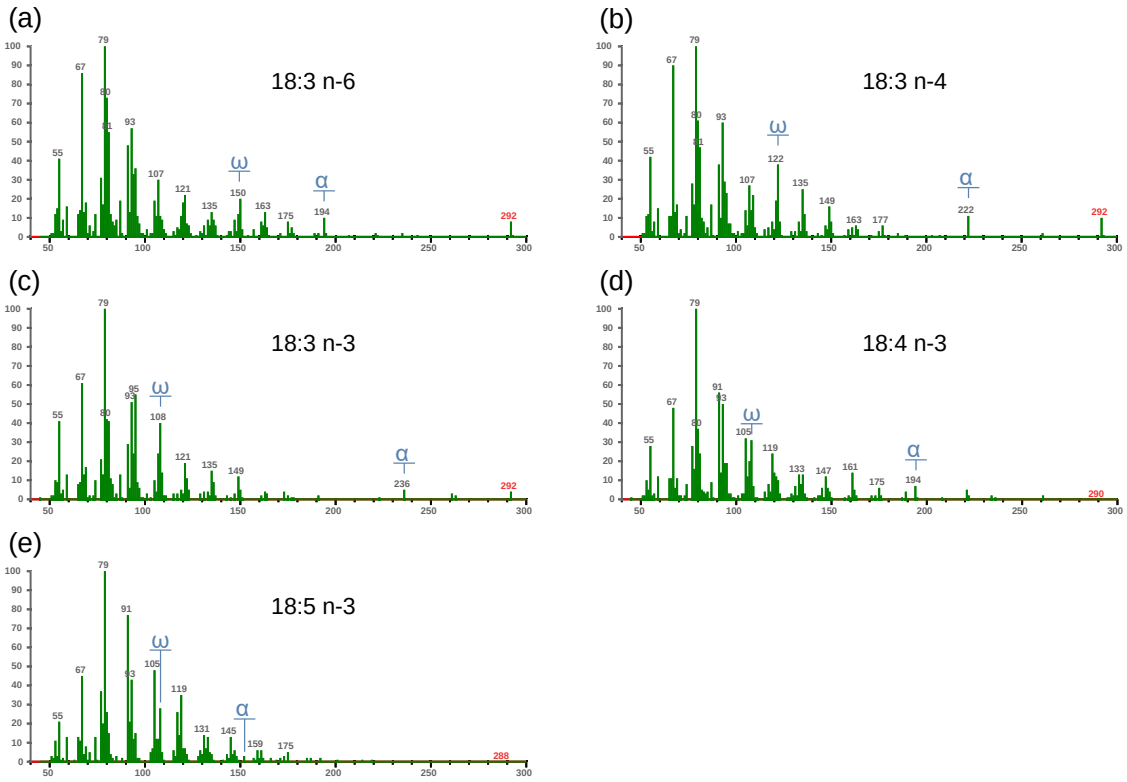

Figure 2.14. Examples of polyunsaturated FAME

2.2.1.7 Hydroxy fatty acids

By looking to Figure 2.15 it can be noticed that hydroxy FAMEs have spectra very different from other FAMEs. Figure 2.15 (a and b) are with the OH-group in 2-position (alpha-hydroxy fatty acids), while Figure 2.15 (c and d) are with OH-group in 3-position (beta-hydroxy fatty acids), these two types are the most common, but the OH-groups can also be in other positions.

The 2-hydroxy FAMEs are best characterized by having m/z 90 as the McLafferty ion and by a very strong $[M-59]^+$ signal, that can be used to confirm the (weak) molecular ion. The 3-hydroxy FAMEs have a very strong signal at m/z 103 and no molecular ion[57].

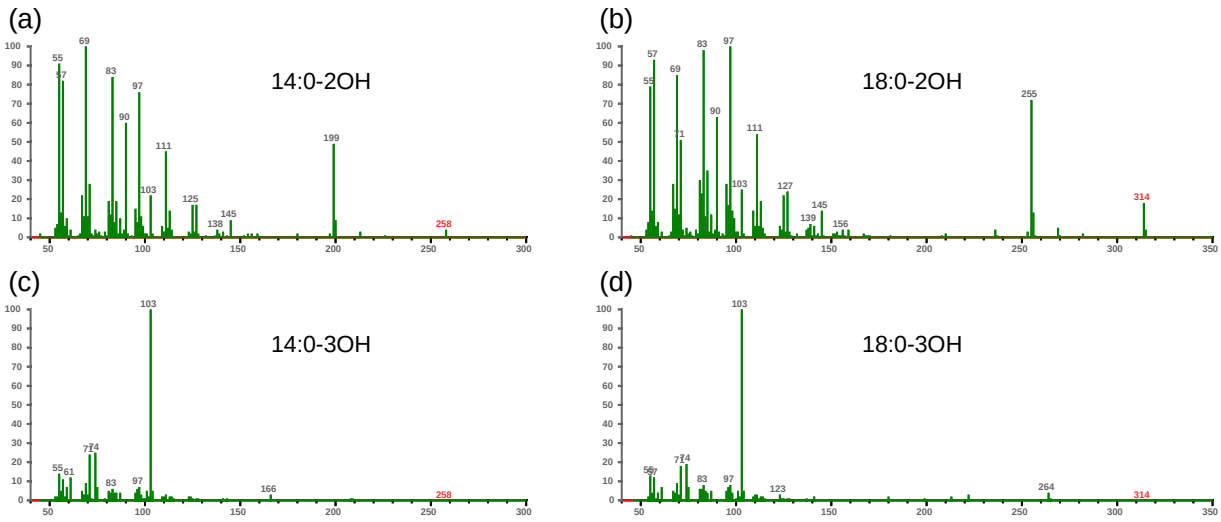

Figure 2.15. Examples of hydroxy FAME

2.2.1.8 Diesters

Figure 2.16 shows examples of dimethyl esters. Dimethyl esters typically have characteristic spectra with m/z 98 as the base peak, no visible molecular ion and relatively strong fragments of $[M-31]^+$, $[M-73]^+$ and $[M-105]^+$, but short diesters, which is shown in Figure 2.16a, may deviate from this pattern.

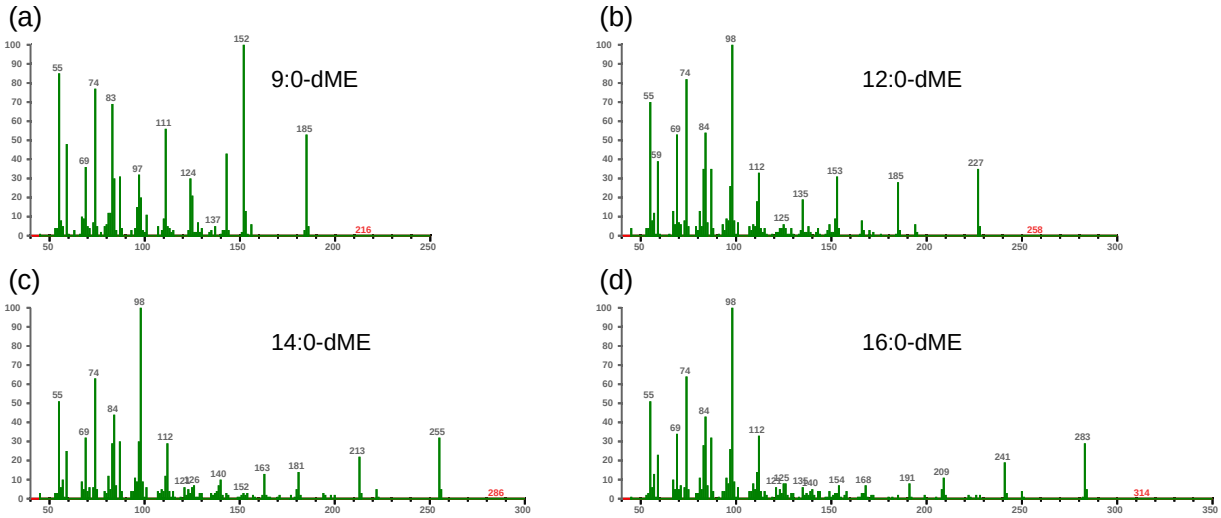

Figure 2.16. Examples of dimethyl esters

2.2.1.9 Other

Other compounds that are typically found in minor amounts in fatty acid chromatograms include branched monoenes (Figure 2.17a), unsaturated hydroxy fatty acids (Figure 2.17b), aldehydes (Figure 2.17c), furan fatty acids (Figure 2.17d), alcohols (Figure 2.17e) and dimethyl acetals (Figure 2.17f).

The furan fatty acids have very characteristic spectra, depending on the position and substitution of the furan group, and the molecular ion is usually abundant. However, in spite of being methyl esters, they have no significant McLafferty ion, and their spectra have no similarities with other FAMEs. It can therefore be difficult to recognize the spectra as furan fatty acids.

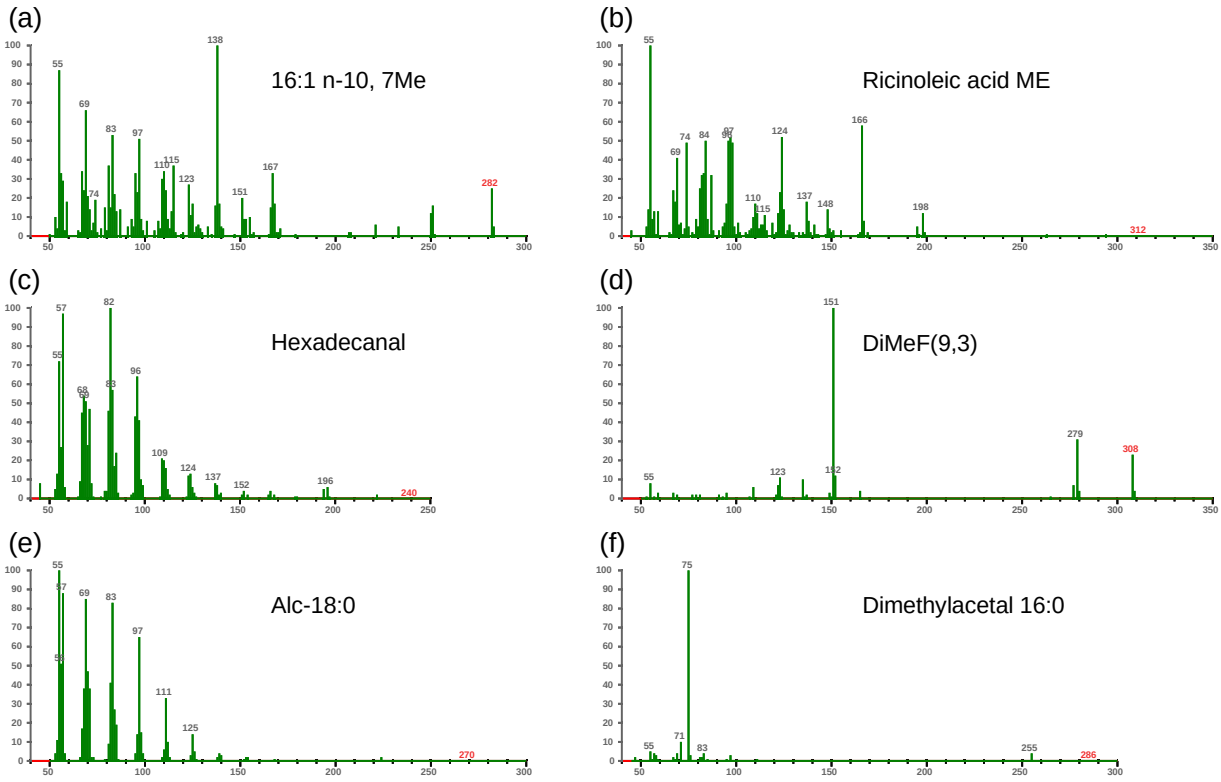

Figure 2.17. Examples of other spectra

3 Materials and methods

3.1 Studies of column properties

To study the retention patterns of FAME the reference mixture GLC793 (Nu-Chek Prep, MN, USA) was analyzed by GC-MS on 10 different capillary columns (Table 3.1). The reference mixture contain the following 28 FAMEs: 12:0, 14:0, 14:1 n-5, 15:0, 16:0, 16:1 n-7, 17:0, 17:1 n-7, 18:0, 18:1 n-9, 18:2 n-6, 18:3 n-3, 18:3 n-6, 20:0, 20:1 n-9, 20:2 n-6, 20:3 n-3, 20:3 n-6, 20:4 n-6, 20:5 n-3, 22:0, 22:1 n-9, 22:4 n-6, 22:5 n-3, 22:6 n-3, 23:0, 24:0, and 24:1 n-9. The sample had a concentration of 3.6 µg/ml of each FAME. A reference mixture of C7 to C30 n-alkanes (49451-U, Supelco/Sigma-Aldrich, St. Louis, MO, USA) was used for retention index calibration. The concentration of each compound in the calibration mixture was 2 µg/ml. Both samples were dissolved in isooctane.

A volume of 1 µl was injected spitless on the different columns, and the following temperature program was applied: injection at 60°C, hold for 2 min, 30°C/min to 80°C and 3°C/min until the last compound had eluted. There are two exceptions from the conditions given above. The rate of the first temperature ramp was 60 °C/min with the DB225 column, and the end temperature of the first ramp was 90°C for the DB5 column. Helium was used as carrier gas at a nominal velocity[58] of 30 cm/s in constant flow mode, and injector temperature was 280°C.

All columns were evaluated using the same Agilent (Santa Clara, CA, USA) 6890/5975 GC–MS system, except DB225 that was evaluated using an Agilent 7890/5977 system. The mass ranges from 45 to 570 Da was recorded with a frequency of 2.8 scans/s. MS interface, ion source and mass filter temperatures were 280°C, 230°C and 150°C, respectively. All columns were 30 m long, had an inner diameter of 0.25 mm, and stationary phase thickness of 0.20 or 0.25 µm. Columns and manufacturers are listed in Table 3.1 below.

Table 3.1. Column dimensions

Column	Manufacturer	Length [m]	Diameter [mm]	Film thickness [µm]
BP20	SGE	30	0.25	0.25
DB5	Agilent	30	0.25	0.25
DB23	Agilent	30	0.25	0.25
DB225	Agilent	30	0.25	0.25
SLB-IL61	Supelco	30	0.25	0.20
SLB-IL82	Supelco	30	0.25	0.20
SLB-IL100	Supelco	30	0.25	0.20
RTX50	Restek	30	0.25	0.25
RTX200	Restek	30	0.25	0.25
RXI1	Restek	30	0.25	0.25

3.2 Algae screening

Data of the fatty acid composition of 258 samples of alga from different strains were available from the Ph.D. project of Pia Steinrücken at Department of Biological Sciences at University of Bergen[28]. A subset of these samples to be analyzed by GC-MS was created by a procedure programmed in Matlab (www.mathworks.com) that tries to pick a subset of samples that covers the variation in the original data set. The Euclidean distance was used as measurement of difference between the samples. Only the 21 most abundant fatty acids in the data set was used, and the objects were normalised (to sum 100 %) and the variables were standardised (each variable was divided by its standard deviation) prior to the selection procedure. Further details and description of the selected samples are given in section 4.2. Principal component analysis (PCA) of the selected samples was performed in Sirius 8.1 (www.prs.no).

Sapling and further details about the original 258 samples are given in[59] and the analytical procedure for the fatty acid determination is given in[60]. The selected samples were diluted so that the largest peak should give an area of approximately 2-3 times the area in the GLC793 reference mixture.

3.3 Algae analyses by GC-MS

The selected algae samples were analyzed by GC-MS on an Agilent 7890/5977 system using four different capillary columns: BPX70 (SGE, Ringwood, Australia), BP20 (SGE), DB225 (Agilent) and HP5 (Agilent). All columns had internal diameter of 0.25 mm and stationary phase thickness of 0.25 µm. The BPX-70 column was 60 m long, while the length of the other was 30 m.

A volume of 1 µl was injected spitless on the different columns. The following temperature program was applied: Injection at 60°C, hold for 3 min, 60°C/min to *A*°C and thereafter *B*°C/min until the end temperature, *C*, where 28:0 FAME had eluted. Helium was used as carrier gas at a nominal velocity of *D* cm/s in constant flow mode. The values of the parameters *A*-*D* are given in Table 3.2. Injector temperature was 280°C and MS interface, ion source and mass filter temperatures were 300°C, 250°C and 180°C, respectively. The mass ranges from 45 to 440 Da was recorded with a frequency of 1.9 scans/s. The chromatographic parameters for BPX70 was tuned to give similar retention indices as in[46] by using the method published in[61].

Table 3.2. Chromatographic parameters.

Column	Start temp, A [°C]	Rate, B [°C/min]	End temperature, C [°C]	Carrier gas velocity, D [cm/s]
HP5	160	3	300	25.9
DB225	160	2	240	30.0
BP20	160	2	258	30.0
BPX70	165.8	1.54	240	26.0

The selected algal samples were divided into analytical sequences with 5 samples in each. In addition, each sequence contained a reference mixture with all saturated FAME from C12 to C28 (except 13:0 and 23:0) and the GLC793 and alkane reference mixtures described above. In every second sequence, the concentration of the GLC793 mixture was diluted to half. The concentrations of each compound in the saturated FAME reference mixture was approximately 1 µg/ml of each compound.

The following FAME references and reference mixtures were also analyzed once for each column:

- Bacterial Acid Methyl Ester (BAME) Mix (Supelco/Sigma-Aldrich 47080-U), approx 1 µg/ml of each compound.
- A mixture of 12:0, 14:0, 16:0, 18:0 dimethyl esters, approx 1 µg/ml of each compound.
- The methyl esters of the hydroxy fatty acids 16:0-3OH, 18:0-2OH, 18:0-12OH and ricinoleic acid, approximately 3 µg/ml of each.
- Mixtures of conjugated 18:3 FAME, approximately 1 µg/ml of each.
- Cod liver oil and two natural sample of salmon testis containing furan fatty acids, where the concentrations were scaled the same way as for the algal samples.

3.4 Data analyses in Chrombox Q

The GC-MS data were analyzed in Chrombox Q 16-05 (www.chrombox.org) using both mass spectra and retention indices for compound identification as described in [46]. Since there already existed databases of marine FAME for BP20 and BPX70 from previous works[46, 62] the identification work started with these columns, and databases of spectra and retention indices for the compounds in algae were gradually built. Spectra from the reference mixtures were used in cases where these were better than the corresponding spectra in algae (e.g. if a compound were found in algae, but with two low concentration to give good spectrum or too high concentration to give accurate retention index). The codes of three letters and three digits associated with each compound can be found at www.chrombox.org/data for compounds that have been found previously. Any compounds not present in the existing libraries and above 0.2% of the total chromatographic area (whether known or unknown) were assigned new codes in the system described in[46]. Once the algal databases for BPX70 and DB20 was finished, these databases were used to identify the same compounds on DB225 and HP5. Because the retention indexes are different on the different columns, this was basically done by comparing mass spectra and by using the reference mixtures where possible.

4 Results and discussions

4.1 The initial evaluation of the columns

The data used to calculate the effects of introducing double bonds and to make the plots in Figure 4.1 and Figure 4.2 are shown in appendices (7.1 and 7.2), respectively.

4.1.1 Effects of introducing double bonds

Figure 4.1 shows how the ECL values are affected by introducing double bonds in the FAME carbon chain. Figure 4.1a shows the effects of adding an n-9 double bond near the centre of the carbon chain. If we look to the effects on the ECL values according to the polarity of the columns, we can see that the effects on the ECL values increase by increasing the polarity of the columns. The Δ ECL are negative on RXI1, DB5 and RTX200 which have lowest polarity. The effect on RTX50 is nearly zero, which means that monounsaturated FAME will overlap with saturated FAMEs of the same chain length. On the other columns the Δ ECL are positive. It is can be noticed that the effect increases with chain length on all columns. Though, by increasing the chain length the n-9 double bond is moved further away from the carboxyl group, therefore this may not be an effect of the chain length. On the other side the increasing of Δ ECL with increasing chain length can also be caused by the change in polarity of columns with temperature. The elution temperature in temperature-programmed GC increase with the analyte chain length and it has been shown that the polarity of some stationary phases are significantly influenced by the temperature [63].

Figure 4.1b shows the effect of introducing an additional double bond in the n-6 position. The effect for RXI1 and DB5 columns, which have non-polar stationary phases, is negative. RTX200 column has effect around 0, which means that n-9 monoenes and n-6 dienes will overlap on this column. The effect for the other columns is positive and it is increasing with increasing the polarity of the columns. The effect of introducing an additional double bond in the n-6 position is stronger than the effect of introducing a single n-9 double bond. The stronger effect can be caused by homoconjugation interactions between n-9 and n-6 double bonds. However, it can also be explained by the position, which is further away from the carboxyl group.

Introduction of a double bond in n-3 position (Figure 4.1c) give stronger effects than those seen for the n-6 position, and these are positive also for the non-polar phases.

The effect of introducing double bonds near the carboxyl group in the Δ4, Δ6 and Δ5 positions shown in Figure 4.1d. The effect in Figure 4.1d are different than the effect in Figure 4.1a, Figure 4.1b and Figure 4.1c which shows fairly consistent patterns. For the three least polar columns the effects are negative, and the value of the effect is similar to introduction of a single double bond in the n-9 position shown in Figure 4.1a.

For RTX50, the effects are almost zero, which means that there will be poor resolution between the compounds that constitute the studied pairs, and possibly between similar pairs of compounds that was not in the reference mixture, such as 22:4 n-6 and 22:5 n-6. For the more polar columns there are large variations in the effects of introducing a double bond near the carboxyl group.

Despite of IL61 being a polar column, the effect of introducing an additional Δ5 double bond is almost zero, and the effect of introducing a Δ4 double bond is slightly negative. This will lead to overlap between biologically important FAME, and for this reason it has been claimed that IL61 is unsuitable for the analyses of marine FAME and for clinical studies [64]. Similarly, on IL100, the most polar column in the study, the effect of an additional Δ4 double bond is zero, which lead to overlap between 22:5 n-3 and 22:6 n-3.

To summarise, introduction of a double bond should lead to change in retention if the column should be generally suitable for fatty acid analysis. This rules out RTX50, where there is minimal effect of introducing the n-9 double bond, and RTX200, which has poor separation between n-9 monoenes and n-6 dienes. There are also issues with some of the ionic liquid phases, where the effect of introducing a double bond near the carboxyl group is low or absent. It was concluded to continue with BPX70 and BP20, for which there exist large collections of reference data (www.chrombox.org/data), and with DB225 and DB5 that can be promising alternatives to these two. DB5 was preferred over RXI1 because the 5% phenyl phase is very common in gas chromatography.

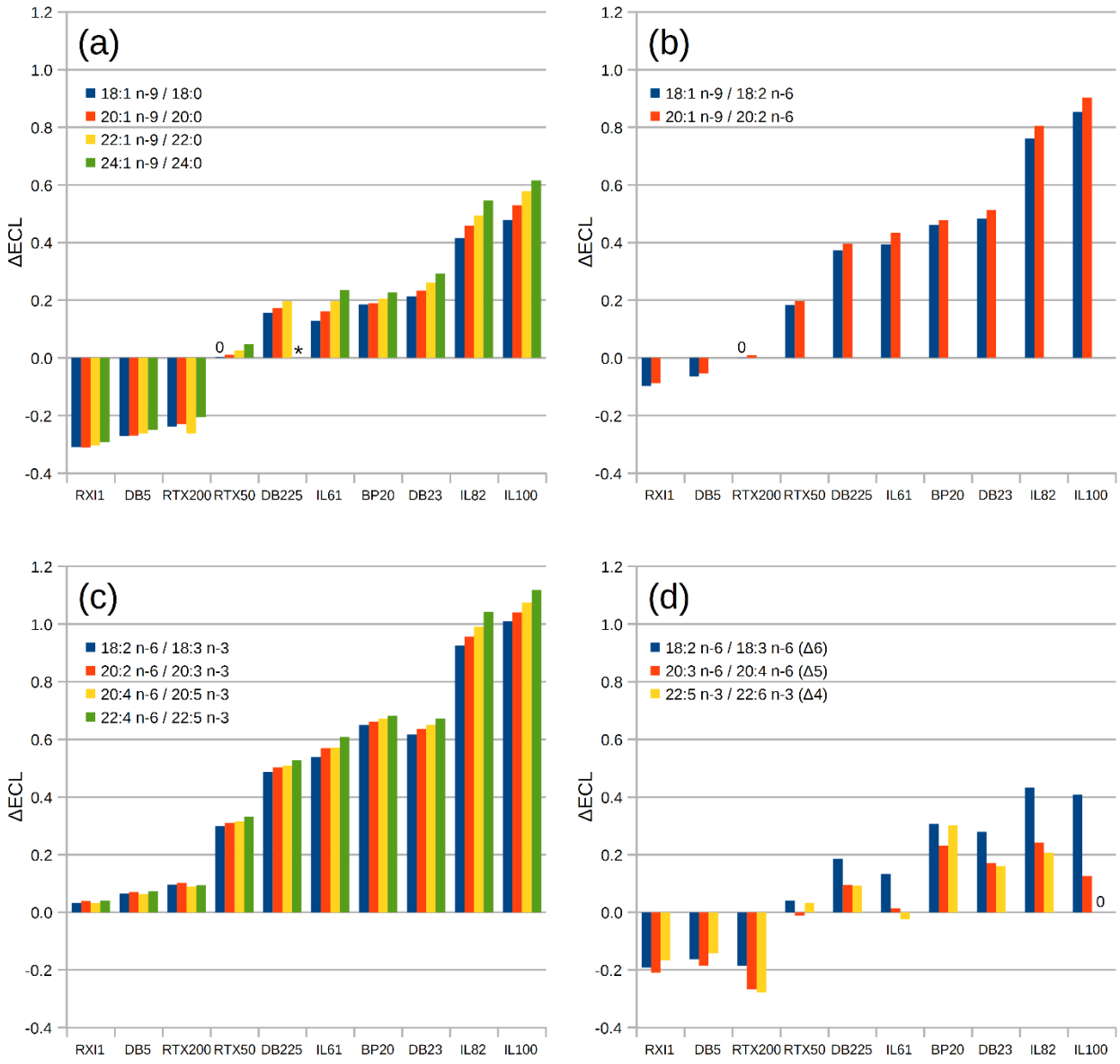

Figure 4.1. Effects on ECL values of introducing double bonds in the n-9 position (a), the n-6 position (b), the n-3 position (c) and near the carboxyl group in the Δ4 to Δ6 positions (d). The asterisk denotes a missing value because 24:1 n-9 was not eluted at the applied conditions. ΔECL was calculated by subtracting the ECL of the least unsaturated compound from the ECL of the most unsaturated compound. Asterisk means that the largest compound was not eluted. 0 means that no effect could be quantified due to complete overlap of the peaks.

4.1.2 The effects of the ester group

In addition to the double bonds, also the carboxyl group has polar interactions. The effects of the ester group can be assessed by comparing the Kovats retention index of the saturated FAMEs with the retention index of a hypothetical *n*-alkane with the same mass.

The effect of the polarity from the ester group given in Figure 4.2. Results are not shown for the most polar columns, because alkanes have very low solubility in these phases, and it was therefore impossible to get proper peak shapes for the n-alkanes.

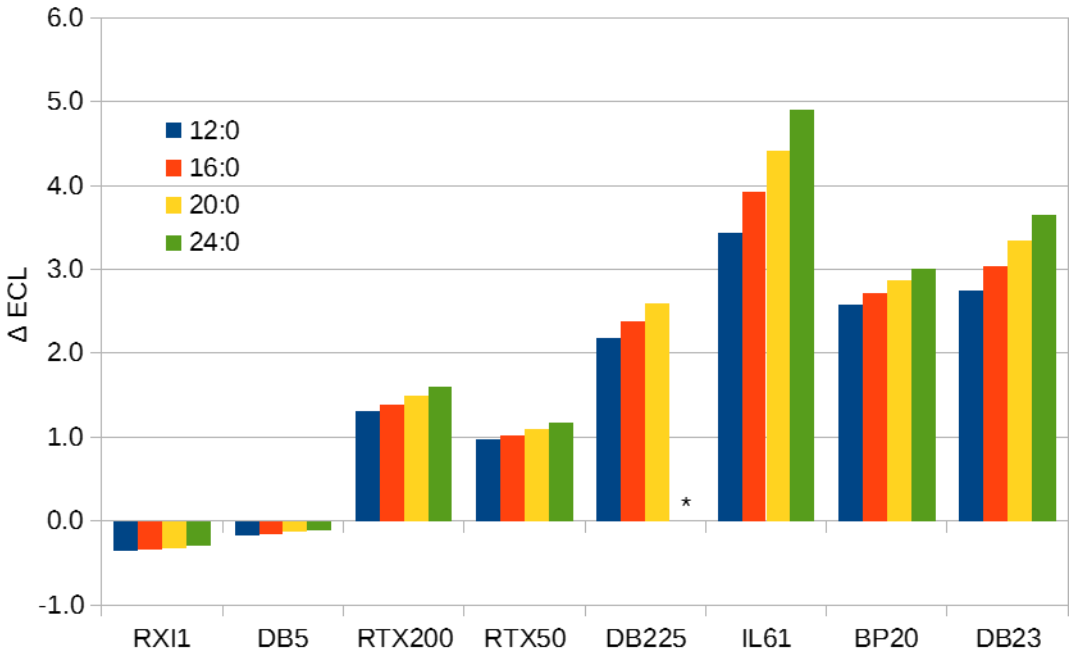

Figure 4.2. Effect of the polarity from the ester group. Asterisk means that the largest compound was not eluted.

The impact of the ester group differs from the impact of the double bonds. RXI1 and DB5 show negative impact, RTX200 has higher values than RTX50. IL61 also show much higher impact than DB225 and BP20, which had similar strength of interactions with the double bonds.

The impact of the ester group will not affect the elution patterns of normal FAMEs, because all have an ester group, but it can affect how diesters elute relative to normal FAMEs and it will affect the relationships between Kovats indexes and ECL values.

4.2 Selection of samples

Originally, 258 samples of algal FAME were available. These were already analysed quantitatively by GC-FID. To reduce the number of samples to be characterized in detail by GC-MS, representative samples that spans the variation in the data set were selected by the method described in the Materials and Methods chapter (3.2). Further details and description of the selected samples are given below.

4.2.1 Explanation of sample selection method

The sample selection method is based on Euclidean distances between the different objects (in this case samples). In two dimensions the Euclidean distance can be calculated by the Pythagorean theorem, stating that the squared distance (c^2) between the two objects p and q in Figure 4.3a is the sum of the squared distances a^2 and b^2.

The Pythagorean theorem can be extended to a higher number of dimensions (n) and the Euclidean distance, *d*, between two points, p and q, can be given as:

$$d(p,q) = \sqrt{\left(x_{1(p)} - x_{1(q)}\right)^2 + \left(x_{2(p)} - x_{2(q)}\right)^2 + \ldots + \left(x_{n(p)} - x_{n(q)}\right)^2} \qquad (9)$$

where *x* are the variables. In this case, the variables were the amounts of 21 fatty acids, meaning that the dimension of the space, *n*, was 21.

The selection algorithm applied with $n = 2$ is illustrated in Figure 4.3b. First the distances between all objects are calculated (red lines), as well as the distance between each object and the mean of all objects, illustrated by the open circle and dotted blue lines. The first object to be selected is the one with largest distance to the mean, in this case object E. The next selected object is the one with largest distance to E, which is object A. The next object to be selected is the one that is furthest away from any of the previously selected objects (has the largest minimum distance to any of the selected), which is object D. The algorithm thereafter selects B (because C is marginally closer to E than B is to A). The algorithm continues until the required number of objects have been selected.

The algorithm has not been published but has previously been applied in a work in the Ph.D. thesis of Chenchen Lin[65].

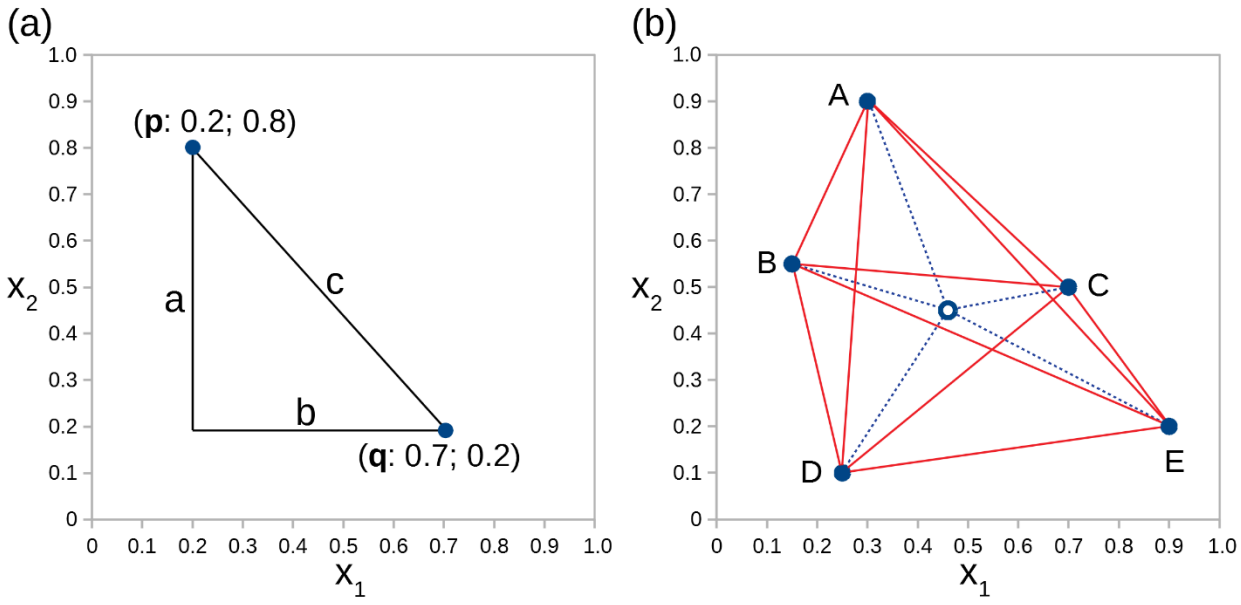

Figure 4.3. Principle of sample selection method. (a) Euclidean distance, (b) Selection of points in two-dimensional space.

4.2.2 Selected samples

The 30 first samples suggested by the algorithm are shown in Table 4.1, column B, where the first row gives the sample that was most different from the mean. Because of limited sample amounts, some of the suggested samples were replaced by other samples of the same algal strain. It was also decided to include both exponential and stationary phase of the suggested strains. Therefore, there are two selected samples for each strain (columns G and H). Finally, the selected samples were given new codes to be used in this work, where odd-numbered codes represent exponential phase and even-numbered codes represent stationary phase (columns H and I). In total 38 samples were selected (both phases of 19 strains).

Both exponential and stationary phase were suggested for some of the strains. In these cases, column E points to the row of the first selection for the strain. However, no combination of strain and phase were repeated among the 30 first selections. There is one suggested sample (PS0023, row 12) that is not selected. This was in an unknown growth phase. The strain was M18, which was selected in row 20.

PCA scores and loading plots of suggested and selected samples are shown in Figure 4.4a and b, respectively. Red dots mark the suggested samples from the algorithm and green circles mark the selected samples. Ideally, each red dot should be in a green circle either because the selected

sample was the same as the suggested, or because the suggested and selected sample are highly similar. In general, the suggested samples in the extremes seems to be well covered by the selected samples, but there are a few near the center of the plot that has relatively large distance to the nearest selected.

It should be noted that the two first principal components only explain 41% of the variance in the data set (24% + 17%), which means it will not show a detailed picture of the difference between the samples. The two first suggested samples, PS0036 and PS0037, are for instance quite close in the score plot because the difference between them are poorly explained by the two first principal components.

The score and loading plots give some indication of the main differences in the data set. In the loading plots typical marine FAME such as the omega-3 PUFA 20:5 n-3 (EPA), 22:6 n-3 (DHA) and 20:4 n-3 are found to in the upper right quadrant, meaning that samples in this direction in the score plot tend to have high amounts of these, and samples in the opposite direction tend to have low amounts. All the samples having a score along PC1 below -4 belong to the kingdom *Plantae* (that terrestrial plants also belong to), while all samples to the right of this limit belong to the kingdom *Chromalveolata*. So PC1 separates the two kingdoms. In general, organisms belonging to *Plantae* do not produce long-chain omega-3, which is why these are not found in terrestrial plants. All of these samples lacked 22:6 n-3, 20:5 n-3 20:4 n-3 and the C16 PUFA 16:3 n-4 and 16:4 n-1. It is worth noting that in addition to being different from the *Chromalveolata* the samples belonging to *Plantae* were also very different from each other. Three of the four most extreme samples (PS0036, PS0037 and PS0127) belonged to the *Plantae* kingdom.

It is more difficult to see a clear trend explained by PC2, but PS0033 (Figure 4.5e), which has the lowest value along PC2 is relatively rich in n-6 PUFA (18:3 n-6 and 20:4 n-6), which are absent or in very low amounts in most samples. It also has low amounts of C18 and C20 fatty acids, except the highly unsaturated.

Table 4.1. Overview of the samples suggested by the algorithm and the samples selected for this project

A	B	C	D	E	F	G	H	I
Order[a]	**Code**	**Strain**	**Phase[b]**	**Repr. by**	**Selected E[b]**	**Selected S[b]**	**RA Code E**	**RA Code S**
1	PS0036	M4	E		PS0210	PS0264	RA01	RA02
2	PS0037	M19	E		PS0213	PS0246	RA03	RA04
3	PS0152	FITO-1	S		PS0133	PS0139	RA07	RA08
4	PS0127	FITO-2	E		PS0127	PS0145	RA05	RA06
5	PS0033	M25	E		PS0204	PS0261	RA19	RA20
6	PS0159	CCAP	E		PS0157	PS0163	RA27	RA28
7	PS0145	FITO-2	S	Row 4				
8	PS0194	M7	S		PS0186	PS0192	RA29	RA30
9	PSF104	FITO-3	LS		PS0102	PS0113	RA25	RA26
10	PS0044	M58	E		PS0231	PS0252	RA13	RA14
11	PS0122	FITO-4	S		PS0109	PS0121	RA09	RA10
12	PS0023	M18	U					
13	PS0047	M27	S		PS0201	PS0240	RA31	RA32
14	PS0264	M4	S	Row 1				
15	PSF078	M21	E		PS0171	PS0174	RA11	RA12
16	PS0260	M20	S		PS0216	PS0258	RA17	RA18
17	PS0025	M25	S	Row 5				
18	PS0297	FITO-3	U	Row 11				
19	PS0063	M46	S		PS0228	PS0276	RA33	RA34
20	PS0209	M18	E		PS0207	PS0243	RA15	RA16
21	PS0051	M19	S	Row 2				
22	PS0232	M58	E	Row 10				
23	PS0178	M28	E		PS0177	PS0195	RA21	RA22
24	PS0263	M20	S	Row 16				
25	PS0198	M29	S		PS0180	PS0198	RA35	RA36
26	PS0286	M21	S	Row 15				
27	PS0237	M65	E		PS0237	PS0249	RA37	RA38
28	PS0106	B58	E		PS0105	PS0117	RA23	RA24
29	PS0139	FITO-1	S	Row 3				
30	PS0201	M27	E	Row 13				

a) The order of the sample as selected by the algorithm

b) E denotes exponential phase, S denotes stationary phase, LS is late stationary phase and U is unknown

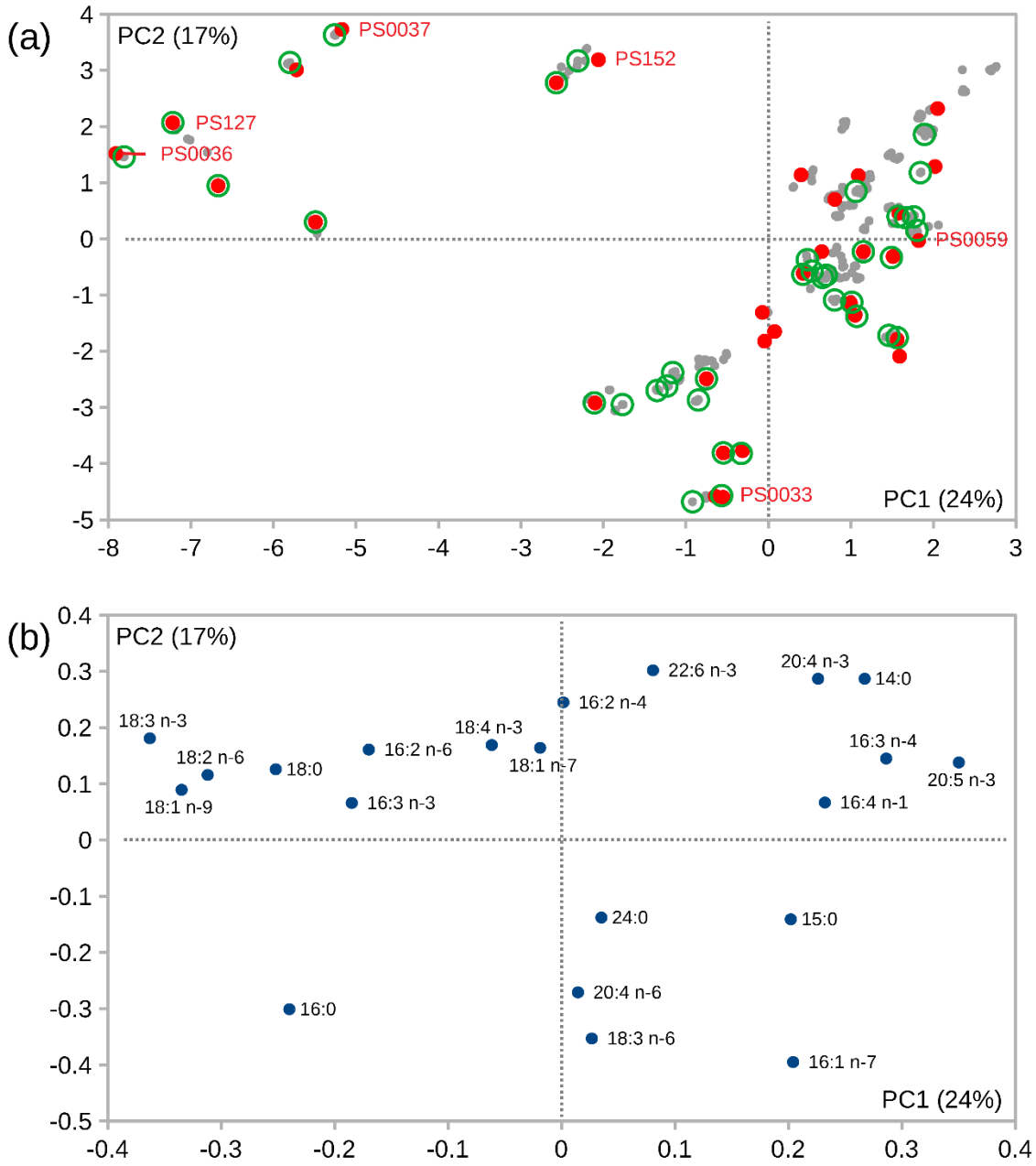

Figure 4.4. PCA scores (a) and loadings (b) of the dataset used for sample selection. Red dots mark the suggested samples from the algorithm. Green circles mark the selected samples. Other samples are shown in grey. The six most different samples are labeled and their chromatograms are shown in Figure 4.5.

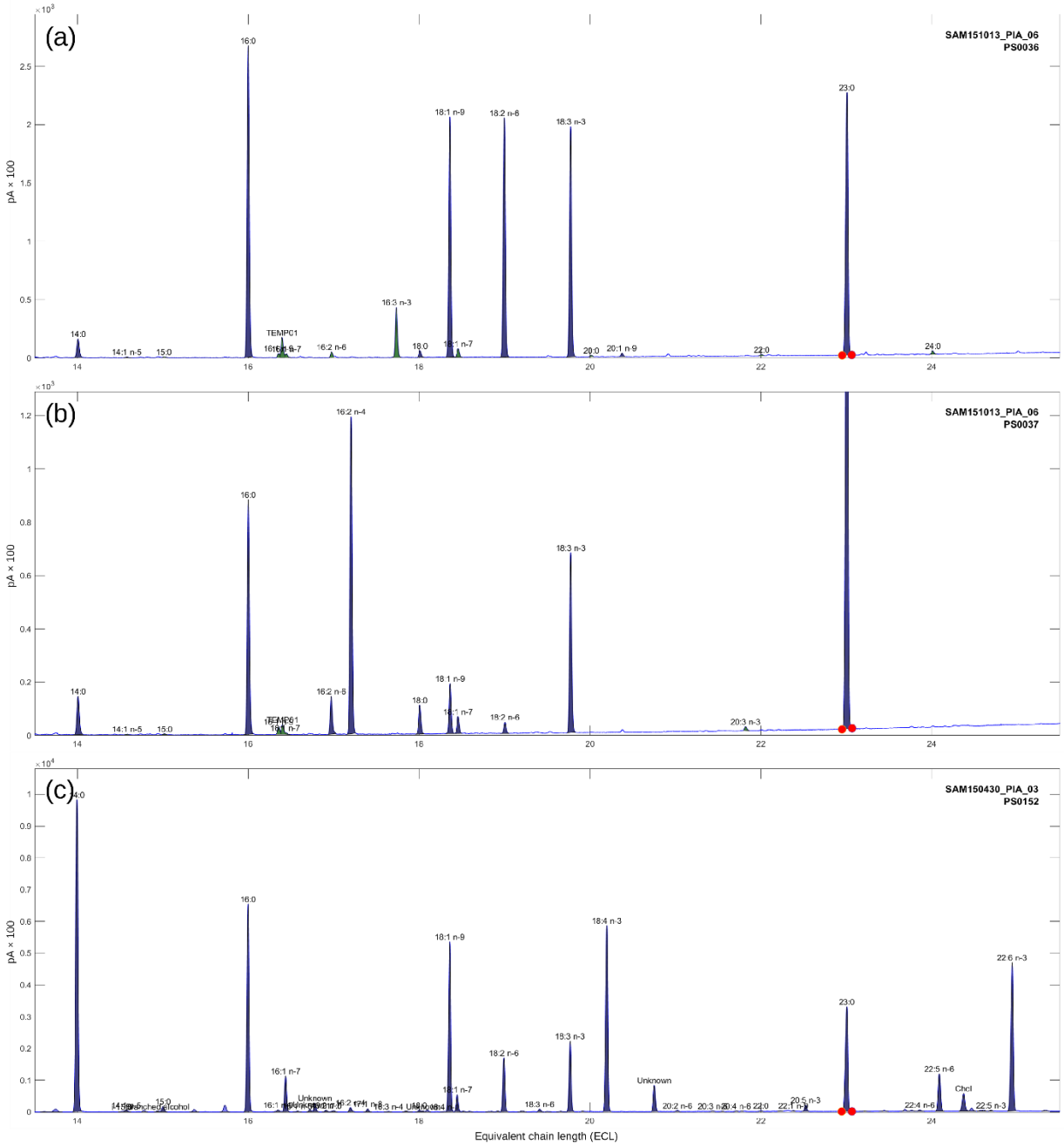

Figure 4.5. GC-FID chromatograms of the six most different samples from the sample selection. Red dots mark 23:0, which is internal standard and not considered in the selection analysis.

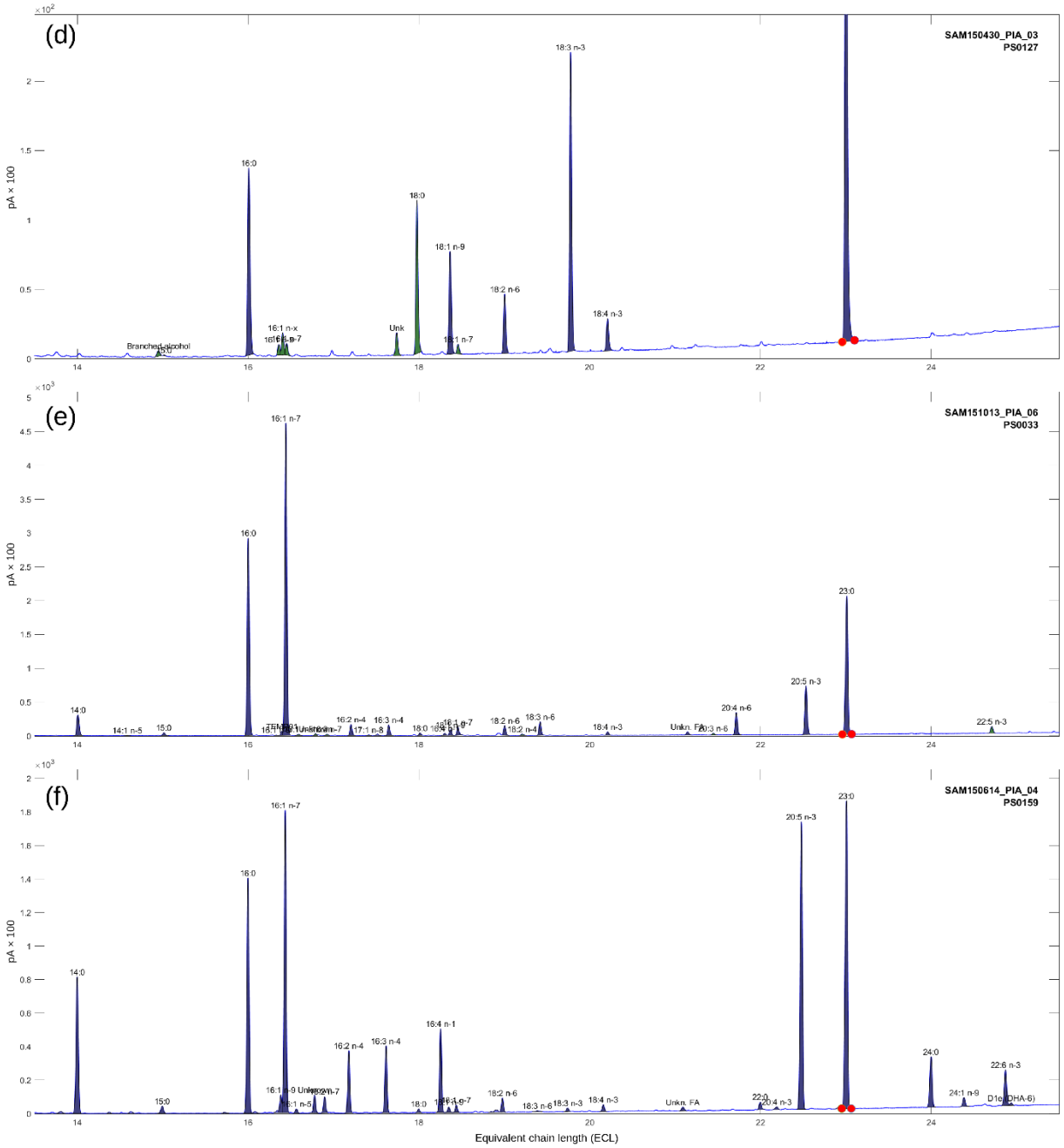

*Figure 4.*5 *continued.*

4.2.3 Overview of selected samples

An overview of the selected samples is given below. Algae are generally classified by species, class phylum and kingdom. However, the classification of algae is not static. As more information become available, classification may change. The classification used below are according to www.algaebase.org by april 2019.

RA01/RA02, Strain: M4

Identified as probably *Micractinium sp.* Belongs to the class *Trebouxiophyceae* (kingdom *Plantae*, Phylum *Chlorophyta*). Isolated from Puddefjorden in March 2014 (N 60° 22.86558′ E 05° 19.52838′)[59].

RA03/RA04, Strain: M19

Could not be identified by molecular methods. Recognized as belonging to the *Chlorophyta* phylum (*Plantae* kingdom) by microscopic examination. Isolated from Raunefjorden in August 2014 (N 60° 16.265′ E 05° 11.456′)[59].

RA05/RA06, Strain: FITO-2

Commercial strain of *Scenedesmus obliquus* (currently regarded as a synonym of *Tetradesmus obliquus*). Belongs to the class *Chlorophyceae* (kingdom *Plantae*, Phylum *Chlorophyta*). Obtained from Fitoplancton marino (Cádiz, Spain). This is a Freshwater species.

RA07/RA08, Strain: FITO-1

Commercial strain of *Isochrysis galbana* (now reassigned to *Tisochrysis lutea*) obtained from Fitoplancton marino. Belongs to the class Coccolithophyceae (phylum *Haptophyta*, kingdom *Chromista*.

RA09/RA10, Strain: FITO-4

Commercial strain of *Nannochloropsis gaditana* (currently regarded as a synonym of *Microchloropsis gaditana*) obtained from Fitoplancton marino. Belongs to the class Eustigmatophyceae (phylum *Ochrophyta*, kingdom *Chromista*).

RA11/RA12, Strain: M21

Identified as *Attheya septentrionalis*. Belongs to the class Mediophyceae (phylum Bacillariophyta, kingdom Chromista). Isolated from the Arctic in May 2014 (N 79° 25.14′ E 08° 18.84′) [59].

RA13/RA14, Strain: M58

Identified as *Thalassiosira hispida*. Belongs to the class *Mediophyceae* (phylum *Bacillariophyta*, kingdom *Chromista*). Isolated from the Arctic in November 2014 (N 78° 59.66′ E 10° 00.17′) [59].

RA15/RA16, Strain: M18

Identified as *Nitzschia laevis*. Belongs to the class *Bacillariophyceae* (phylum *Bacillariophyta*, kingdom *Chromista*). Isolated from Raunefjorden in August 2014 (N 60° 16.265′ E 05° 11.456′) [59].

RA17/RA18, Strain: M20

Identified as *Arcocellulus cornucervis*. Belongs to the class *Mediophyceae* (phylum *Bacillariophyta*, kingdom *Chromista*). Isolated from Raunefjorden in August 2014 (N 60° 16.265′ E 05° 11.456′) [59].

RA19/RA20, Strain: M25

Identified as *Nanofrustulum shiloi*. Belongs to the class *Bacillariophyceae* (phylum *Bacillariophyta*, kingdom *Chromista*). Isolated from Sognefjorden in August 2012 (N 61° 02.467′ E 05° 24.962′) [59].

RA21/RA22, Strain: M28

Identified as *Phaeodactylum tricornutum.* Belongs to the class *Bacillariophyta classis incertae sedis* (phylum *Bacillariophyta*, kingdom *Chromista*). Isolated from Puddefjorden in March 2014 (N 60° 22.86558′ E 05° 19.52838′) [59].

RA23/RA24, Strain: B58

Identified as *Phaeodactylum tricornutum.* Belongs to the class *Bacillariophyta classis incertae sedis* (phylum *Bacillariophyta*, kingdom *Chromista*). Isolated from Puddefjorden in 1997 [66].

RA25/RA26, Strain: FITO-3

Commercial strain of *Phaeodactylum tricronutum* obtained from Fitoplancton Marino. Belongs to the class *Bacillariophyta classis incertae sedis* (phylum *Bacillariophyta*, kingdom *Chromista*).

RA27/RA28, Strain: CCAP

*Phaeodactylum tricronutum s*train CCAP 1052/1A, obtained from the Culture Collection of Algae and Protozoa in Oban, UK. Belongs to the class *Bacillariophyta classis incertae sedis* (phylum *Bacillariophyta*, kingdom *Chromista*). The experiment wwith this strain is described in [60].

RA29/RA30, Strain: M7

Identified as *Thalassiosira hispida.* Belongs to the class *Mediophyceae* (phylum *Bacillariophyta*, kingdom *Chromista*). Isolated from the Arctic in August 2014 (N 80° 39.72′ E 15° 26.55′) [59].

RA31/RA32, Strain: M27

Unknown species identified as belonging to the phylum Bacillariophyta and kingdom Chromista. Isolated from Store Lungegårdsvann in August 2014 (N 60° 22.93733′ E 05° 20.17962′) [59].

RA33/RA34, Strain: M46

Identified as *Thalassiosira hispida.* Belongs to the class *Mediophyceae* (phylum *Bacillariophyta*, kingdom *Chromista*). Isolated from the Arctic in November 2014 (N 78° 59.66′ E 10° 00.17′) [59].

RA35/RA36, Strain: M29

Identified as *Phaeodactylum tricornutum* Belongs to the class *Bacillariophyta classis incertae sedis* (phylum *Bacillariophyta*, kingdom *Chromista*). Isolated from Puddefjorden in March 2014 (N 60° 22.86558′ E 05° 19.52838′) [59].

RA37/RA38, Strain: M65

Identified as *Thalassiosira hispida.* Belongs to the class *Mediophyceae* (phylum *Bacillariophyta*, kingdom *Chromista*). Isolated from the Arctic in November 2014 (N 78° 59.66′ E 10° 00.17′) [59].

4.3 Identification by retention indices

Chrombox Q uses mass spectra and retention indices for identification, but it does not take benefit of the information that can be found by combining retention indices from several columns. Because of that, the FAMEs are analyzed on four different columns. There are several methods to combine the information from the different columns. The simplest method is to plot the ECLs from different columns against each other in simple two-dimensional scatter plots. As a result of this, a data set consisting of standards and fatty acids with quite certain identities were utilized. The selection of compounds is given in Appendix 7.4 and spans chain lengths from C12 to C24 and cover the range of typical polarities of FAME by including hydroxy FAMEs and a multibranched saturated FAME (phytanic acid). It also includes furan fatty acids, diesters and PUFA with conjugated double bonds.

With four columns there are six possible combinations of two. The scatter plots are shown in Figure 4.6, where the most polar column is always plotted at the y-axis. Due to high correlation, it is difficult to see any clear groupings that are of diagnostic value. The information that can read from the plot is that BP20 and DB225 are the two most similar columns (highest correlation) and that BPX70 and HP5 are most dissimilar (lowest correlation).

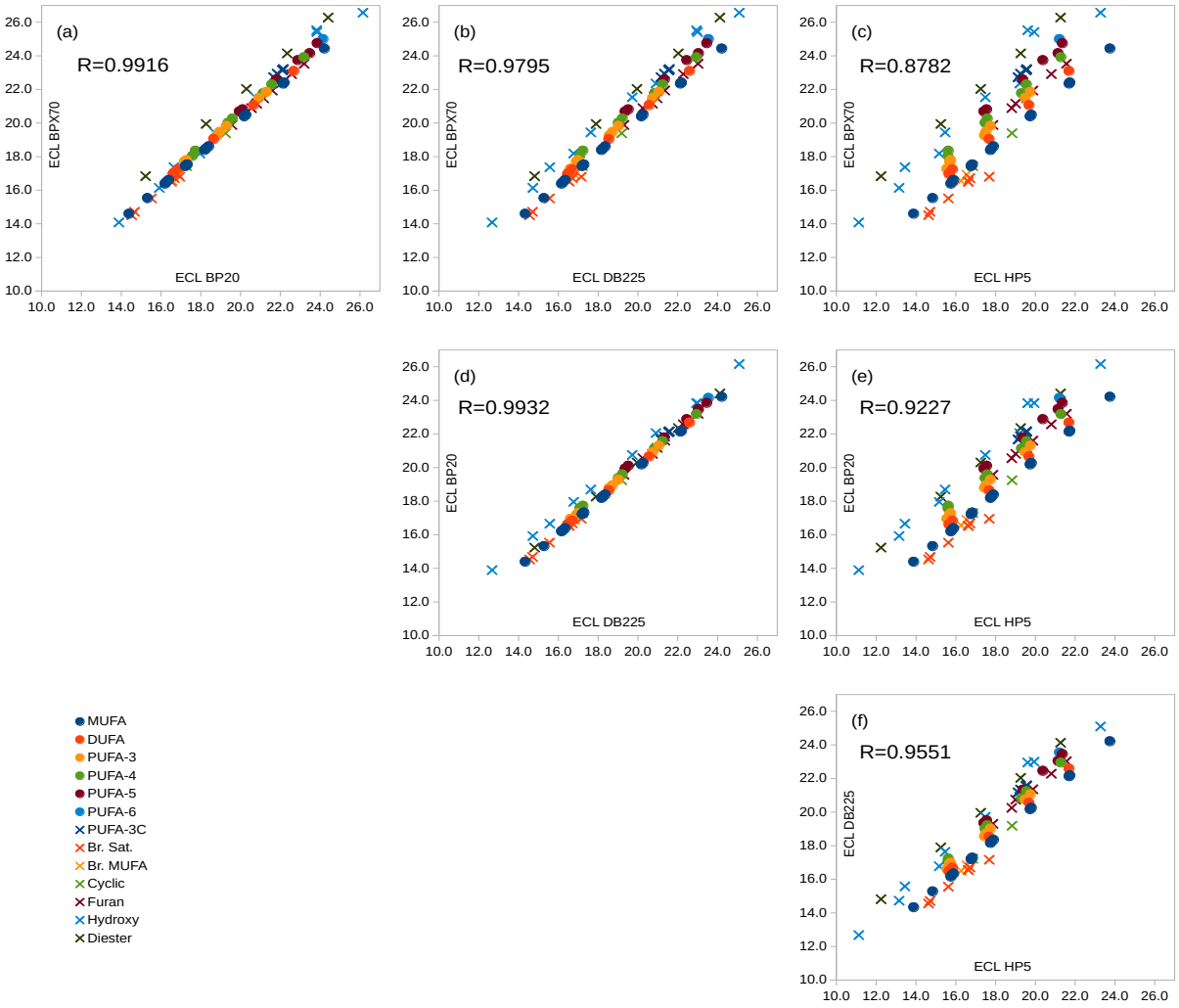

Figure 4.6. Scatter plots of ECL on the different columns

4.3.1 Difference plots

Better diagnostic plots could be accomplished by plotting the difference between the two columns on the y-axis (Figure 4.7). In these cases, the x-axis explains chain lengths and there are clear bands associated to double bonds and functional groups along the y-axis. Although all plots show similar patterns, the clearest grouping according to the structures seems to be in Figure 4.7c, where BP20 and DB5 is combined. It was decided to use this plot further for identification of unknowns.

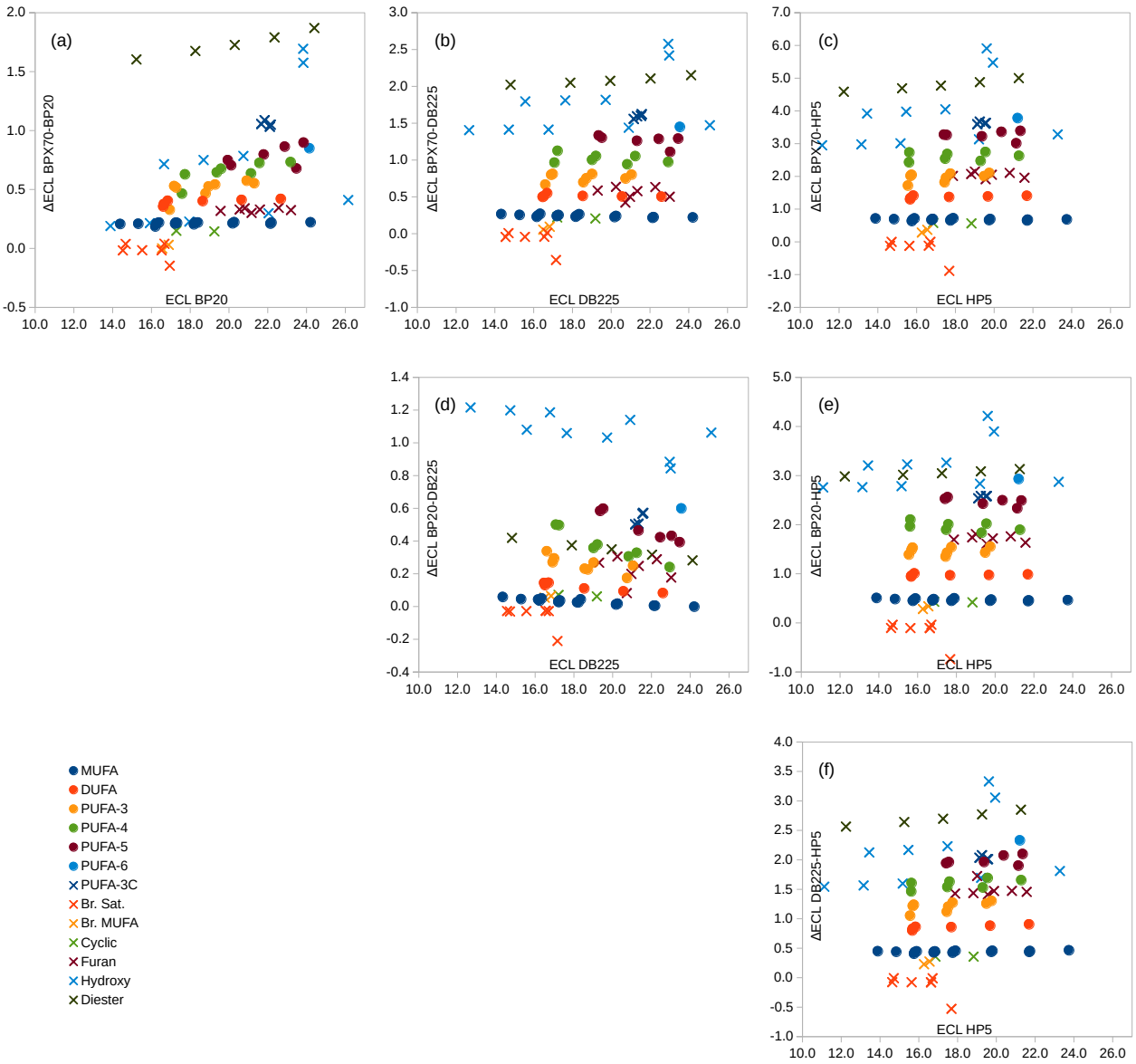

Figure 4.7. Scatter plots with the difference in ECL between two columns on the y-axis and the ECL-values for the least polar column on the y-axis

4.3.2 Difference-difference plots

By using differences on both axes, the information from more than two columns could be included (e.g. A-B on x-axis and C-D on y-axis). However, there is a large number of combinations of such differences, and it was therefore decided to use the combination that gives the lowest correlation between the two axes. A matrix of correlation plots are given in Figure 4.8, where it can be seen that the lowest correlation (R=0.43) was achieved with the ECL for

DB225 subtracted from the ECL of BP20 on the x-axis, and the ECL of BP20 subtracted from the ECL of BPX70 on the y-axis. In this plot BP20 is used on both axes, and HP5 is not applied.

The plot shows 4 groups that are clearly separated from the main group of FAME. Additional details are shown in Figure 4.9, which show that three of these groups are hydroxy FAME, while the last is diesters. Although BP20 and DB225 are the most similar columns, it can be seen that the difference between the two (x-axis) is critical for separating the hydroxy FAME from the main group. Diesters and conjugated trienes are separated from the main group by the y-axis (BPX70-BP20).

Further details for each group of FAME are shown in Figure 4.10 and Figure 4.11. In Figure 4.10a the normal MUFA are plotted together with cyclopropan FAME and branched MUFA. The plot clearly separates the cyclopropanes from the MUFA (which cannot be done by MS). A closer look at the normal MUFA (Figure 4.10b) reveals patterns related to double bond position and chain length. Similar patterns can be seen for dienes (Figure 4.10c) and PUFA (Figure 4.10d-f). In the plots of PUFA it can be seen that FAME with the first double bond close to the carboxyl group (16:3 n-6 and 16:4 n-3) are outliers.

Conjugated linolenic acids are separated in four groups (Figure 4.11a). The different CLnA isomers are not completely identified, but the groups may be related to the total number of trans double bonds (0, 1, 2, and 3) that are possible. In each group there are two positional isomers.

The hydroxy fatty acids are clearly separated according to the position of the OH-group (Figure 4.11b). Within each group the compounds are distributed according to chain length. It is worth noting that the position of the OH-group is much more important than the presence of a double bond, which is the difference between 18:0-12OH and Ricinoleic acid.

Diesters are distributed according to the chain length. For the furan fatty acids (Figure 4.11d) there is a tendency to distribution according to the chain length of the acid (first number in the bracket) and the propyl/pentyl substituent (last number in the bracket). Iso and ante-iso branched FAME are clearly separated in Figure 4.11e, and phytanic acid methyl ester is far from these.

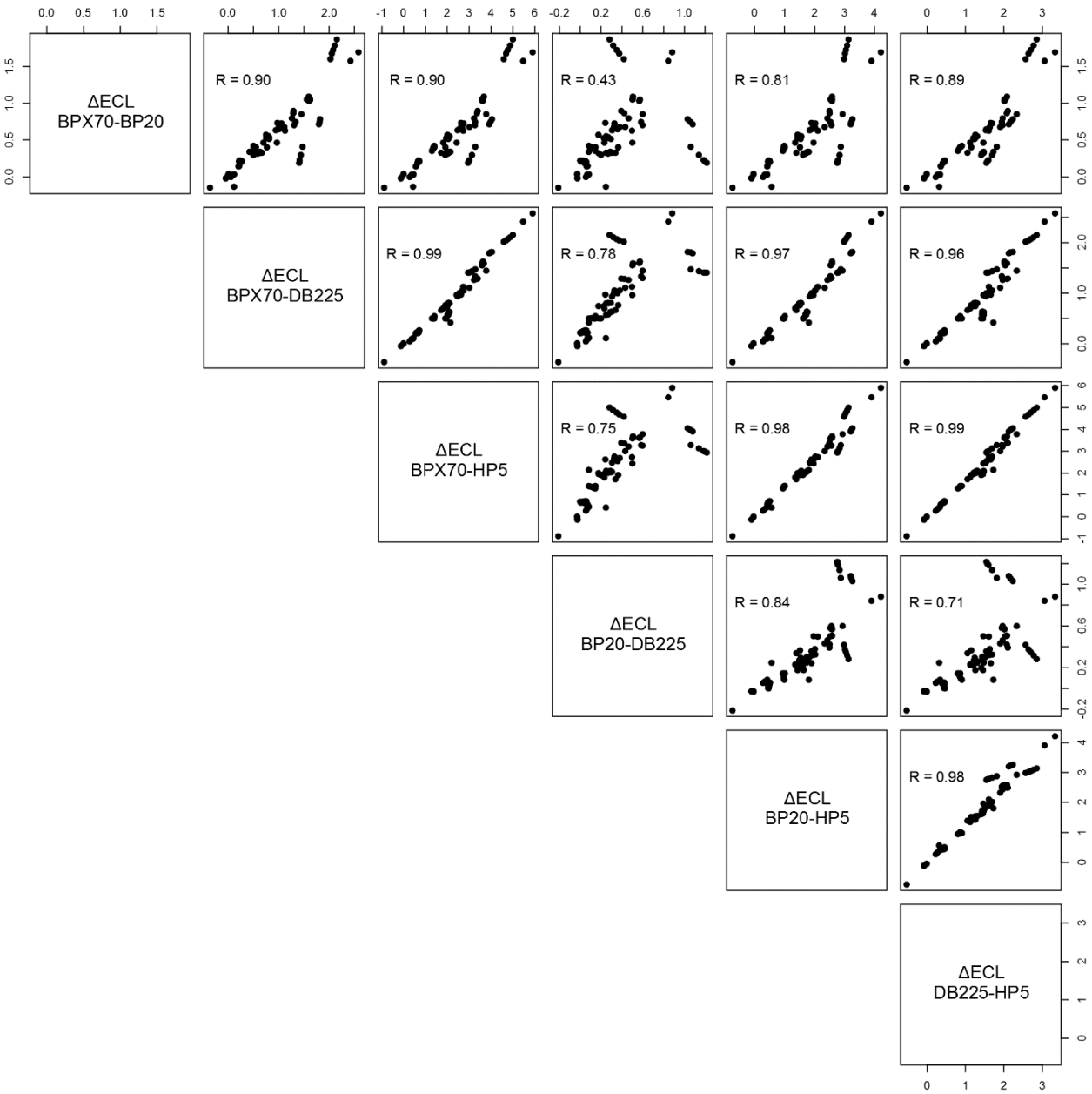

Figure 4.8. Matrix of correlation plots for the ECL differences

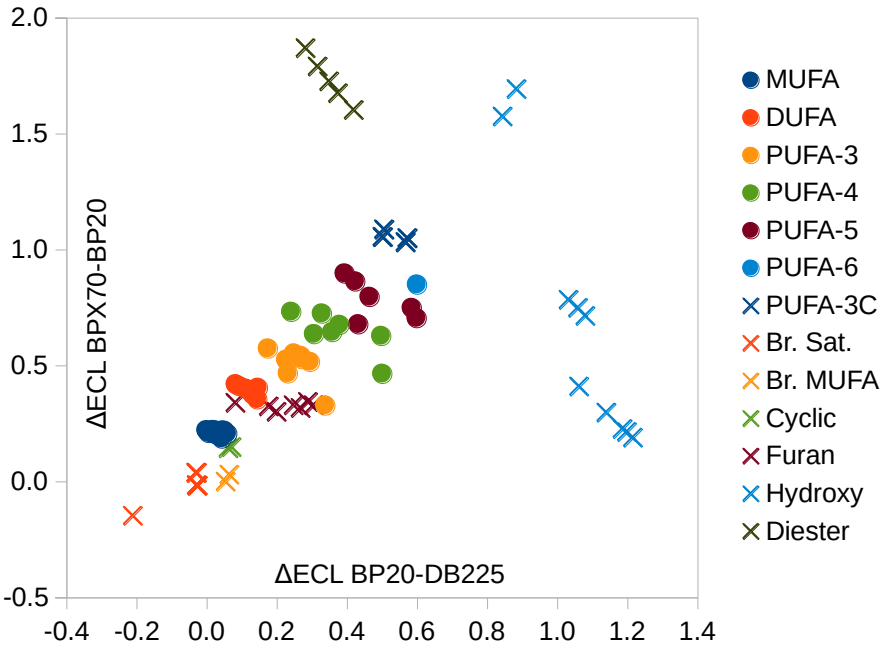

Figure 4.9. Plot of ECL differences. ECL for DB225 subtracted from the ECL of BP20 on the x-axis, and the ECL of BP20 subtracted from the ECL of BPX70 on the y-axis

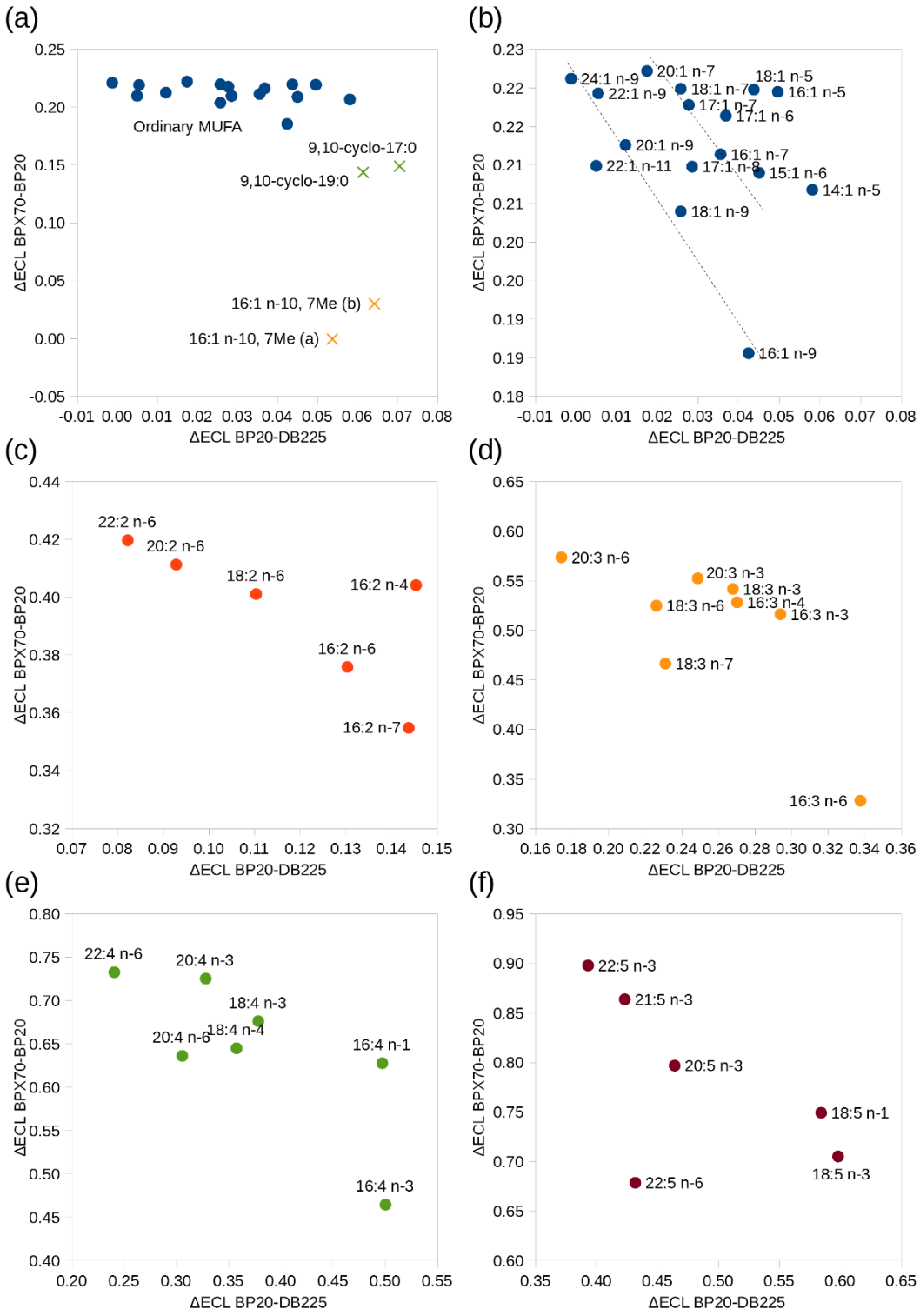

Figure 4.10. Plot of ECL differences. ECL for DB225 subtracted from the ECL of BP20 on the x-axis, and the ECL of BP20 subtracted from the ECL of BPX70 on the y-axis, normal FAME and cyclopropane FAME

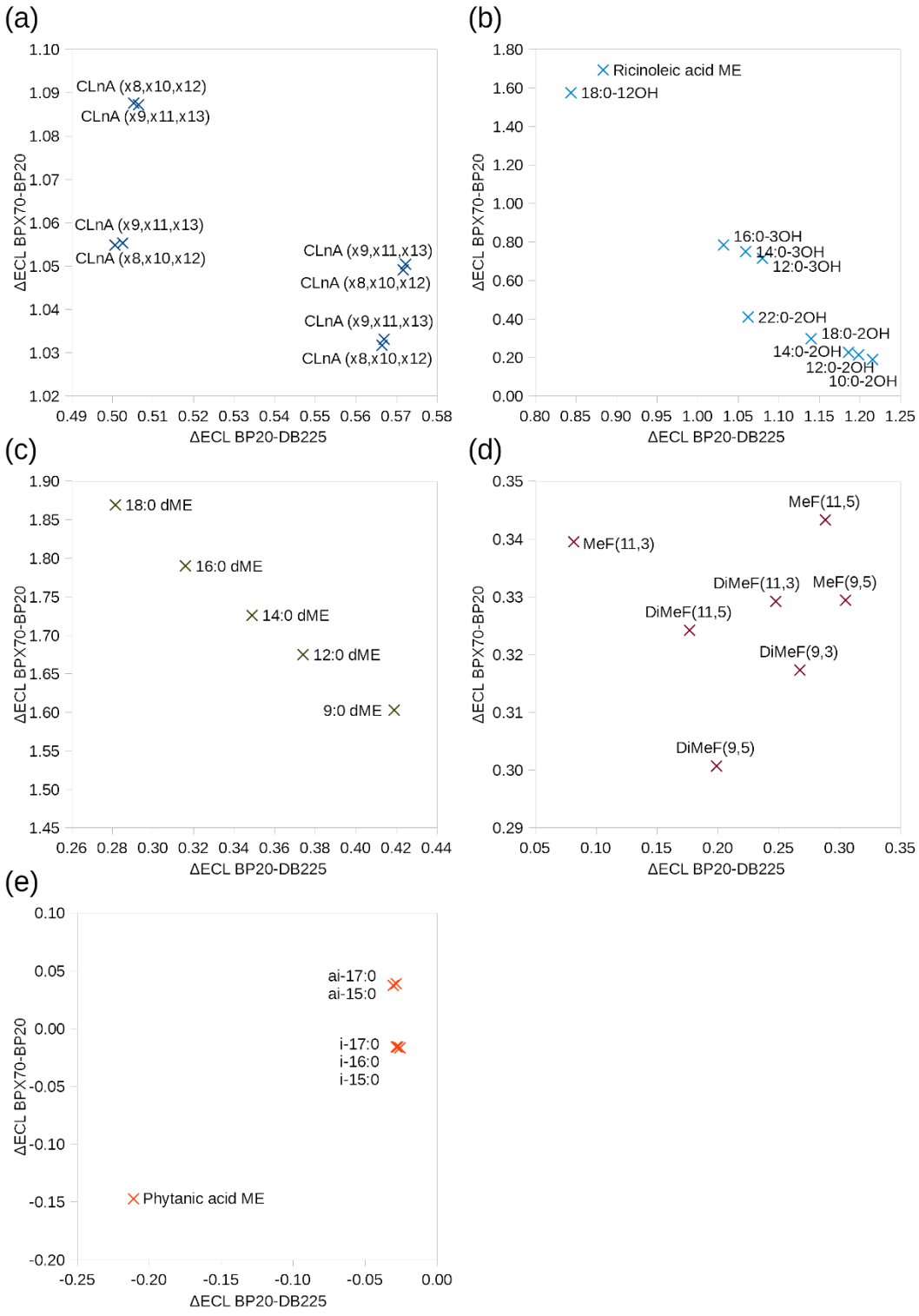

Figure 4.11. Plot of ECL differences. ECL for DB225 subtracted from the ECL of BP20 on the x-axis, and the ECL of BP20 subtracted from the ECL of BPX70 on the y-axis, conjugated, hydroxy, branched and furan FAME and dimethylesters.

4.4 The identification of the compounds

4.4.1 Methodology

The ECL maximal area percent of each compound that was found, and ECL values on the four columns BPX70, BP20, DB225 and HP5, are listed in appendix 7.3. Based on the results from Section 4.3 it was decided to base identifications on the two plots shown in Figure 4.7 (ECL on HP5 against ΔECL between BP20 and HP5) and Figure 4.9 (ΔECL between BPX70 and BP20 against ΔECL between BP20 and DB225). These two "ECL maps" together with the mass spectrum forms an identification sheet. An example of an identification sheet for a compound assumed to be 16:3 n-4 is given in Figure 4.12. It can be seen that the ECL values marked by the blue cross lie in the regions of triunsaturated PUFA in both plots. In the first ECL plot (ECL on HP5 against ΔECL between BP20 and HP5) thee is also a distribution by chain length by ECL on HP5, and the compounds group with the other C16 FAME.

In the mass spectrum the molecular ion (m/z 164), the alpha ion (m/z 194) and the omega ion (m/z 122) is visible. Identification sheets for other compounds are given in Appendix 7.5. Identification sheets were prepared for compounds shown with bold text in appendix 7.3, and focus will be on these compounds, that had identifications that needed to be confirmed, partial identifications , or that were completely unknown.

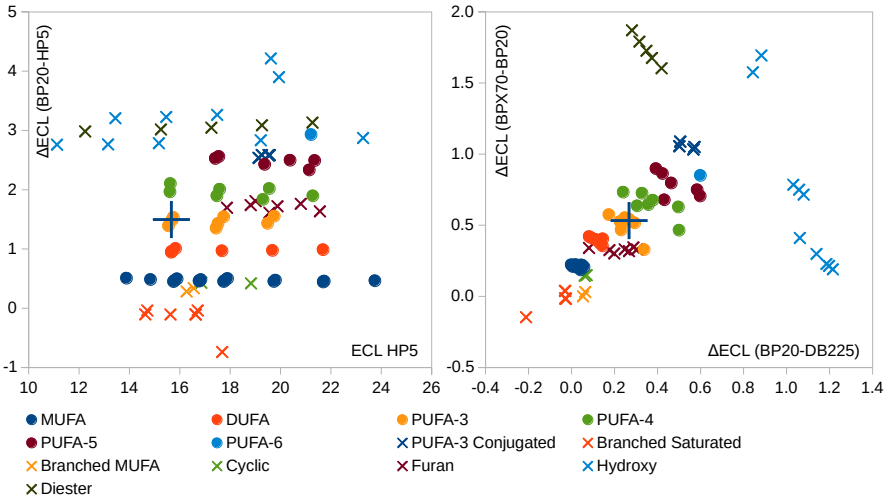

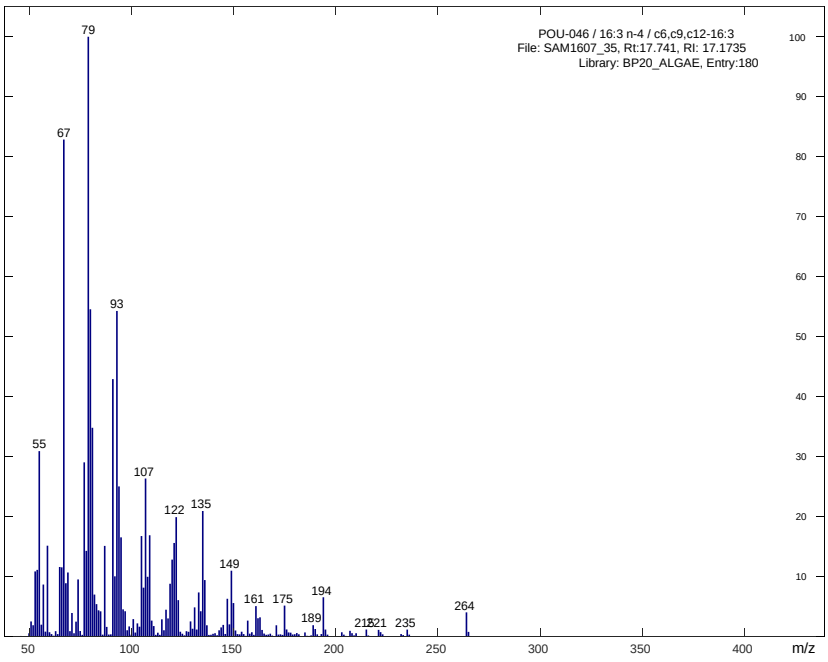

Figure 4.12. An example of identification sheet for the compound POU-046, assumed to be 16:3 n-4.

4.4.2 Overview

Table 4.2 gives an overview of the compounds that was worked with regarding identification. The other compounds listed in section 7.3 are available as standards or so common that their identities can be regarded as quite certain. In the table the compounds are listed alphabetically by the code, a reference to the identification sheet and the section with further information is given. The status before and after the identification work is also given.

Table 4.2. Overview of unknowns and tentatively identified compounds, sorted by Chrombox code.

Code	Short name	Max %[a]	Sheet[b]	Section[c]	Status B[d]	Status A[e]
ALK-752	Unknown	0.22	7.5.48	4.4.11.1	U	N, PI
DIU-779	16:2 conj	0.83	7.5.18	4.4.9.1	TD	F, PI
MOU-297	16:1 n-x	1.35	7.5.12	4.4.8.1	TM	F, PI
MOU-571	24:1 n-x	0.46	7.5.24	4.4.8.3	TM	F, PI
MOU-769	22:1 n-x	0.77	7.5.19	4.4.8.2	TM	F, PI
MOU-770	24:1 n-x	0.40	7.5.29	4.4.8.3	TM	F, PI
MOU-795	26:1 n-x	1.42	7.5.11	4.4.8.4	TM	F, PI
MOU-807	27:1 n-x	0.25	7.5.49	4.4.8.5	TM	F, PI
POU-046	16:3 n-4	4.76	7.5.4	4.4.5.1	TP	F, I
POU-049	16:3 n-3	3.12	7.5.5	4.4.3.1	TP	F, I
POU-051	16:4 n-3	7.67	7.5.2	4.4.3.2	TP	F, I
POU-052	16:4 n-1	5.93	7.5.3	4.4.6.1	TP	F, I
POU-054	20:4 n-3	0.86	7.5.17	4.4.3.4	TP	F, I
POU-059	18:4 n-4	1.77	7.5.9	4.4.5.2	TP	F, I
POU-066	22:5 n-6	2.66	7.5.6	4.4.4.2	TP	F, I
POU-068	18:5 n-1	1.24	7.5.13	4.4.6.2	TP	F, I
POU-069	21:5 n-3	0.35	7.5.35	4.4.3.5	TP	F, I
POU-163	18:5 n-3	2.31	7.5.7	4.4.3.3	TP	F, I
POU-245	20:4 NMI	0.26	7.5.44	4.4.7.3	TP	F, PI
POU-307	18:3 n-7	0.97	7.5.14	4.4.7.1	TP	F, I
POU-313	16:3 n-6	20.16	7.5.1	4.4.4.1	TP	F, I
POU-318	24:6 n-3	0.21	7.5.53	4.4.3.6	TP	F, I
POU-583	Unkn. FAME (PUFA)	0.36	7.5.33	4.4.7.2	TP	F, PI
POU-751	24:5 n-6	0.11	7.5.58	4.4.4.3	TP	F, I
SAD-691	9:0 dME	0.15	7.5.57	4.4.9.4	TDE	F, I
SOH-742	22:0-2OH	0.69	7.5.20	4.4.9.3	TOH	F, I
SOH-769	16:0-3OH	0.28	7.5.40	4.4.9.2	TOH	F, I
UNK-165	Unknown	0.91	7.5.15	4.4.11.3	U	N, U

Table 4.2 continued

Code	Short name	Max %[a]	Sheet[b]	Section[c]	Status B[d]	Status A[e]
UNK-166	Unkn. FAME	0.89	7.5.16	4.4.10.1	U	F, U
UNK-292	Unknown	2.13	7.5.8	4.4.11.1	U	N, PI
UNK-478	Unknown	0.69	7.5.21	4.4.11.1	U	N, PI
UNK-492	Unkn. FAME	0.30	7.5.39	4.4.10.1	U	F, U
UNK-730	Unknown	0.36	7.5.32	4.4.11.1	U	N, U
UNK-732	Unknown	0.22	7.5.50	4.4.11.7	U	N, U
UNK-735	Unknown	0.20	7.5.56	4.4.11.1	U	N, U
UNK-736	Unknown	0.27	7.5.42	4.4.11.1	U	N, U
UNK-740	Unknown	1.50	7.5.10	4.4.11.1	U	N, U
UNK-741	Unknown	0.21	7.5.52	4.4.11.1	U	N, U
UNK-743	Unknown	0.58	7.5.22	4.4.10.8	U	F, PI
UNK-747	Unknown	0.26	7.5.45	4.4.11.3	U	N, U
UNK-759	Unknown	0.21	7.5.51	4.4.11.1	U	N, U
UNK-760	Unknown	0.42	7.5.26	4.4.10.2	U	F, U
UNK-761	Unknown	0.45	7.5.25	4.4.10.2	U	F, U
UNK-767	Unknown	0.27	7.5.43	4.4.10.5	U	F, PI
UNK-768	Unknown	0.50	7.5.23	4.4.11.5	U	N, U
UNK-778	Unknown	0.22	7.5.49	4.4.10.6	U	F, PI
UNK-780	Unknown	0.40	7.5.28	4.4.11.2	U	N, U
UNK-781	Unknown	0.30	7.5.38	4.4.11.2	U	N, U
UNK-782	Unknown	0.32	7.5.36	4.4.11.4	U	N, U
UNK-784	Unknown	0.21	7.5.54	4.4.11.8	U	N, U
UNK-798	Unknown	0.37	7.5.31	4.4.11.2	U	N, U
UNK-801	Unknown	0.38	7.5.30	4.4.10.9	U	F, PI
UNK-804	Unknown	0.35	7.5.34	4.4.10.3	U	F, PI
UNK-805	Unknown	0.31	7.5.37	4.4.10.4	U	F, PI
UNK-810	Unknown	0.23	7.5.47	4.4.11.1	U	N, U
UNK-814	Unknown	0.28	7.5.41	4.4.11.1	U	N, U
UNK-820	Sterol Der.	0.42	7.5.27	4.4.11.6	U	N, PI
UNK-822	Unknown	0.20	7.5.55	4.4.10.7	U	F, PI

Notes:

a) Maximal area percent in any sample

b) Refers to the section with interpretation

b) Refers to section with discussion

c) Tentative status, TD: DUFA, TDE: diester, TM: MUFA, TOH: Hydroxy FAME, TP: PUFA, U: Unknown

d) Status after interpretation, F: FAME, N: not FAME, I: identified, PI: partly identified, U: Unknown

4.4.3 Compounds tentatively identified as omega-3 PUFA

The omega-3 series is the most abundant class of PUFA in most algae. The diagnostic omega-ion for omega-3 PUFA is m/z 108.

4.4.3.1 POU-049 / 16:3 n-3

The identification sheet is available in Section 7.5.5. Both alpha (m/z 208) and omega (m/z 108) are visible. The molecular ion (m/z 264) is visible but weak. The lower masses show a pattern typical for PUFA with m/z 79 as base peak. The ECL plots indicates that the chain lengths and the number of double bonds is correct. The tentative identification seems correct.

4.4.3.2 POU-051 / 16:4 n-3

The identification sheet is available in Section 7.5.2. Both alpha (m/z 166) and omega (m/z 108) ions are visible. There is no visible molecular ion (m/z 262). The lower masses show a pattern typical for PUFA with m/z 79 as base peak. The ECL plots indicates that the chain lengths and the number of double bonds is correct. The tentative identification seems correct.

4.4.3.3 POU-163 / 18:5 n-3

The identification sheet is available in Section 7.5.7. Both alpha (m/z 152) and omega (m/z 108) are visible, but the alpha ion is only around 3% relative to the base peak. in the molecular ion (m/z 288) is not visible. The lower masses show a pattern typical for PUFA with m/z 79 as base peak. The ECL plots indicates that the chain lengths and the number of double bonds is correct. The tentative identification seems correct.

4.4.3.4 POU-054 / 20:4 n-3

The identification sheet is available in Section 7.5.17. Both alpha (m/z 222) and omega (m/z 108) are visible. The molecular ion (m/z 318) is not visible. The lower masses show a pattern typical for PUFA with m/z 79 as base peak. The ECL plots indicates that the chain lengths and the number of double bonds is correct. The tentative identification seems correct.

4.4.3.5 POU-069 / 21:5 n-3

The identification sheet is available in Section 7.5.35. Both alpha (m/z 194) and omega (m/z 108) are visible. The molecular ion (m/z 330) is not visible. The lower masses show a pattern typical for PUFA with m/z 79 as base peak. The ECL plots indicates that the chain lengths and the number of double bonds is correct. The tentative identification seems correct.

4.4.3.6 POU-318 / 24:6 n-3

The identification sheet is available in Section 7.5.53. Both alpha (m/z 194) and omega (m/z 108) are visible. The molecular ion (m/z 370) is not visible in the identification sheet, but could be seen in other spectra of this compound. The lower masses show a pattern typical for PUFA with m/z 79 as base peak. The ECL plots indicates that the chain lengths is correct. The tentative identification seems correct.

4.4.4 Compounds tentatively identified as omega-6 PUFA

The diagnostic omega-ion for omega-6 PUFA is m/z 150.

4.4.4.1 POU-313 / 16:3 n-6

The identification sheet is available in Section 7.5.1. Both alpha (m/z 166) and omega (m/z 150) are visible. The molecular ion (m/z 264) is also visible, but weak. The lower masses show a pattern typical for PUFA with m/z 79 as base peak. The ECL plots indicates that the chain lengths and the number of double bonds is correct. The tentative identification seems correct.

4.4.4.2 POU-066 / 22:5 n-6

The identification sheet is available in Section 7.5.6. The mass spectrum shows the alpha ion (m/z 166) and the omega ion (m/z 150). The molecular ion (m/z 344) is not visible. The lower masses show a pattern typical for PUFA with m/z 79 as base peak. The ECL plots indicate that the chain lengths and the number of double bonds is correct. The tentative identification seems correct.

4.4.4.3 POU-751 / 24:5 n-6

The identification sheet is available in Section 7.5.58. Both alpha (m/z 194) and omega (m/z 150) are visible. The molecular ion (m/z 372) is not visible. The lower masses show a pattern typical for PUFA with m/z 79 as base peak. The ECL plots indicates that the chain lengths and the number of double bonds is correct. The tentative identification seems correct.

4.4.5 Compounds tentatively identified as omega-4 PUFA

The omega-4 series is a less abundant class of PUFA than omega-3 and omega-6. The diagnostic omega-ion for omega-4 PUFA is m/z 122.

4.4.5.1 POU-046 / 16:3 n-4

The identification sheet is available in Section 7.5.4. Both alpha (m/z 194) and omega (m/z 122) are visible. The molecular ion (m/z 264) is visible. The lower masses show a pattern typical for PUFA with m/z 79 as base peak. The ECL plots indicates that the chain lengths and the number of double bonds is correct. The tentative identification seems correct.

4.4.5.2 POU-059 / 18:4 n-4

The identification sheet is available in section (Appendix 7.5.9). Both alpha (m/z 180) and omega (m/z 122) are visible. The molecular ion (m/z 290) is not visible. The lower masses show a pattern typical for PUFA with m/z 79 as base peak. The ECL plots indicates that the chain lengths and the number of double bonds is correct. The tentative identification seems correct.

4.4.6 Compounds tentatively identified as omega-1 PUFA

The omega-1 series is also a minor series of PUFA in most organisms. The omega-1 series has no omega-ion, and they can therefore only be identified by their alpha ion or molecular ion in addition to the chromatographic properties.

4.4.6.1 POU-052 / 16:4 n-1

The identification sheet is found in Section 7.5.3. The ECL plots indicates that the chain lengths and the number of double bonds is correct. The lower masses show a pattern typical for PUFA with m/z 79 as base peak. The alpha ion (m/z 194) is available but the molecular ion is not seen. The tentative identification seems correct, but with only one diagnostic ion it is less certain than the other. The compound is also present in the NIST library, and search against NIST gave 16:4 n-1 as the best match.

4.4.6.2 POU-068 / 18:5 n-1

The identification sheet is found in Section 7.5.13. The ECL plots indicates that the chain lengths and the number of double bonds is correct. The lower masses show a pattern typical for PUFA with m/z 79 as base peak. The alpha ion (m/z 180) is available. The tentative identification seems correct, but with only one diagnostic ion it is less certain than the other. The compound is also present in the NIST library, and search against NIST gave 18:5 n-1 as the best match.

4.4.7 Compounds tentatively identified as other PUFA

4.4.7.1 POU-307 / 18:3 n-7

The identification sheet is available in Section 7.5.14. The ECL plots indicates that the chain lengths and the number of double bonds is correct. The lower masses show a pattern typical for PUFA with m/z 79 as base peak. The molecular ion (m/z 292), the alpha ion (m/z 180) and the omega ion (m/z 164) are visible and relatively strong. The tentative identification seems correct.

4.4.7.2 POU-583 / Unkn. FAME (PUFA)

The identification sheet is available in section 7.5.33. The ECL plots indicates that the compound is in the PUFA-5 region. The chain length is between C18 and C20. The lower masses show a pattern typical for PUFA with m/z 79 as base peak. The spectrum is very similar to the spectrum of 20:5 n-3, which indicates 5 double bonds and double bonds in the same distance from the carboxyl group as in 20:5 n-3 [37]. This should correspond to a $\Delta^{5,8,11,14,17}$ 19:5 (19:5 n-2). The main difference between the spectra is higher abundance of m/z 94 (omega ion for n-2) and lower abundance of m/z 108 (omega ion of n-3). The alpha ion for the Δ5 series (m/z 180) is also visible. The compound is therefore tentatively identified as 19:5 n-2.

4.4.7.3 POU-245 / 20:4 NMI

The identification sheet is available in Section 7.5.44. The lower masses show a pattern typical for PUFA-4 with m/z 79 as base peak. The ECL plots indicates that the chain lengths and the number of double bonds is correct. A search in the NIST library gave hits for $\Delta^{5,11,14,17}$ 20:4 at the three best matches. The strong signal for m/z 108 also indicates that there is a methylene-interrupted double bond system from Δ11 to Δ17, but the position of the first double bond cannot be accurately determined. The compound is tentatively identified as $\Delta^{x,11,14,17}$ 20:4.

4.4.8 Compounds tentatively identified as MUFA

4.4.8.1 MOU-297 / 16:1 n-x

The identification sheet is available in section 7.5.12. The molecular ion (m/z 268) is visible and the [M+-32] ion (m/z 236) is strong. The spectrum also has a strong signal at [M+-74] (m/z 194). The McLafferty ion (m/z 74) is base peak, which can happen in MUFA when the double bond is close to the carboxyl group. The ECL plots indicates that the chain length is correct, but it is

positioned far from the other MUFA in one of the plots. The deviation from normal MUFA can be explained by a double bond very close to the carboxyl group, which gives low retention compared to other positions on BPX70, or it can have a branched carbon chain. A stronger signal for m/z 74 than m/z 55 indicates that the double bond is close to the carboxyl group.

4.4.8.2 MOU-769 / 22:1 n-x

The identification sheet is available in Section 7.5.19. The lower masses show a pattern typical for MUFA with m/z 55 as base peak. The molecular ion (m/z 352) is visible and the [M+-32] ion (m/z 320) is strong, also $[M-74]^+$ and $[M-116]^+$ ions are visible at m/z = 278 and 236, respectively. The ECL plots confirms the chain length and number of double bonds, but it is not possible to tell the double bond position accurately. A relatively weak signal for m/z 74 compared to other MUFA indicates that the double bond is far from the carboxyl group.

4.4.8.3 MOU-571 / 24:1 n-x and MOU-770 / 24:1 n-x

The identification sheet is available in Sections 7.5.24 and 7.5.29. The lower masses show a pattern typical for MUFA with m/z 55 as base peak. The molecular ion (m/z 380) is visible and the [M+-32] ion (m/z 348) is strong, also $[M-74]^+$ and $[M-116]^+$ ions are visible at m/z = 306 and 264, respectively. The ECL plots confirms the chain length and number of double bonds, but it is not possible to tell the double bond position accurately. Relatively weak signals for m/z 74 compared to other MUFA indicates that the double bonds are far from the carboxyl group.

4.4.8.4 MOU-795 / 26:1 n-x

The identification sheet is available in Section 7.5.11. The molecular ion (m/z 408) is visible and the [M+-32] is very strong. The lower masses show a pattern typical for MUFA with m/z 55 as base peak. The ECL plots confirms the chain length and number of double bonds, but it is not possible to tell the double bond position accurately. A relatively weak signal for m/z 74 compared to other MUFA indicates that the double bond is far from the carboxyl group.

4.4.8.5 MOU-807 / 27:1 n-x

The identification sheet is available in Section 7.5.49. The molecular ion (m/z 422) is visible and the [M+-32] is very strong. The lower masses show a pattern typical for MUFA with m/z 55 as base peak. The ECL plot indicates that the chain length is correct, but it is positioned little far

from the other MUFA the plot. The deviation from normal MUFA can be explained by a double bond very close to the carboxyl group, which gives low retention compared to other positions on BPX70, or it can have a branched carbon chain. A relatively weak signal for m/z 74 compared to other MUFA indicates that the double bond is far from the carboxyl group.

4.4.9 Other tentative identifications

4.4.9.1 DIU-779 / 16:2 conj

The identification sheet is available in Section 7.5.18. The lower masses show a pattern typical for DUFA with m/z 67 as base peak. The molecular ion (m/z 266) is visible. The ECL plots indicates that the chain length is correct, but it is positioned far from the DUFA region in both plots and it is closer to PUFA-3. This indicates that it is not a normal double bond system. The deviation from normal DUFA is in the same direction as conjugated PUFA-3 deviates from normal PUFA-3. The molecular ion is also relatively strong, which is typical for conjugated systems.

4.4.9.2 SOH-769 / 16:0-3OH

The identification sheet is available in Section 7.5.40. The lower masses show a pattern typical for Hydroxy with m/z 103 as base peak. The molecular ion (m/z 286) is not visible, which is common for 3-hydroxy FAME. In the ECL plots the compound is positioned with other 3-hydroxy FAME. The tentative identification seems correct.

4.4.9.3 SOH-742 / 22:0-2OH

The identification sheet is available in Section 7.5.20. The molecular ion (m/z 370) is visible and the $[M-59]^+$ at (m/z 311) is very strong. The McLafferty ion at m/z 90 is strong. The ECL plots confirms the chain length and the compound is positioned with other 2-hydroxy FAME. With the molecular ion and the diagnostic McLafferty ion present, and ECL data that fits with chain length and the 2-hydroxy group, this identification is regarded as quite certain.

4.4.9.4 SAD-691 / 9:0 dME

The identification sheet is available in section 7.5.57. The mass spectrum for this compound is very characteristic, but it deviates from the spectrum of the longer diesters (Section 2.2.1.8). A

search in the NIST library gave good match with very similar spectra and the four closest matches were all 9:0 dimethyl ester.

4.4.10 Previously unknowns expected to be FAME

4.4.10.1 UNK-166 and UNK-492

The identification sheet is available in Sections 7.5.16 and 7.5.39. These two compounds have similar spectra and similarities in the ECL plots. The McLafferty ion of FAME at (m/z 74) is visible and more dominating than seen in regular saturated FAME. The ECL plots indicates that these are compounds with high polarity, but it does not match any of the other classes in the plots. At higher masses there are prominent ions at m/z 236 and m/z 264 are separated by 28 mass units that these belong to the same homologous series, which is also supported by the ECL value at HP5, where UNK-166 are positioned as C18 FAME and UNK-492 are positioned as C20 FAME. This indicates that they are homologues separated by two methylene units, but the chain length can be different from C18 and C20. There were a large number of these compounds from different sources in the existing libraries, which means that these are common.

4.4.10.2 UNK760 and UNK761

The identification sheet is available in Section 7.5.26 and 7.5.25. These two compounds always appeared together. Both have weak ions at m/z 74 (approx. 5-10% of the base peak), but there is little else in the spectra that indicates that they are FAME. They are found at the same place in the ECL plots, which indicates structural similarity, and they are found in regions covered by regular FAME, indicating a polarity similar to FAME of MUFA or DUFA. Search in the NIST database gave no reliable identification. These are regarded as possible FAME, but this conclusion is uncertain.

4.4.10.3 UNK-804

The identification sheet is available in Section 7.5.34. The McLafferty ion (m/z 74) is around 45% of the base peak. The ECL plots indicate that the compound may be Hydroxy FAME similar to Ricinoleic acid or 18:0-12OH, but possibly with shorter chain length. The best match in the NIST library spectrum was with 16:0-10OH. In Figure 4.13 the spectrum of UNK-804 is compared to the spectrum of 18:0-12OH, that was analysed as a qualitative standard. It can be

seen that the spectra are very similar at lower masses and that higher masses are shifted down by 28 mass units, corresponding to the mass of two methylene units. It is therefore likely that this compound is 16:0-10OH.

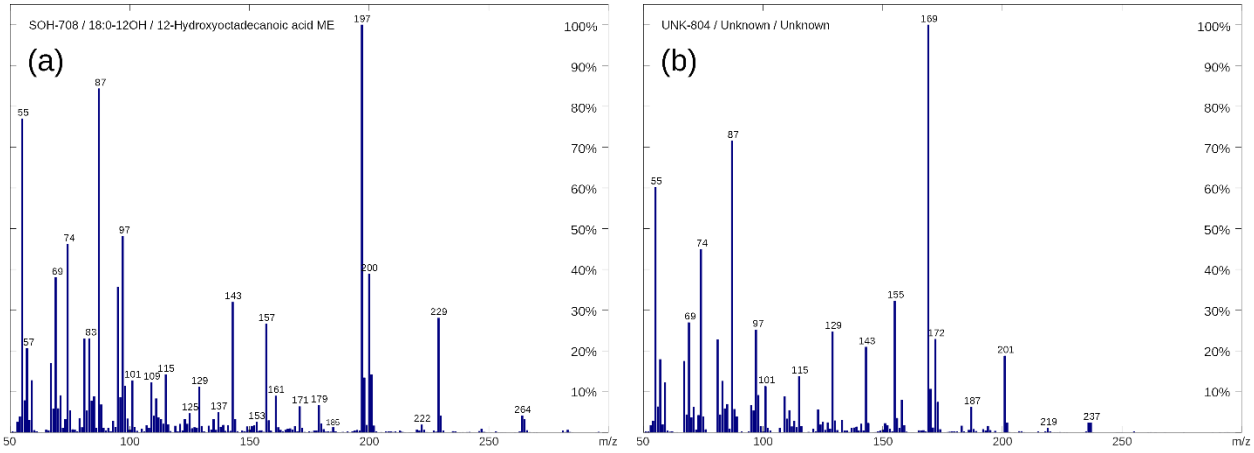

Figure 4.13. Comparison of the spectra of 18:0-12OH (a) and UNK804 (b)

4.4.10.4 UNK-805

The identification sheet is available in Section 7.5.37. The ECL plots indicate that the compound may be a C16 DUFA. The McLafferty ion (m/z 74) at about 10% of the base peak. The ion at m/z 266 (9% of base peak) corresponds with the molecular ion of C16 DUFA. The best match in the NIST library was 16:2 n-6 (which is DIU-494). The mass spectrum has some deviations from a normal DUFA, with a more prominent m/z 81 and m/z 113. This may indicate a methyl branch or a non-methylene-interrupted double bond system. The ECL values also indicated slightly lower polarity than in normal DUFA. The compound is identified as a 16:2 isomer, but it is not possible to conclude on the position of the double bonds or if it has a branch.

4.4.10.5 UNK-767

The identification sheet is available in Section 7.5.43. The available ECL plot indicate that the compound is a 24:1 MUFA. The spectrum is very similar to those of MOU-571 (section 7.5.24) and MOU-770 (section 7.5.29). The spectra were of low quality and m/z 55 were base peak in some of the spectra. The compound is identified as 24:1, but it is not possible to tell the double bond position.

4.4.10.6 UNK-778

The identification sheet is available in Section 7.5.49. The spectrum looks like the spectra of normal PUFA. The McLafferty ion has an intensity of around 13% relative to the base peak. The spectra were of poor quality. There is no ECL plots available for this compound because it only eluted on BP20 (ECL 25.17) and BPX70 (ECL 27.39). Identified as long clain PUFA, but more information is necessary to give a more detailed identification.

4.4.10.7 UNK-822

The identification sheet is available in Section 7.5.55. The spectrum looks like the spectra of normal PUFA. The McLafferty ion has an intensity of around 18% relative to the base peak. The spectra were of poor quality. There is no ECL plots available for this compound because it only eluted on BP20 and BPX70. Identified as a PUFA, but more information is necessary to give a more detailed identification.

4.4.10.8 UNK-743

The identification sheet is available in Section 7.5.22. The spectrum has similarities with hydroxy fatty acids and the ECL plot in the identification sheet indicates it may be a C22 hydroxy fatty acid because it has similar values as 22:0-2OH. The molecular ion of C22 hydroxy FAME (m/z 370) was clearly visible in some of the spectra. The McLafferty ion (m/z 74) was around 6%. Search in the NIST spectrum gave the best match with 22:0-2OH, but it cannot be this compound because it elutes later on BPX70 and BP20, The McLafferty ion of 2-hydroxy FAME is also very weak (approximately 2%). Most likely this is a different C22 hydroxy fatty acid. It cannot be 22:0-3OH because 3-hydroxy FAME have very different spectra dominated by m/z 103. When the hydroxy group is nearer the center of the carbon chain, the McLafferty ion tend to be higher (Figure 4.13).

4.4.10.9 UNK-801

The identification sheet is available in Section 7.5.30. The ECL plots indicates a polarity near the 2-hydroxy FAME but it is slightly outside this group. The spectrum also shows similarities with 2-hydroxy FAME and the McLafferty ion of 2-hydroxy FAME (m/z 90) is very strong (>60%). The ion at m/z 284 corresponds to the mass of a monounsaturated hydroxy C16 FAME. It is

therefore concluded that this can be a 16:1-2OH, but it is not possible to say anything about the double bond position.

4.4.11 Previously unknowns not expected to be FAME

4.4.11.1 Apolar compounds

Many of the unknown compounds could be classified as not being FAME from their polarity. While FAME can have polar groups, making it difficult to set an upper limit for the polarity, they cannot be much less polar than the highly branched phytanic acid, which is present in the ECL plots in the identification sheets. The following compounds were found to be significantly less polar than the phytanic acid methyl ester:

- UNK-292 (Section 7.5.8) and UNK-478 (Section 7.5.21). Both these have an abundant ion at m/z 278, which may be the base peak and many of the same fragments (but differing in abundance). The best match in the NIST library for both compounds was with phytol isomers (3,7,11,15-Tetramethyl-2-hexadecen-1-ol). It is therefore concluded that this is a phytol isomer or a closely related compound.
- UNK-740 (Section 7.5.10) and UNK-741 (Section 7.5.52). Both have abundant ions at 432, which may be the base peak, very similar spectra and a large degree of fragmentation at lower masses. The ECL value along HP5 indicates a long carbon chain. Both spectra had the best match in the NIST library with a long chain unsaturated formate (14-Tricosenyl formate) but there were also good matches with unsaturated unbranched aliphatic compounds.
- UNK-730 (Section 7.5.32) also has a spectrum with large degree of fragmentation and an ECL value along HP5 indicates a long carbon chain. The best match in the NIST library was with 1-heptacosanol, which may indicate that this is a long chain alcohol.
- UNK-736 (Section 7.5.42) and ALK-752 (Section 7.5.48). ALK-752 has no ELC plots, but the spectrum is almost identical to UNK-736 at lower masses and the two spectra has pairs of ions at higher masses separated by 28 mass units. They are therefore assumed to belong to the same homologous series. Both spectra had their best matches in the NIST library with branched alkanes.

- UNK-814 and UNK-810 (Appendix 7.5.41 and Appendix 7.5.47). These two compounds both have very similar spectra and similar ECL maps. The spectra are dominated by m/z 99, accounting for close to 100% of the signal. The NIST library only gave matches with small molecules that do not fit with an ECL value on HP5 around 16.
- UNK-759 and UNK-735 (Appendix 7.5.51 and Appendix 7.5.56). The two spectra are similar at lower masses and have pairs of ions at high masses that are separated by 56 mass units, corresponding to 4 methylene units. They are therefore expected to belong to the same homologous series. The ECL values at HP5 also differ by approximately 4. For both compounds the best match in the NIST library is with iso-branched alkanes.

4.4.11.2 UNK-780, UNK-781 and UNK-798

The identification sheet is available in Section 7.5.28, 7.5.38 and 7.5.31 These three compounds are considered together because they have highly similar ECL-plots, suggesting that they may belong to the same compound class. In the ECL plot of HP5 against the difference between BP20 and HP5 they are grouped together with hydroxy FAME, but in the other plot they are far from any FAME. All three have weak signals for m/z 74 (McLafferty ion of most FAME) of approx. 3-5% of the base peak. Besides of that there is limited similarity between the three spectra. None of the spectra gave any good match against the NIST library, and the best matches were not structurally similar.

4.4.11.3 UNK-165 and UNK-747

The identification sheet is available in Section 7.5.15. The compound has a spectrum that looks like a PUFA, but it lacks the McLafferty ion. Even FAME of highly of unsaturated PUFA has a significant McLafferty ion (e.g. approx. 10% of the base peak in 22:6 n-3). The ECL plots also show that the compound has much lower polarity than regular FAME. A similar case is seen with UNK-747 that has spectral similarities with DUFA FAME, but with no significant McLafferty ion. There is no ELC plots available for UNK-747, but the NIST database gave the best match with a tri-unsaturated alkene.

4.4.11.4 UNK-782

The identification sheet is available in Section 7.5.36. The compound was only found on BP20 and BPX70 and the ECL maps in the identification sheets are therefore not available. ECL on

BP20 and PBX70 was 22.2 and 25.2, respectively. The large difference indicates a very high polarity. For comparison, the ECL differences between the two columns for dimethyl esters and hydroxy fatty acids are less than 2. The NIST database gave no reliable suggestions. Even though m/z 74 is present in low amounts (approx. 4%), this is regarded as not being a FAME.

4.4.11.5 UNK-768

The identification sheet is available in Section 7.5.23. The compound was only found on BP20 and BPX70, and the ECL plots are therefore not available in the identification sheets. The ECL values were higher on BP20 than on BPX70, which indicates a low polarity. Search in the NIST library gave no reliable suggestions, but the best matches were with long chain aldehydes, ethers or epoxides. The McLafferty ion for FAME was absent.

4.4.11.6 UNK-820

The identification sheet is available in Section 7.5.27. The compound was too heavy to elute on BPX70 and DB225, it is therefore no ECL plots in the identification sheet. There was a good match with Stigmasta-5,22-dien-3-ol acetate in the NIST database, but there are many similar spectra. It is therefore concluded that this is some kind of sterol or a closely related compound.

4.4.11.7 UNK-732

The identification sheet is available in Section 7.5.50. The ECL plots indicate that the compound is slightly less polar than branched saturated FAME. The McLafferty ion of FAME is absent. Search in the NIST library gave no reliable suggestions. It is concluded that this is a FAME, but it was not possible to tell more about the structure

4.4.11.8 UNK-784

The identification sheet is available in Section 7.5.54. The ECL plots indicate that the compound has chromatographic properties similar to Hydroxy FAME. There is a weak signal from m/z 74 (approx. 3%), but lower than typically seen in FAME. Search in the NIST spectrum gave no reliable suggestions. In spite of being in the region with hydroxy FAME in the ECL plot, there is no similarity with any of the other FAME in the mass spectrum. It is therefore concluded that this is not a FAME.

5 Conclusions and suggestions for further work

In the first part of this study, GC-MS was used to study the retention patterns of FAME on 10 different capillary columns to find if they were suitable for analysis of FAME in marine algae. To be suitable for fatty acid analysis, the introduction of a double bond should lead to a significant change in retention. Several of the evaluated columns, in particular RXI1, RTX50, RTX200, IL61 and IL100, failed to give the required separation when the double bonds were introduced in certain positions. It was decided to continue with DB225 and DB5, in addition to BP20 and BPX70 for which there exist a large collection of reference data (www.chrombox.org/data)

It was found that simple two-dimensional scatter plots of ECL values gave information useful for identification of the FAME in combination with the mass spectra. The applied plots were the ECL on DB5 plotted against the difference in ECL between BP20 and DB5, and the difference between BP20 and DB225 plotted against the difference between BPX70 and BP20.

It total 114 compounds were found above the 0.2% limit in the algae, meaning that they constituted 0.2% or more of the chromatographic are percent in at least one sample. 58 compounds (including two that were below the 0.2% limit) had unknown structure or tentative identities that needed to be confirmed. The 26 compounds with tentative identification as FAME included 6 omega-3 PUFA, 3 omega-6 PUFA, 2 omega-4 PUFA, 2 omega-1 PUFA, 1 omega-7 PUFA and 2 other PUFA with unknown structure. There were also 6 identified as MUFA with unknown double bond position, 2 compounds identified as hydroxy fatty acids, one DUFA and one diester. All the tentative identifications were confirmed, but the complete structure of some of them are still unknown. The other 35 compounds were unknowns, 11 of these are expected to be FAMEs. While 21 are not expected to be FAMEs.

After studying the identification sheets of the compounds, new information about some of the FAMEs could be gained. One PUFA (POU-583) was tentatively identified as 19:5 n-2 and one NMI PUFA (POU-245) is tentatively identified as Δx,11,14,17 20:4. For all compounds tentatively identified as MUFA it was possible to tell if the double bond is close to or far from the carboxyl group, but without determining the double bond position accurately.

Two compounds (UNK-804 and UNK-801) were identified as 16:0-10OH and as 16:1-2OH, respectively. The double bond position of the 16:1-2OH is not known. More information could also be told about other previously unknowns, but a reliable or full identification could not be given.

The largest peak that remains unknown is UNK-740 that constituted 1.5% of the area in one of the samples, but this is not expected to be a FAME. The largest unknown peak expected to be FAME is UNK-166 that constituted 0.9% in one of the samples. This is also expected to have a homologous compound in UNK-492 (0.3%). There were a large number of these compounds from different sources in the existing libraries, which means that these are common. There are also several monoenes with unknown double bond position. The largest of these, 26:1 (MOU-795) constituted 1.4 % of the area in one of the samples.

More studies can be done to identify the largest unknowns. Softer ionization methods like chemical ionization may tell the molecular mass in cases where the mass is not certain. They may also give less fragmentation that can give diagnostic fragments. Derivatization of the double bonds or functional groups may also give information about their position. In cases where there is doubt about whether a compound is FAME or not, the samples can be hydrolyzed, which will produce free fatty acids from FAME (or from the original lipids). Free fatty acids can be easily separated from non-acids by extraction or chromatography.

6 References:

1. Kohlmeier, M., *Nutrient metabolism*. Food science and technology, international series. 2003, Amsterdam ; Boston: Academic Press. viii, 829 p.
2. Cammack, R., *Oxford dictionary of biochemistry and molecular biology*. Rev. ed. 2006, Oxford ; New York: Oxford University Press. xv, 720 p.
3. Wang, T.Y., et al., *New insights into the molecular mechanism of intestinal fatty acid absorption.* Eur J Clin Invest, 2013. **43**(11): p. 1203-23.
4. *Fatty Acids*, in *Encyclopedia of Genetics, Genomics, Proteomics and Informatics*. 2008, Springer Netherlands: Dordrecht. p. 675-675.
5. Berg, J.M., et al., *Biochemistry*. 5th ed. 2002, New York: W.H. Freeman.
6. Laposata, M., *Fatty acids. Biochemistry to clinical significance.* Am J Clin Pathol, 1995. **104**(2): p. 172-9.
7. Davidson, B.C. and R.C. Cantrill, *Fatty acid nomenclature. A short review.* S Afr Med J, 1985. **67**(16): p. 633-4.
8. Jacobson, T.A., et al., *Effects of eicosapentaenoic acid and docosahexaenoic acid on low-density lipoprotein cholesterol and other lipids: a review.* J Clin Lipidol, 2012. **6**(1): p. 5-18.
9. Shoji, T., et al., *Serum n-3 and n-6 polyunsaturated fatty acid profile as an independent predictor of cardiovascular events in hemodialysis patients.* Am J Kidney Dis, 2013. **62**(3): p. 568-76.
10. Song, C., et al., *The role of omega-3 polyunsaturated fatty acids eicosapentaenoic and docosahexaenoic acids in the treatment of major depression and Alzheimer's disease: Acting separately or synergistically?* Prog Lipid Res, 2016. **62**: p. 41-54.
11. Jho, D.H., et al., *Role of omega-3 fatty acid supplementation in inflammation and malignancy.* Integr Cancer Ther, 2004. **3**(2): p. 98-111.
12. Virtanen, J.K., et al., *Serum omega-3 polyunsaturated fatty acids and risk of incident type 2 diabetes in men: the Kuopio Ischemic Heart Disease Risk Factor study.* Diabetes Care, 2014. **37**(1): p. 189-96.
13. MacLean, C.H., et al., *Effects of omega-3 fatty acids on cancer risk: a systematic review.* JAMA, 2006. **295**(4): p. 403-15.
14. Weylandt, K.H., et al., *Omega-3 Polyunsaturated Fatty Acids: The Way Forward in Times of Mixed Evidence.* Biomed Res Int, 2015. **2015**: p. 143109.
15. Kaur, N., V. Chugh, and A.K. Gupta, *Essential fatty acids as functional components of foods- a review.* J Food Sci Technol, 2014. **51**(10): p. 2289-303.
16. Siri-Tarino, P.W., et al., *Saturated Fats Versus Polyunsaturated Fats Versus Carbohydrates for Cardiovascular Disease Prevention and Treatment.* Annu Rev Nutr, 2015. **35**: p. 517-43.

17. Tur, J.A., et al., *Dietary sources of omega 3 fatty acids: public health risks and benefits.* Br J Nutr, 2012. **107 Suppl 2**: p. S23-52.

18. Zivkovic, A.M., et al., *Dietary omega-3 fatty acids aid in the modulation of inflammation and metabolic health.* Calif Agric (Berkeley), 2011. **65**(3): p. 106-111.

19. Ablikim, U., et al., *Identification of absolute geometries of cis and trans molecular isomers by Coulomb Explosion Imaging.* Sci Rep, 2016. **6**: p. 38202.

20. Rabinovichb, A.P.L.a.a.A.L., *Recent development in computer simulations of lipid bilayers.* Soft Matter, 2011, 7, 25.

21. Barnathan, G., *Non-methylene-interrupted fatty acids from marine invertebrates: Occurrence, characterization and biological properties.* Biochimie, 2009. **91**(6): p. 671-8.

22. Tanaka, T., et al., *Methylene-interrupted double bond in polyunsaturated fatty acid is an essential structure for metabolism by the fatty acid chain elongation system of rat liver.* Biochim Biophys Acta, 1998. **1393**(2-3): p. 299-306.

23. Otera, J., *Transesterification.* Chemical Reviews, 1993. **93**(4): p. 1449.

24. de Boer, K. and P.A. Bahri, *Supercritical methanol for fatty acid methyl ester production: A review.* Biomass and Bioenergy, 2011. **35**(3): p. 983-991.

25. Cesarini, S., et al., *Moving towards a Competitive Fully Enzymatic Biodiesel Process.* Sustainability, 2015. **7**(6): p. 7884.

26. Hamilton, M.L., et al., *Heterotrophic Production of Omega-3 Long-Chain Polyunsaturated Fatty Acids by Trophically Converted Marine Diatom Phaeodactylum tricornutum.* Mar Drugs, 2016. **14**(3).

27. Ahlgren, et al., *Fatty acid content and chemical composition of freshwater microalgae1*. Journal of Phycology, 1992. **28**(1): p. 37-50.

28. Steinrücken, P. and B. Universitetet i, *High-value fatty acids from microalgae : bioprospecting and outdoor cultivation at northern latitudes*. 2018, University of Bergen: Bergen.

29. Guiochon, G. and C.L. Guillemin, *Gas chromatography*. Review of Scientific Instruments, 1990. **61**(11): p. 3317-3339.

30. Coskun, O., *Separation techniques: Chromatography*. North Clin Istanb, 2016. **3**(2): p. 156-160.

31. Kolomnikov, I.G., et al., *Early stages in the history of gas chromatography.* Journal of Chromatography A, 2018. **1537**: p. 109-117.

32. Kuyper, B., *An investigation into the source and distribution of bromoform in the southern African and Southern Ocean marine boundary layer*. 2014.

33. McNair, H.M. and J.M. Miller, *Basic gas chromatography*. Techniques in analytical chemistry series. 1998, New York: Wiley. xii, 200 p.

34. Mjøs, S.A., *Interpretation of chromatographic and mass spectrometric data from analyses of fatty acid methyl esters Application of multivariate methods*. 2006, The University of Bergen.

35. Hübschmann, H.-J. and H.-J. Bschmann, *Handbook of GC-MS : Fundamentals and Applications*. 2015, Weinheim, GERMANY: John Wiley & Sons, Incorporated.

36. Wasta, Z., *Identifikasjon av fettsyrer i omega-3 produkter ved hjelp av gasskromatografi med massespektrometrisk deteksjon.* 2012.

37. Mjøs, S.A., *The prediction of fatty acid structure from selected ions in electron impact mass spectra of fatty acid methyl esters.* European Journal of Lipid Science and Technology, 2004. **106**(8): p. 550-560.

38. Kováts, E., *Gas-chromatographische Charakterisierung organischer Verbindungen. Teil 1: Retentionsindices aliphatischer Halogenide, Alkohole, Aldehyde und Ketone.* Helvetica Chimica Acta, 1958. **41**(7): p. 1915-1932.

39. Mjos, S.A., *Prediction of equivalent chain lengths from two-dimensional fatty acid retention indices.* J Chromatogr A, 2006. **1122**(1-2): p. 249-54.

40. Blumberg, L. and M.S. Klee, *Optimal heating rate in gas chromatography.* J. Microcolumn Sep., 2000. **12**(9): p. 508-514.

41. Waktola, H.D. and B. Universitetet i, *Optimization of separation efficiency in temperature programmed gas chromatography : application of response surface methodology*. 2014, H.D. Waktola: Bergen.

42. Morken, P.H., *Sammenhenger mellom gasskromatografisk retensjon og fysikalsk-kjemiske egenskaper for miljøgifter*. 2012.

43. Rahman, M.M., et al., *Basic Overview on Gas Chromatography Columns*, in *Analytical Separation Science*.

44. Rodriguez-Sanchez, S., et al., *Characterization by the solvation parameter model of the retention properties of commercial ionic liquid columns for gas chromatography.* J Chromatogr A, 2014. **1326**: p. 96-102.

45. Smith, R.M., *Understanding mass spectra : a basic approach*. 2nd ed. 2004, Hoboken, N.J.: Wiley Interscience. xviii, 372 p.

46. Wasta, Z. and S.A. Mjos, *A database of chromatographic properties and mass spectra of fatty acid methyl esters from omega-3 products.* J Chromatogr A, 2013. **1299**: p. 94-102.

47. Ryhage, R.a.S.E., *Mass spectrometric studies. I. Saturated normal long-chain methyl esters.* Arkiv Kemi, 1959. **13**: p. 523-542

48. Apon, J.M. and N. Nicolaides, *The determination of the position isomers of the methyl branches fatty acids methyl esters by capillary GC/MS.* J Chromatogr Sci, 1975. **13**(10): p. 467-73.

49. Lough, A.K., *The chemistry and biochemistry of phytanic, pristanic and related acids.* Prog Chem Fats Other Lipids, 1973. **14**(1): p. 1-48.

50. Ran-Ressler, R.R., P. Lawrence, and J.T. Brenna, *Structural characterization of saturated branched chain fatty acid methyl esters by collisional dissociation of molecular ions generated by electron ionization.* J Lipid Res, 2012. **53**(1): p. 195-203.

51. Fardin-Kia, A.R., et al., *Separation of the fatty acids in menhaden oil as methyl esters with a highly polar ionic liquid gas chromatographic column and identification by time of flight mass spectrometry.* Lipids, 2013. **48**(12): p. 1279-95.

52. Christie, W.W. and R.T. Holman, *Mass spectrometry of lipids. I. Cyclopropane fatty acid esters.* Lipids, 1966. **1**(3): p. 176-82.

53. Hallgren, B., Ryhage, R. and Stenhagen, E. , *The mass spectra of methyl oleate, methyl linoleate and methyl linolenate.* Acta Chem. Scand, 1959. **13**: p. 845-847

54. Iversen, S.A., et al., *Identification of a diene conjugated component of human lipid as octadeca-9,11-dienoic acid.* FEBS Lett, 1984. **171**(2): p. 320-4.

55. Brauner, A., H. Budziewicz, and W. Boland, *Organic Mass Spectrometry 17* 1982: p. 161–64.

56. Dobson, G. and W.W. Christie, *Mass spectrometry of fatty acid derivatives.* European Journal of Lipid Science and Technology, 2002. **104**(1): p. 36-43.

57. Ryhage, R.a.S., E., *Mass spectrometric studies. VI. Methyl esters of normal chain oxo-, hydroxy-, methoxy- and epoxy-acids.* Arkiv Kemi, 1960. **15**: p. 545-574

58. Mjos, S.A. and H.D. Waktola, *Optimizing the relationship between chromatographic efficiency and retention times in temperature-programmed gas chromatography.* J Sep Sci, 2015. **38**(17): p. 3014-27.

59. Steinrucken, P., et al., *Bioprospecting North Atlantic microalgae with fast growth and high polyunsaturated fatty acid (PUFA) content for microalgae-based technologies.* Algal Res, 2017. **26**: p. 392-401.

60. Prestegard, S.K., et al., *Specific Metabolites in a Phaeodactylum tricornutum Strain Isolated from Western Norwegian Fjord Water.* Mar Drugs, 2015. **14**(1): p. 9.

61. Chhaganlal, M., L.K. Skartland, and S.A. Mjos, *Transfer of retention patterns in gas chromatography by means of response surface methodology.* J Chromatogr A, 2014. **1332**: p. 64-72.

62. Mjos, S.A. and B.O. Haugsgjerd, *Trans fatty acid analyses in samples of marine origin: the risk of false positives.* J Agric Food Chem, 2011. **59**(8): p. 3520-31.

63. Castello, G., et al., *Effect of temperature on the polarity of some stationary phases for gas chromatography.* Journal of Chromatography A, 1997. **779**(1): p. 275-286.

64. Lin, C.C., Z. Wasta, and S.A. Mjos, *Evaluation of the retention pattern on ionic liquid columns for gas chromatographic analyses of fatty acid methyl esters.* J Chromatogr A, 2014. **1350**: p. 83-91.

65. Lin, C. and B. Universitetet i, *Multivariate analysis of human serum fatty acid profiles*. 2016, University of Bergen: Bergen.

66. Prestegard, S.K., et al., *Marine benthic diatoms contain compounds able to induce leukemia cell death and modulate blood platelet activity.* Mar Drugs, 2009. **7**(4): p. 605-23.

7 Appendixes

7.1 ECL-values for FAME in GLC793 on 10 different columns

FAME	BP20	DB225	DB23	DB5	IL100	IL61	IL82	RTX200	RTX50	RXI1
12:0	12.00	12.00	12.00	12.00	12.00	12.00	12.00	12.00	12.00	12.00
14:0	14.00	14.00	14.00	14.00	14.00	14.00	14.00	14.00	14.00	14.00
14:1 n-5	14.36	14.29	14.37	13.87	14.66	14.28	14.58	13.92	14.13	13.83
15:0	15.00	15.00	15.00	15.00	15.00	15.00	15.00	15.00	15.00	15.00
16:0	16.00	16.00	16.00	16.00	16.00	16.00	16.00	16.00	16.00	16.00
16:1 n-7	16.25	16.21	16.27	15.78	16.55	16.18	16.47	15.82	16.05	15.74
17:0	17.00	17.00	17.00	17.00	17.00	17.00	17.00	17.00	17.00	17.00
17:1 n-7	17.25	17.22	17.28	16.78	17.58	17.20	17.50	16.83	17.06	16.74
18:0	18.00	18.00	18.00	18.00	18.00	18.00	18.00	18.00	18.00	18.00
18:1 n-9	18.18	18.16	18.21	17.73	18.48	18.13	18.42	17.76	18.00	17.69
18:2 n-6	18.65	18.53	18.70	17.66	19.33	18.52	19.18	17.76	18.18	17.59
18:3 n-3	19.30	19.02	19.31	17.73	20.34	19.06	20.10	17.86	18.48	17.62
18:3 n-6	18.95	18.71	18.98	17.50	19.74	18.65	19.61	17.58	18.22	17.40
20:0	20.00	20.00	20.00	20.00	20.00	20.00	20.00	20.00	20.00	20.00
20:1 n-9	20.19	20.17	20.23	19.73	20.53	20.16	20.46	19.77	20.01	19.69
20:2 n-6	20.67	20.57	20.75	19.68	21.43	20.59	21.26	19.78	20.21	19.60
20:3 n-3	21.33	21.07	21.38	19.75	22.47	21.16	22.22	19.88	20.52	19.64
20:3 n-6	20.94	20.76	21.03	19.48	21.94	20.76	21.74	19.60	20.23	19.37
20:4 n-6	21.17	20.85	21.20	19.29	22.07	20.77	21.98	19.33	20.22	19.17
20:5 n-3	21.84	21.36	21.85	19.36	23.15	21.35	22.97	19.42	20.54	19.20
22:0	22.00	22.00	22.00	22.00	22.00	22.00	22.00	22.00	22.00	22.00
22:1 n-9	22.21	22.20	22.26	21.74	22.58	22.20	22.49	21.78	22.03	21.70
22:4 n-6	23.23	22.98	23.35	21.29	24.51	22.98	24.29	21.40	22.29	21.15
22:5 n-3	23.91	23.51	24.02	21.36	25.62	23.59	25.33	21.49	22.62	21.19
22:6 n-3	24.21	23.60	24.18	21.22	25.62	23.56	25.54	21.21	22.65	21.02
23:0	23.00	23.00	23.00	23.00	23.00	23.00	23.00	23.00	23.00	23.00
24:0	24.00	*	24.00	24.00	24.00	24.00	24.00	24.00	24.00	24.00
24:1 n-9	24.23	*	24.29	23.75	24.62	24.23	24.55	23.79	24.05	23.71

* Not eluted

7.2 Kovats indexes for FAME in GLC793 on 10 different columns

FAME	BP20	DB225	DB23	DB5	IL100[a]	IL61	IL82[a]	RTX200	RTX50	RXI1
12:0	1801	1760	1817	1525	-	1887	-	1673	1640	1507
14:0	2007	1970	2031	1726	-	2110	-	1877	1842	1707
14:1 n-5	2045	2001	2071	1713	-	2141	-	1869	1856	1690
15:0	2111	2075	2139	1826	-	2222	-	1979	1944	1807
16:0	2214	2181	2246	1927	-	2335	-	2082	2045	1908
16:1 n-7	2240	2202	2275	1905	-	2355	-	2064	2050	1882
17:0	2318	2286	2354	2027	-	2447	-	2184	2147	2008
17:1 n-7	2344	2309	2384	2005	-	2470	-	2167	2152	1983
18:0	2422	2391	2462	2128	-	2559	-	2287	2249	2109
18:1 n-9	2441	2408	2485	2101	-	2574	-	2262	2249	2078
18:2 n-6	2489	2447	2537	2094	-	2618	-	2262	2267	2068
18:3 n-3	2556	2498	2603	2101	-	2679	-	2272	2297	2071
18:3 n-6	2521	2467	2567	2078	-	2633	-	2243	2271	2049
20:0	2629	2602	2678	2329	-	2784	-	2492	2452	2310
20:1 n-9	2649	2620	2703	2302	-	2802	-	2468	2453	2279
20:2 n-6	2699	2662	2758	2296	-	2851	-	2470	2473	2270
20:3 n-3	2767	2715	2827	2304	-	2915	-	2480	2505	2274
20:3 n-6	2727	2682	2788	2277	-	2870	-	2450	2476	2247
20:4 n-6	2751	2692	2807	2258	-	2871	-	2423	2475	2226
20:5 n-3	2820	2745	2876	2264	-	2936	-	2432	2507	2229
22:0	2837	2812	2893	2531	-	3009	-	2697	2656	2511
22:1 n-9	2858	2833	2921	2504	-	3031	-	2674	2658	2481
22:4 n-6	2964	2916	3038	2459	-	3118	-	2635	2685	2425
22:5 n-3	3035	2971	3110	2466	-	3186	-	2645	2719	2429
22:6 n-3	3066	2981	3128	2452	-	3184	-	2616	2722	2413
23:0	2940	2918	3001	2631	-	3121	-	2800	2757	2612
24:0	3044	[b]	3108	2732	-	3233	-	2902	2859	2712
24:1 n-9	3068	[b]	3139	2707	-	3259	-	2881	2864	2683

Notes:

a) Kovats indexes are not available for the two most polar columns

b) Not eluted

7.3 ECL values for all compounds on four columns

			ECL[b]			
Max %[a]	**Code**	**Short name**	**BPX70**	**BP20**	**DB225**	**HP5**
47.35	MOU-021	16:1 n-7	16.4760	16.2646	16.2291	15.7973
43.09	MOU-023	18:1 n-9	18.3950	18.1910	18.1653	17.7418
40.26	SAN-014	23:0 (INTERNAL STANDARD)	23.0000	23.0000	23.0029	23.0008
35.89	SAN-007	16:0	16.0000	16.0000	16.0006	16.0002
21.62	POU-036	20:5 n-3	22.5931	21.7962	21.3323	19.3689
20.16	**POU-313**	16:3 n-6	17.2703	16.9422	16.6046	15.5537
17.92	DIU-027	18:2 n-6	19.0468	18.6457	18.5354	17.6779
17.15	POU-032	18:3 n-3	19.8281	19.2864	19.0186	17.7449
16.40	SAN-005	14:0	14.0000	14.0000	14.0004	14.0004
12.38	POU-039	22:6 n-3	24.9958	24.1458	23.5466	21.2160
9.16	POU-035	20:4 n-6	21.7754	21.1392	20.8337	19.3037
8.49	POU-053	18:4 n-3	20.2694	19.5932	19.2149	17.5848
7.67	**POU-051**	16:4 n-3	18.0402	17.5755	17.0753	15.6113
5.93	**POU-052**	16:4 n-1	18.3595	17.7317	17.2346	15.6280
4.76	**POU-046**	16:3 n-4	17.7036	17.1753	16.9052	15.6896
4.13	SAN-015	24:0	24.0000	24.0000	24.0024	24.0004
3.12	**POU-049**	16:3 n-3	17.7931	17.2769	16.9830	15.7461
2.96	DIU-201	16:2 n-4	17.2472	16.8430	16.6977	15.8356
2.87	SAN-009	18:0	18.0000	18.0000	18.0010	18.0002
2.66	**POU-066**	22:5 n-6	24.1553	23.4766	23.0450	21.1433
2.31	**POU-163**	18:5 n-3	20.8173	20.1121	19.5140	17.5511
2.29	DIU-494	16:2 n-6	17.0195	16.6436	16.5133	15.6848
2.13	**UNK-292**	Unknown	12.3490	13.5340	13.6901	15.4485
1.99	MOU-079	18:1 n-7	18.4833	18.2634	18.2377	17.7947
1.93	SAN-006	15:0	15.0000	15.0000	15.0008	15.0002
1.77	**POU-059**	18:4 n-4	20.0152	19.3703	19.0128	17.4740
1.62	POU-030	18:3 n-6	19.4721	18.9472	18.7212	17.5191
1.55	MOU-275	16:1 n-9	16.3858	16.2002	16.1578	15.7518
1.50	**UNK-740**	Unknown	24.3373	25.3599	ne	27.3963
1.47	MOU-026	24:1 n-9	24.4337	24.2125	24.2138	23.7499
1.46	SAN-017	26:0	26.0000	26.0000	ne	26.0000
1.42	**MOU-795**	26:1 n-x	26.2208	26.2022	ne	25.7881
1.35	**MOU-297**	16:1 n-x	16.3946	16.5253	16.2792	15.9630
1.28	ALC-291	Branched alcohol	12.0707	13.1809	13.3860	15.2334
1.27	ALC-152	Branched alcohol	12.9250	13.9987	14.1478	15.8000
1.24	**POU-068**	18:5 n-1	20.6880	19.9387	19.3545	17.4123
1.13	OTH-744	Ster. degr. prod.	27.5032	26.9641	ne	25.9114
0.97	**POU-307**	18:3 n-7	19.2598	18.7933	18.5624	17.4442
0.91	**UNK-165**	Unknown	16.7816	17.3364	17.0851	17.2840
0.89	**UNK-166**	Unkn. FAME	21.2160	19.7483	19.8876	18.0586
0.87	POU-038	22:5 n-3	24.7500	23.8521	23.4592	21.3597
0.86	**POU-054**	20:4 n-3	22.2989	21.5737	21.2457	19.5536
0.86	OTH-681	C16H22O4	23.1182	20.5108	20.3062	16.3892
0.84	DMA-809	DMA	17.9094	15.6164	14.7561	10.7741
0.83	DIU-091	16:2 n-7	16.9616	16.6068	16.4631	15.6632
0.83	**DIU-779**	16:2 conj	18.5105	18.1099	17.7459	16.5970

Continued

			ECL[b]			
Max %[a]	**Code**	**Short name**	**BPX70**	**BP20**	**DB225**	**HP5**
0.77	**MOU-769**	22:1 n-x	22.2595	22.2238	22.1413	21.8038
0.70	OTH-796	Sterol. Degr.	26.8168	26.2931	19.0322	25.0856
0.69	POU-033	20:3 n-6	21.4919	20.9182	20.7442	19.4878
0.69	**SOH-742**	22:0-2OH	26.5640	26.1542	25.0922	23.2821
0.69	**UNK-478**	Unknown	12.5766	13.6318	13.8474	15.5824
0.68	SAN-013	22:0	22.0000	22.0000	22.0023	22.0004
0.58	**UNK-743**	Unknown	27.4680	26.9363	ne	23.2961
0.50	**UNK-768**	Unknown	26.7962	27.4195	ne	nd
0.47	DMA-802	DMA	14.6257	14.9152	14.9502	15.2840
0.46	**MOU-571**	24:1 n-x	24.2707	MOU-026	24.1562	23.8137
0.45	ALD-710	14:0 Ald	14.0225	13.1532	13.5263	12.8735
0.45	**UNK-761**	Unknown	18.9509	18.3773	18.3325	17.3810
0.43	MOU-255	16:1 n-5	16.6105	16.3910	16.3414	15.8949
0.42	**UNK-760**	Unknown	18.9245	18.3494	18.3084	17.3644
0.42	**UNK-820**	Sterol Der.	ne	27.8509	ne	26.8807
0.41	SAN-003	12:0	12.0000	12.0000	12.0001	12.0003
0.40	**UNK-780**	Unknown	25.5028	22.0534	22.3140	18.2404
0.40	**MOU-770**	24:1 n-x	24.2160	24.1881	24.1132	23.7776
0.39	OTH-745	Ster. degr. prod.	27.2859	26.8299	ne	25.8765
0.39	POU-034	20:3 n-3	21.8581	21.3057	21.0571	19.7531
0.38	**UNK-801**	Unknown	20.7655	20.2737	19.0710	16.9816
0.38	DMA-811	DMA	26.9862	27.5186	ne	28.4219
0.37	MOU-024	20:1 n-9	20.3981	20.1855	20.1734	19.7353
0.37	**UNK-798**	Unknown	25.1949	22.1735	22.3781	18.7340
0.36	**UNK-730**	Unknown	18.2586	21.2659	21.3775	23.6368
0.36	**POU-583**	Unkn. FAME (PUFA)	22.0651	21.2298	20.6891	18.6248
0.36	MOU-436	17:1 n-8	17.4330	17.2232	17.1947	16.7660
0.35	MOU-442	15:1 n-6	15.5321	15.3231	15.2781	14.8396
0.35	**UNK-804**	Unknown	23.3230	21.8367	20.9440	17.9315
0.35	**POU-069**	21:5 n-3	23.7421	22.8784	22.4554	20.3814
0.34	ART-746	Benzyl butyl phthalate	25.1128	27.5562	ne	20.1738
0.33	ALC-728	Branched alcohol	sd	12.8466	13.0947	14.9906
0.32	**UNK-782**	Unknown	25.1966	22.1772	nd	nd
0.32	DMA-788	DMA	15.8901	14.8574	14.5415	12.6932
0.32	OTH-797	Sterol. Degr.	26.6059	26.1654	ne	25.0441
0.32	OTH-816	Methyl 4-ketohex-5-enoate	12.7301	sd	sd	sd
0.31	MOU-327	17:1 n-6	17.5387	17.3223	17.2855	16.8397
0.31	**UNK-805**	Unknown	nd	17.4708	17.3409	16.2830
0.30	OTH-178	Cholestadiene	27.1465	26.4670	ne	25.4507
0.30	OTH-772	Sterol	28.4072	27.5817	ne	26.5157
0.30	**UNK-781**	Unknown	25.4184	22.0052	22.2695	18.2596
0.30	**UNK-492**	Unkn. FAME	23.2937	21.7708	21.9513	20.0671
0.30	ALC-295	Branched alcohol	14.8607	15.5903	15.8361	17.1021
0.28	**SOH-769**	16:0-3OH	21.5316	20.7473	19.7155	17.4853
0.28	**UNK-814**	Unknown	13.0600	14.1950	14.4428	16.4929
0.27	**UNK-736**	Unknown	13.5972	14.6222	15.0240	17.3319
0.27	SAN-008	17:0	17.0000	17.0000	17.0000	17.0000
0.27	**UNK-767**	Unknown	24.3961	24.5234	ne	23.9445
0.26	POU-037	22:4 n-6	23.9164	23.1838	22.9433	21.2874

Continued

			ECL[b]			
Max %[a]	**Code**	**Short name**	**BPX70**	**BP20**	**DB225**	**HP5**
0.26	**POU-245**	20:4 NMI	22.1383	21.4616	21.1392	19.5087
0.26	**UNK-747**	Unknown	26.8467	27.8290	ne	nd
0.26	SAN-011	20:0	20.0000	20.0000	20.0023	20.0003
0.25	MOU-020	14:1 n-5	14.5984	14.3916	14.3335	13.8851
0.25	SAN-019	28:0	28.0000	28.0000	ne	28.0000
0.25	**MOU-807**	27:1 n-x	27.2234	27.2056	ne	26.7887
0.24	MOU-025	22:1 n-9	22.4144	22.1951	22.1897	21.7377
0.23	DMA-817	DMA	17.7692	15.3489	14.6737	10.6624
0.23	**UNK-810**	Unknown	13.6536	14.5261	14.8397	16.4929
0.22	**ALK-752**	Unknown	12.0598	13.2146	sd	sd
0.22	**UNK-778**	Unknown	27.3884	25.1700	ne	nd
0.22	**UNK-732**	Unknown	17.2193	17.4867	17.7491	18.5378
0.21	**UNK-759**	Unknown	16.7252	17.8387	18.2269	20.7932
0.21	**UNK-741**	Unknown	24.4260	25.4533	ne	27.4551
0.21	**POU-318**	24:6 n-3	27.2869	26.1814	ne	23.1910
0.21	**UNK-784**	Unknown	25.2699	22.2264	ne	18.7680
0.20	**UNK-822**	Unknown	26.9516	24.8533	nd	nd
0.20	SAN-016	25:0	25.0000	25.0000	25.0000	25.0000
0.20	**UNK-735**	Unknown	12.7708	13.9020	14.3394	16.7940
0.18	DMA-791	DMA	14.8577	13.8370	13.4827	11.7322
0.15	**SAD-691**	9:0 dME	16.8315	15.2287	14.8099	12.2470
0.11	**POU-751**	24:5 n-6	26.4063	25.4883	ne	23.1116
0.11	DIU-028	20:2 n-6	21.0662	20.6549	20.5621	19.6809
0.09	SOH-222	12:0-2OH	16.1331	15.9193	14.7211	13.1565
0.09	SAB-077	ai-15:0	14.7114	14.6741	14.7047	14.7138
0.08	SAB-078	i-15:0	14.5096	14.5272	14.5553	14.6328
0.08	SOH-223	12:0-3OH	17.3667	16.6517	15.5720	13.4471
0.02	SAN-012	21:0	21.0000	21.0000	21.0000	20.9999
0.01	SAN-004	13:0	13.0000	13.0000	13.0000	13.0000
F	FUR-185	DiMeF(9,3)	19.8849	19.5676	19.3003	17.8732
F	FUR-186	MeF(9,5)	20.8835	20.5541	20.2493	18.8147
F	FUR-187	MeF(11,3)	21.1548	20.8153	20.7338	19.0094
F	FUR-188	DiMeF(9,5)	21.4702	21.1695	20.9707	19.5611
F	FUR-189	DiMeF(11,3)	21.9295	21.6003	21.3528	19.8819
F	FUR-190	MeF(11,5)	22.9115	22.5682	22.2800	20.8072
F	FUR-191	DiMeF(11,5)	23.5242	23.2000	23.0234	21.5677
C	MOB-286	16:1 n-10, 7Me (b)	16.9214	16.8914	16.8272	16.5551
C	MOB-289	16:1 n-10, 7Me (a)	16.5520	16.5525	16.4988	16.2717
C	MOU-087	20:1 n-7	20.4971	20.2749	20.2575	19.8015
C	MOU-258	18:1 n-5	18.6166	18.3968	18.3531	17.8961
C	MOU-262	22:1 n-11	22.3491	22.1392	22.1343	21.6972
C	POU-067	24:5 n-3	26.8258	25.8727	ne	23.3539
C	SAB-071	Phytanic acid ME	16.7969	16.9443	17.1553	17.6846
C	SAB-073	ai-17:0	16.7133	16.6745	16.7030	16.7135
C	SAB-074	i-17:0	16.5068	16.5235	16.5494	16.6290
C	UNK-288	Unknown	19.7199	19.1361	19.0860	18.1261
S	ALC-713	Isophytol	16.1235	16.6900	16.1542	16.2050
S	ALC-714	Phytol isom.	19.1660	19.4078	18.4658	17.5991
S	ALC-715	Phytol isom.	19.5936	19.8226	18.8351	17.8397

Continued

			ECL[b]			
Max %[a]	**Code**	**Short name**	**BPX70**	**BP20**	**DB225**	**HP5**
S	ALD-484	16:0 Ald	16.0632	15.2171	15.5813	14.9228
S	ALD-712	12:0 Ald	11.9506	11.1562	11.5017	sd
S	CYC-220	9,10-cyclo-17:0	17.4337	17.2846	17.2141	16.8559
S	CYC-221	9,10-cyclo-19:0	19.3893	19.2456	19.1842	18.8281
S	DIU-029	22:2 n-6	23.0974	22.6777	22.5955	21.6911
S	MOH-709	Ricinoleic acid ME	25.5222	23.8293	22.9458	19.6167
S	MOU-022	17:1 n-7	17.4774	17.2596	17.2319	16.7935
S	OXP-716	Ox18:3 n-3	23.0935	21.2620	21.1857	18.4249
S	POU-717	CLnA (x8,x10,x12)	22.7231	21.6683	21.1677	19.1336
S	POU-718	CLnA (x8,x10,x12)	22.9303	21.8431	21.3367	19.2593
S	POU-719	CLnA (x8,x10,x12)	23.1417	22.1100	21.5436	19.5316
S	POU-720	CLnA (x8,x10,x12)	23.2044	22.1553	21.5837	19.5713
S	POU-721	CLnA (x9,x11,x13)	22.7227	21.6674	21.1649	19.1316
S	POU-722	CLnA (x9,x11,x13)	22.9292	21.8416	21.3364	19.2582
S	POU-723	CLnA (x9,x11,x13)	23.1402	22.1071	21.5402	19.5287
S	POU-724	CLnA (x9,x11,x13)	23.2027	22.1523	21.5801	19.5684
S	SAB-072	i-16:0	15.5089	15.5248	15.5532	15.6323
S	SAD-703	12:0 dME	19.9423	18.2673	17.8934	15.2527
S	SAD-704	14:0 dME	22.0269	20.3010	19.9523	17.2560
S	SAD-705	16:0 dME	24.1394	22.3493	22.0334	19.2633
S	SAD-706	18:0 dME	26.2737	24.4045	24.1231	21.2734
S	SAN-001	8:0	sd	8.0000	8.0000	sd
S	SAN-002	10:0	10.0000	10.0000	10.0000	sd
S	SAN-010	19:0	19.0000	19.0000	19.0000	19.0000
S	SAN-018	27:0	27.0000	27.0000	ne	27.0000
S	SAN-218	11:0	11.0000	11.0000	11.0000	11.0000
S	SOH-219	10:0-2OH	14.0784	13.8889	12.6735	11.1295
S	SOH-224	14:0-2OH	18.1821	17.9555	16.7697	15.1731
S	SOH-225	14:0-3OH	19.4412	18.6914	17.6325	15.4654
S	SOH-226	16:0-2OH	20.2567	SAN-011	18.8305	17.1953
S	SOH-707	18:0-2OH	22.3459	22.0483	20.9086	19.2156
S	SOH-708	18:0-12OH	25.4123	23.8377	22.9939	19.9398
S	SOH-771	10:0-3OH	15.3079	14.6245	sd	sd

Notes:

(a) A numeric value refers to the highest percentage found in algae with either BPX70 or BP20, F, C and S denotes the source of supporting compounds, furan fatty acid sample, cod liver oil or standard, respectively.

(b) A compound code instead of a numeric value means that the compound was overlapping with that of the corresponding compound code, sd means that the compound was lost in the solvent delay, ne means not eluted and nd refers to peaks that are assumed to be present in the chromatogram, but that were not detected.

To be included in the list the compound had to be present above the 0.2% limit and detected on more than one column, or identified and detected on all columns if it was below the 0.2% limit.

7.4 Compounds used in the ECL-evaluation and identification sheets

Code	Name	Code	Name	Code	Name
CYC-220	9,10-cyclo-17:0	MOU-262	22:1 n-11	POU-718	CLnA (x8,x10,x12)
CYC-221	9,10-cyclo-19:0	MOU-275	16:1 n-9	POU-719	CLnA (x8,x10,x12)
DIU-027	18:2 n-6	MOU-327	17:1 n-6	POU-720	CLnA (x8,x10,x12)
DIU-028	20:2 n-6	MOU-436	17:1 n-8	POU-721	CLnA (x9,x11,x13)
DIU-029	22:2 n-6	MOU-442	15:1 n-6	POU-722	CLnA (x9,x11,x13)
DIU-091	16:2 n-7	POU-030	18:3 n-6	POU-723	CLnA (x9,x11,x13)
DIU-201	16:2 n-4	POU-032	18:3 n-3	POU-724	CLnA (x9,x11,x13)
DIU-494	16:2 n-6	POU-033	20:3 n-6	SAB-071	Phytanic acid ME
FUR-185	DiMeF(9,3)	POU-034	20:3 n-3	SAB-072	i-16:0
FUR-186	MeF(9,5)	POU-035	20:4 n-6	SAB-073	ai-17:0
FUR-187	MeF(11,3)	POU-036	20:5 n-3	SAB-074	i-17:0
FUR-188	DiMeF(9,5)	POU-037	22:4 n-6	SAB-074	i-17:0
FUR-189	DiMeF(11,3)	POU-038	22:5 n-3	SAB-077	ai-15:0
FUR-190	MeF(11,5)	POU-039	22:6 n-3	SAB-078	i-15:0
FUR-191	DiMeF(11,5)	POU-046	16:3 n-4	SAD-691	9:0 dME
MOB-286	16:1 n-10, 7Me (b)	POU-049	16:3 n-3	SAD-703	12:0 dME
MOB-289	16:1 n-10, 7Me (a)	POU-051	16:4 n-3	SAD-704	14:0 dME
MOH-709	Ricinoleic acid ME	POU-052	16:4 n-1	SAD-705	16:0 dME
MOU-020	14:1 n-5	POU-053	18:4 n-3	SAD-706	18:0 dME
MOU-021	16:1 n-7	POU-054	20:4 n-3	SOH-219	10:0-2OH
MOU-022	17:1 n-7	POU-059	18:4 n-4	SOH-222	12:0-2OH
MOU-023	18:1 n-9	POU-066	22:5 n-6	SOH-223	12:0-3OH
MOU-024	20:1 n-9	POU-068	18:5 n-1	SOH-224	14:0-2OH
MOU-025	22:1 n-9	POU-069	21:5 n-3	SOH-225	14:0-3OH
MOU-026	24:1 n-9	POU-163	18:5 n-3	SOH-707	18:0-2OH
MOU-079	18:1 n-7	POU-307	18:3 n-7	SOH-708	18:0-12OH
MOU-087	20:1 n-7	POU-313	16:3 n-6	SOH-742	22:0-2OH
MOU-255	16:1 n-5	POU-717	CLnA (x8,x10,x12)	SOH-769	16:0-3OH
MOU-258	18:1 n-5				

7.5 Identification sheets

7.5.1 POU-313 / 16:3 n-6 / c4,c7,c10-16:3

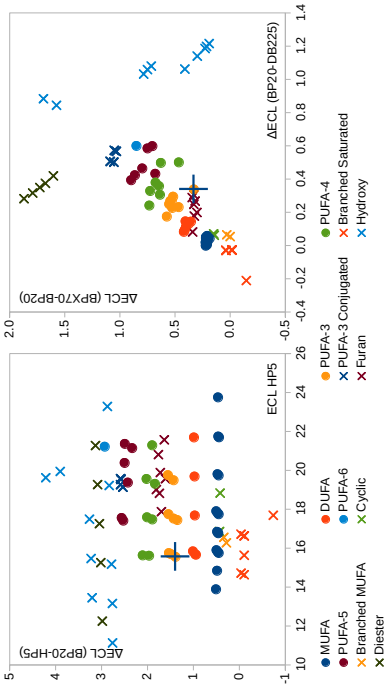

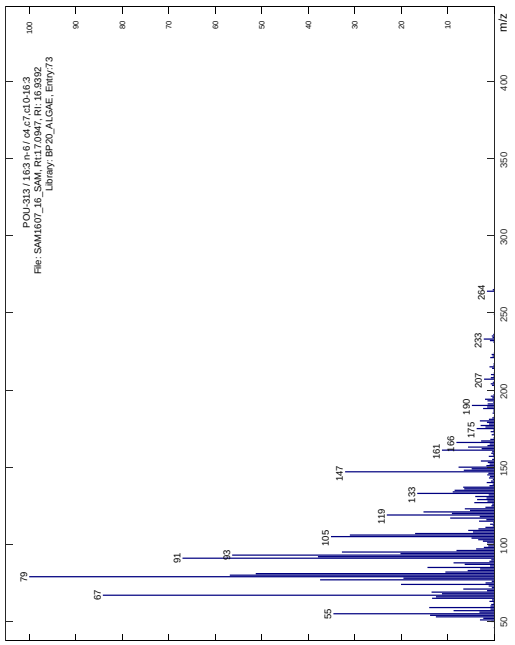

7.5.2 POU-051 / 16:4 n-3 / c4,c7,c10,c13-16:4

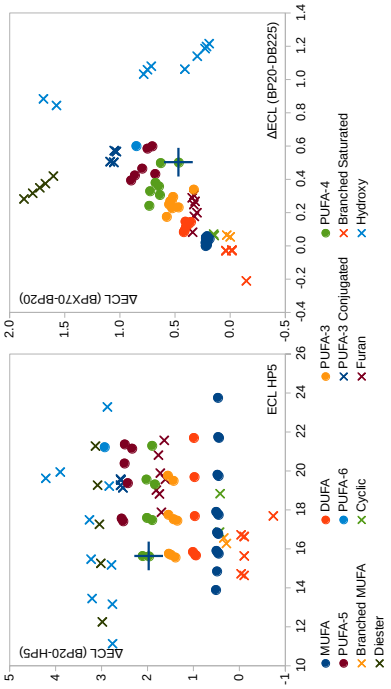

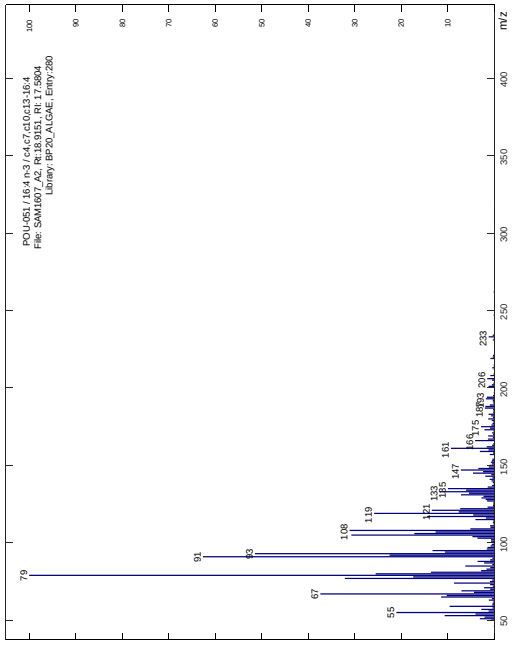

7.5.3 POU-052 / 16:4 n-1 / c6,c9,c12,c15-16:4

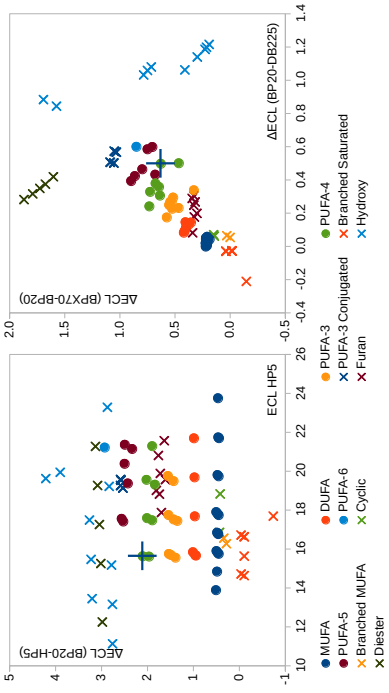

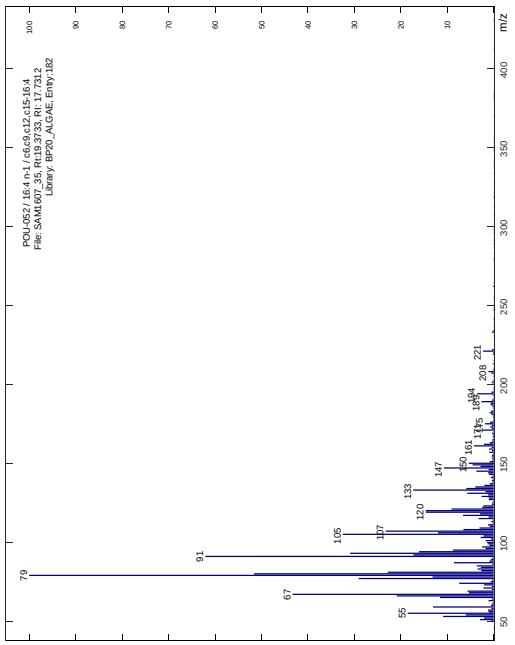

7.5.4 POU-046 / 16:3 n-4 / c6,c9,c12-16:3

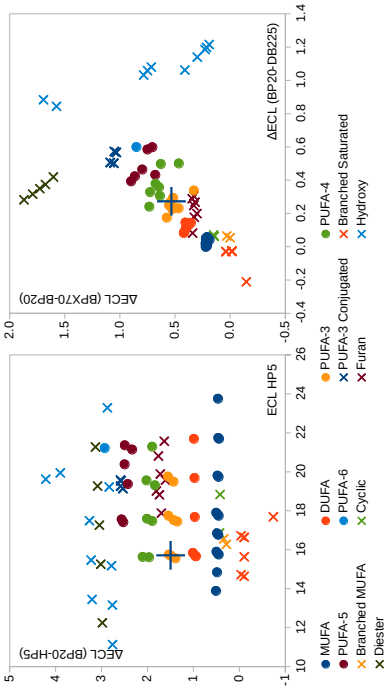

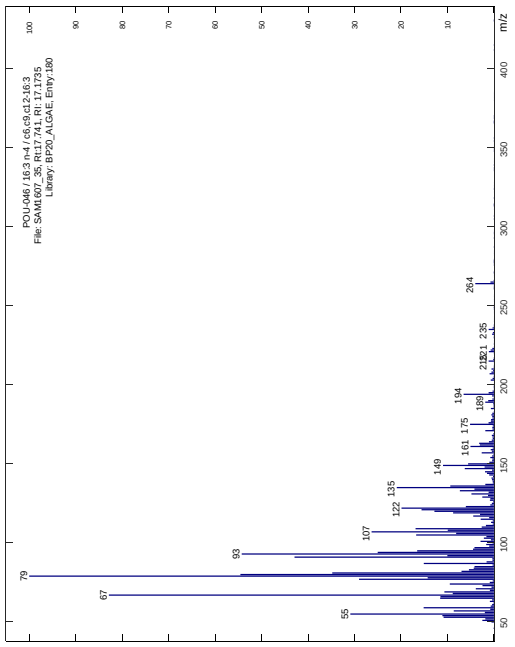

7.5.5 POU-049 / 16:3 n-3 / c7,c10,c13-16:3

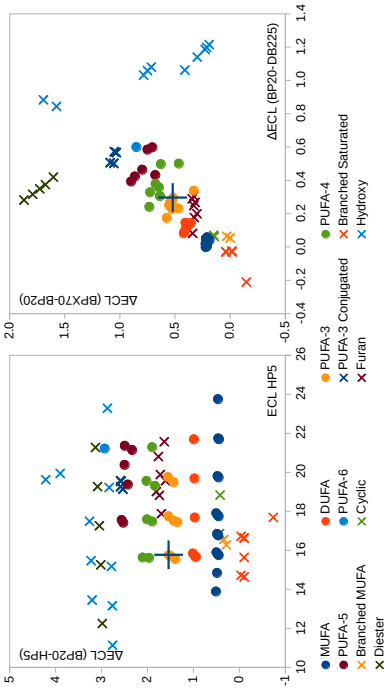

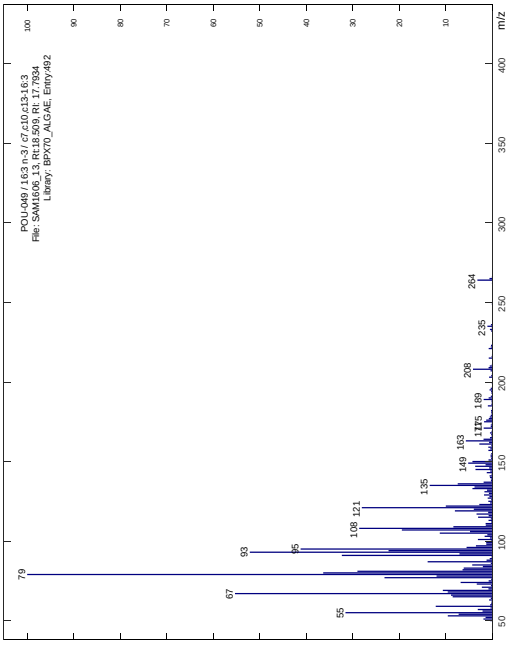

7.5.6 POU-066 / 22:5 n-6 / c4,c7,c10,c13,c16-22:5

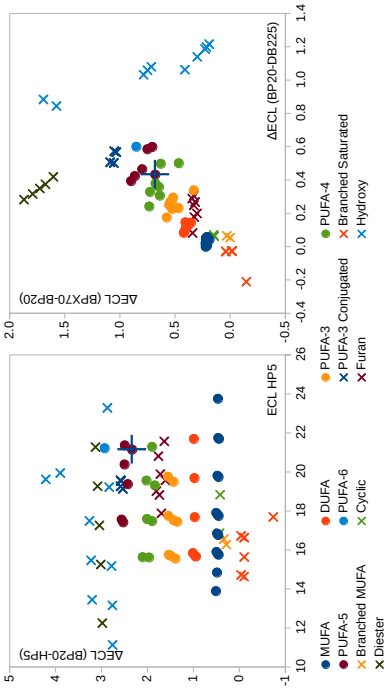

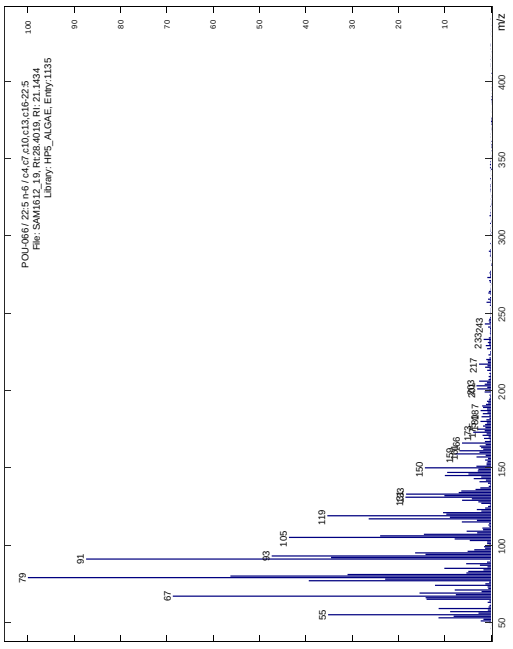

7.5.7 POU-163 / 18:5 n-3 / c3,c6,c9,c12,c15-18:3

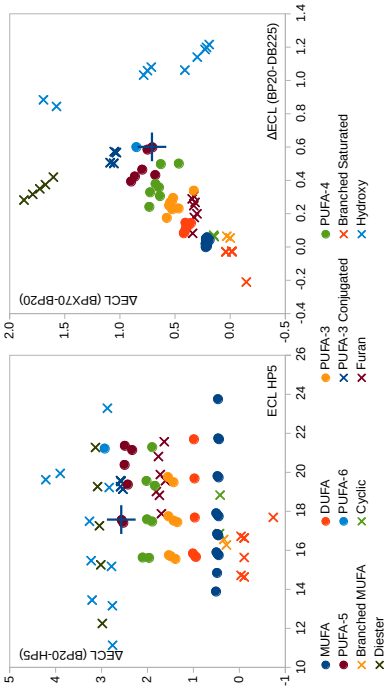

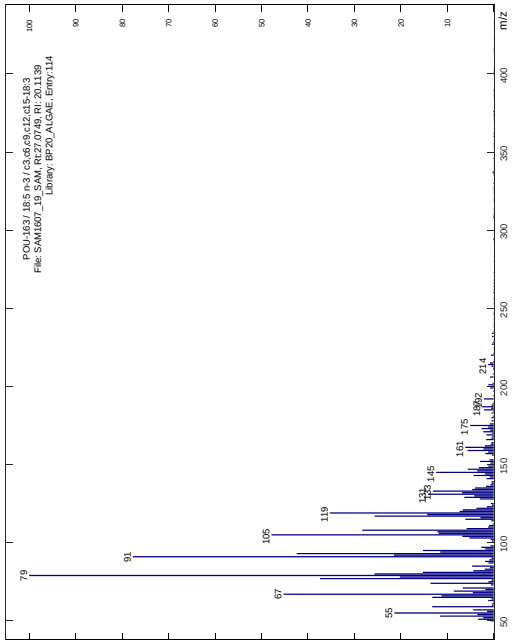

7.5.8 UNK-292 / Unknown / Unknown

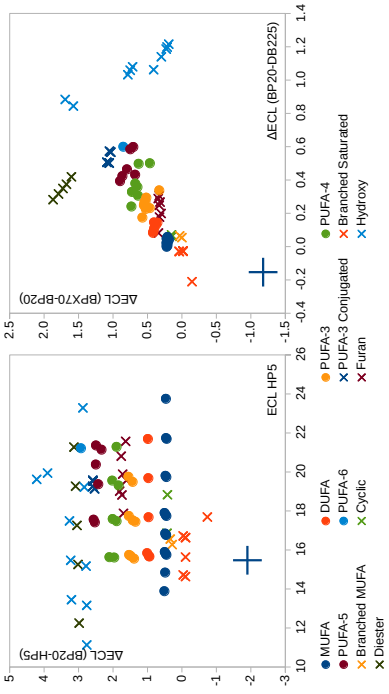

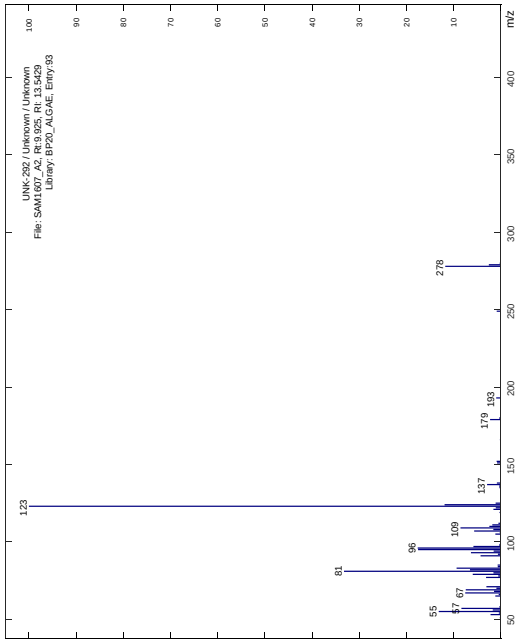

7.5.9 POU-059 / 18:4 n-4 / c5,c8,c11,c14-18:4

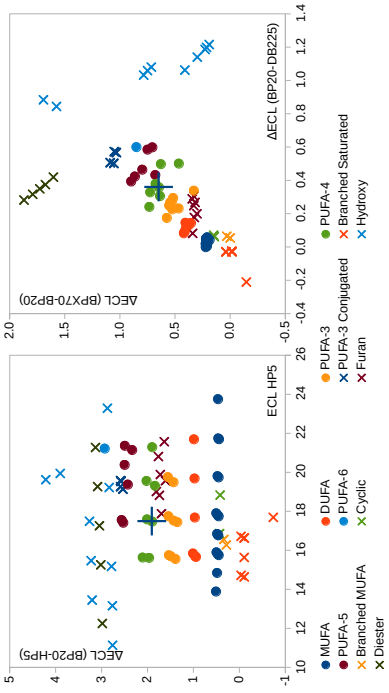

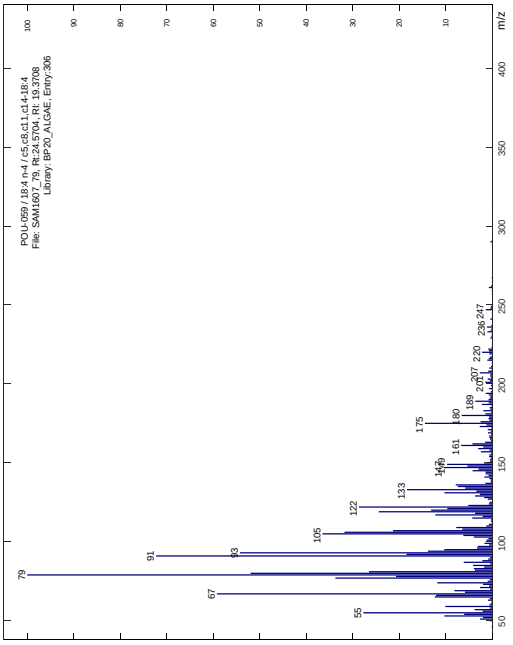

7.5.10 UNK-740 / Unknown / Unknown

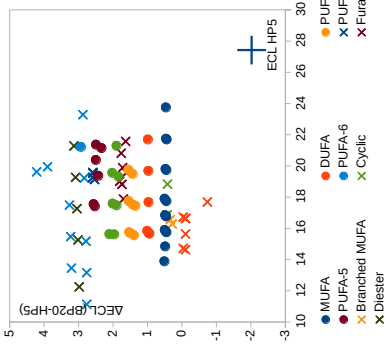

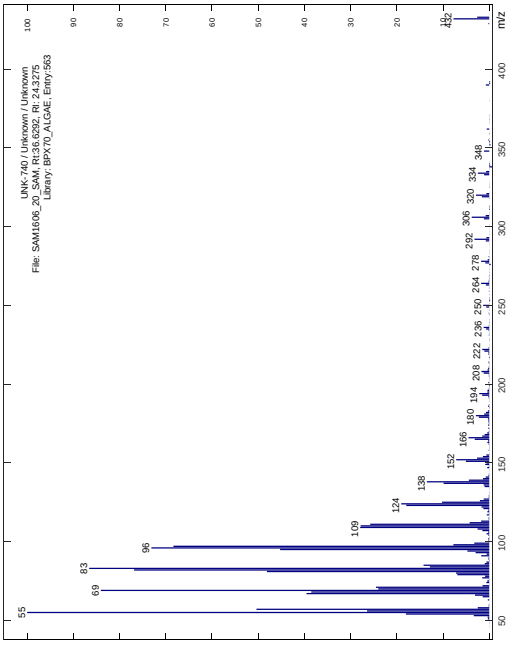

7.5.11 MOU-795 / 26:1 n-x / x-26:1

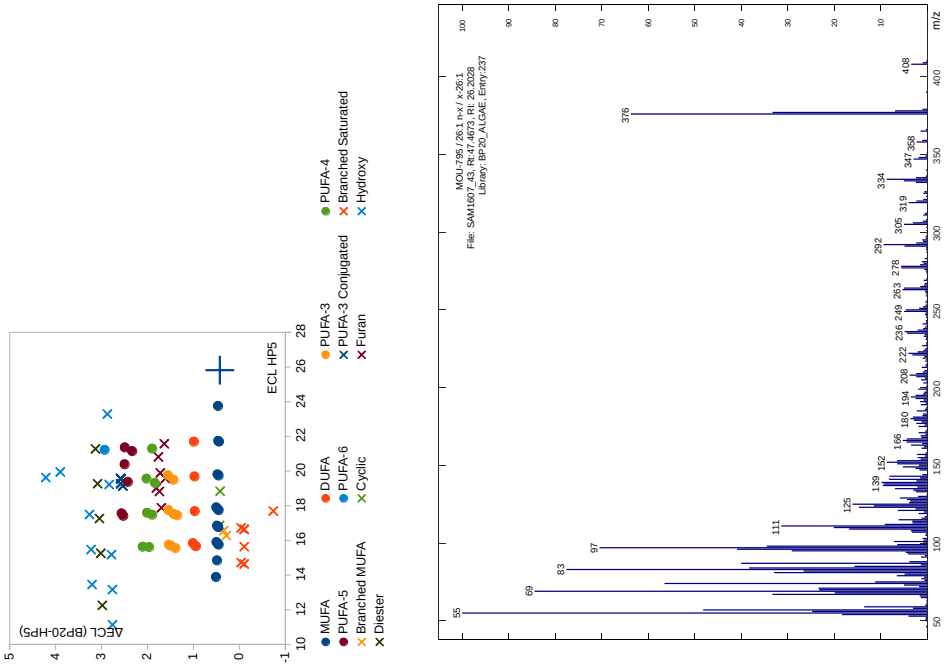

7.5.12 MOU-297 / 16:1 n-x / x-16:1

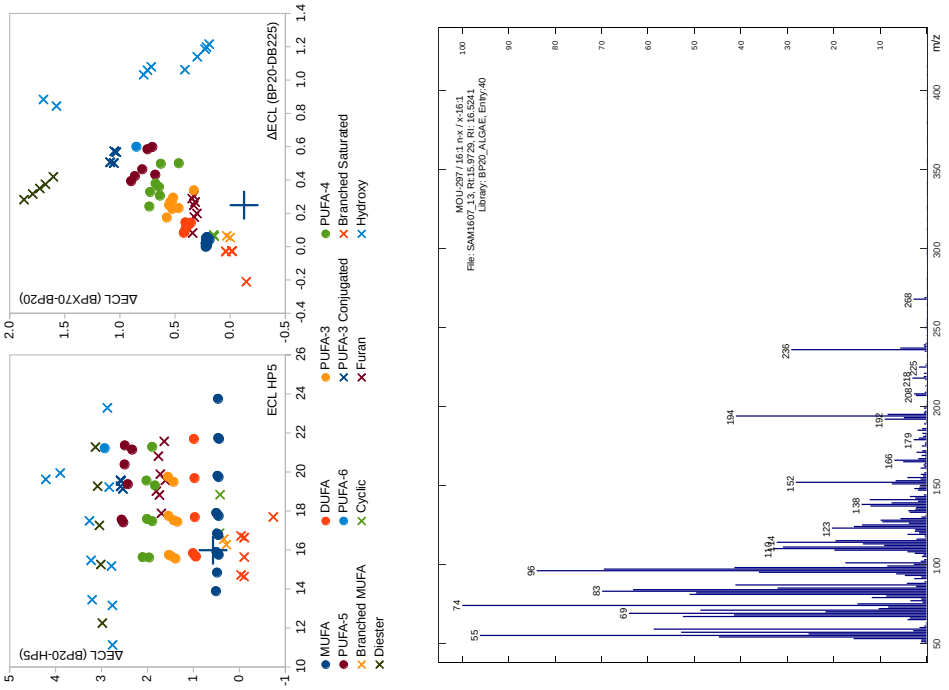

7.5.13 POU-068 / 18:5 n-1 / c5,c8,c11,c14,c17-18:5

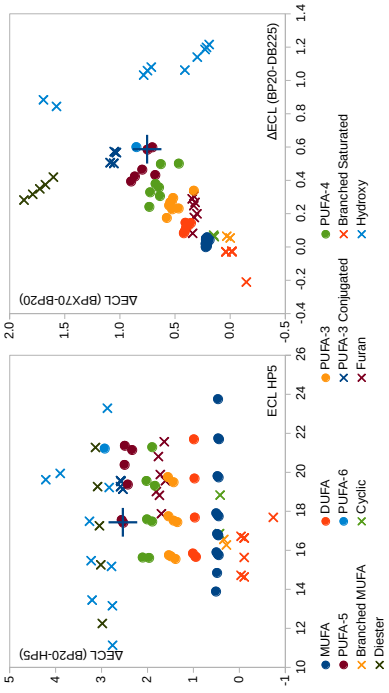

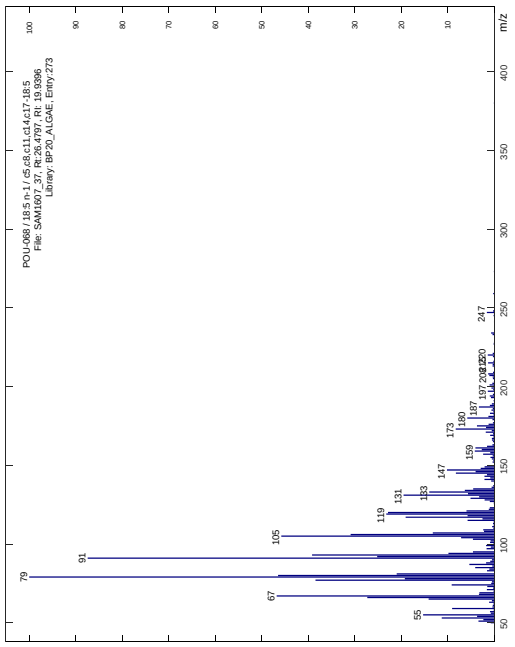

7.5.14 POU-307 / 18:3 n-7 / 5,8,11-18:3

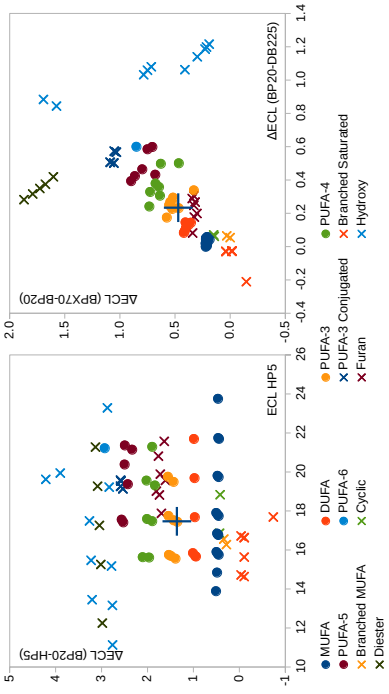

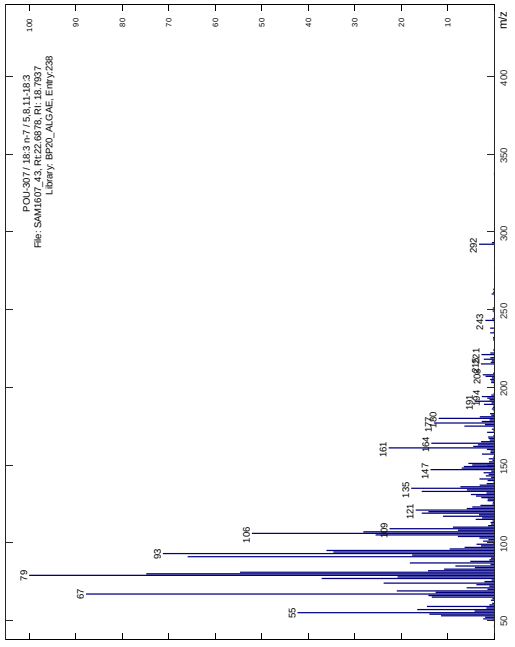

7.5.15 UNK-165 / Unknown / Unknown

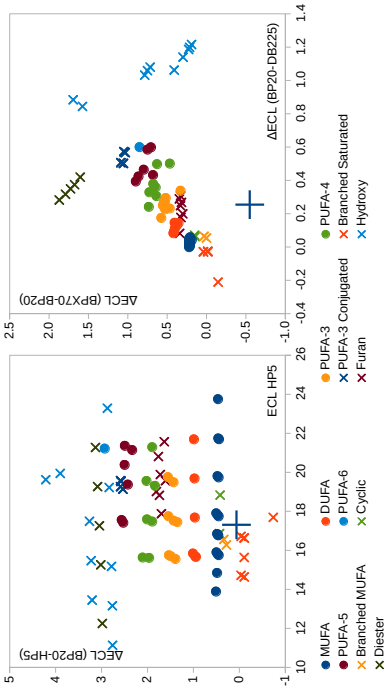

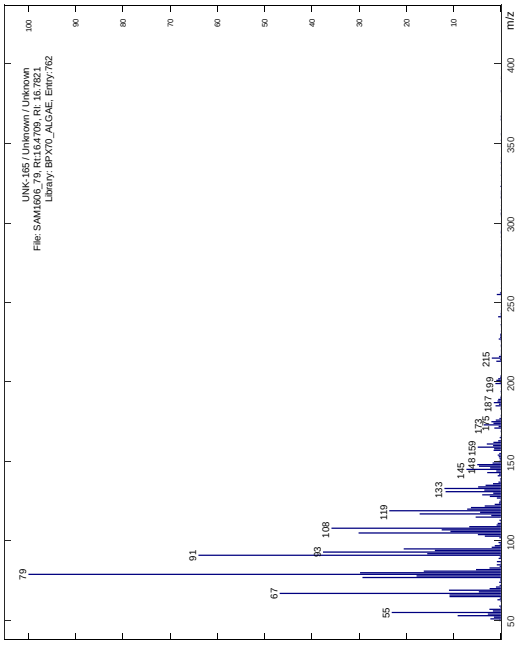

7.5.16 UNK-166 / Unkn. FAME / Unknown FAME

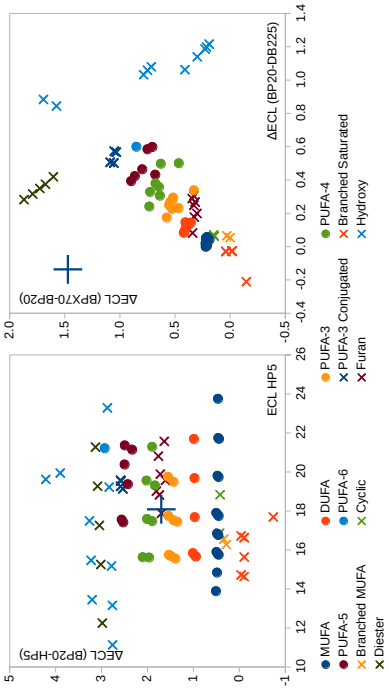

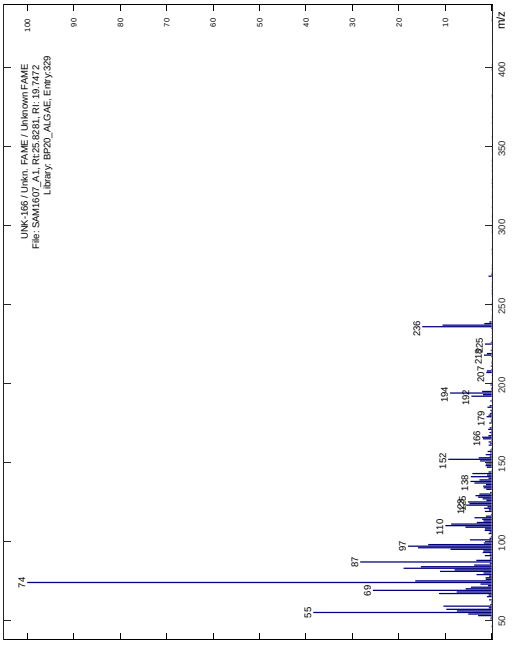

7.5.17 POU-054 / 20:4 n-3 / c8,c11,c14,c17-20:4

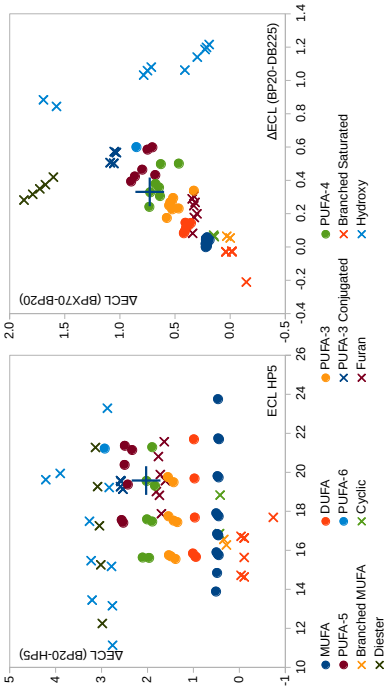

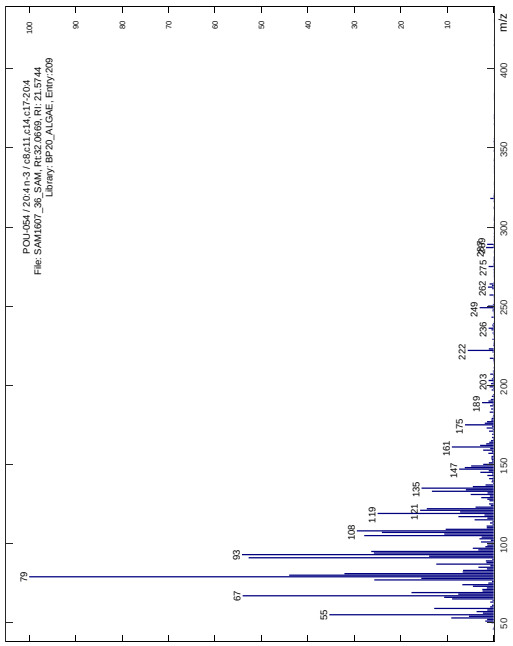

7.5.18 DIU-779 / 16:2 conj / x,x-16:2 (conj.)

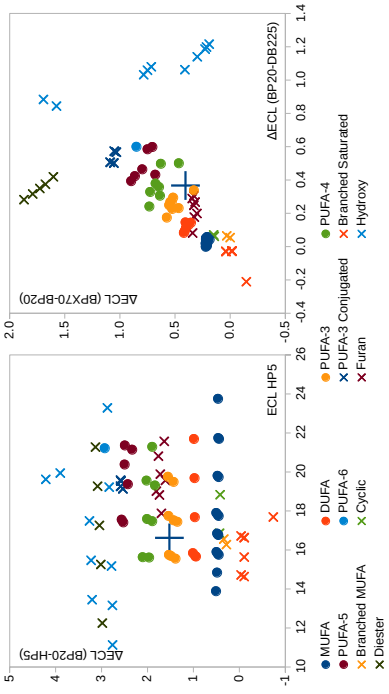

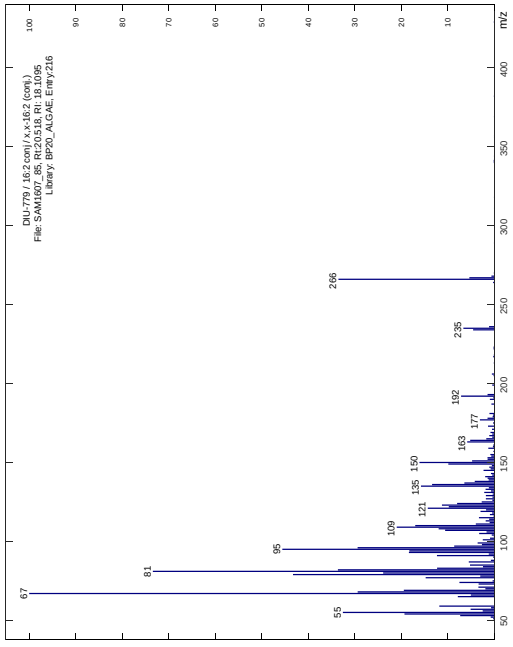

7.5.19 MOU-769 / 22:1 n-x / x-22:1

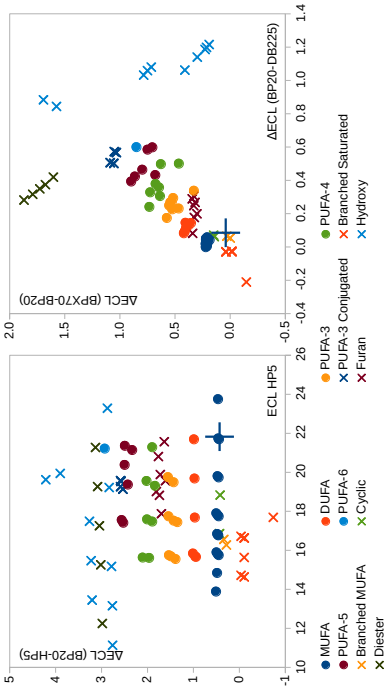

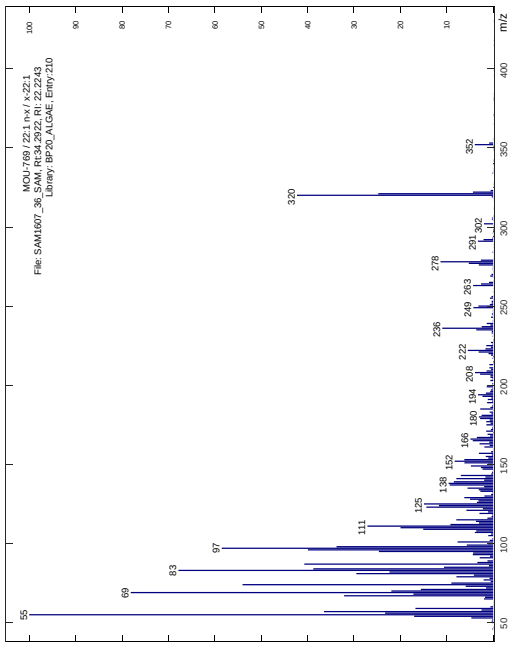

7.5.20 SOH-742 / 22:0-2OH / 2-Hydroxydocosanoic acid ME

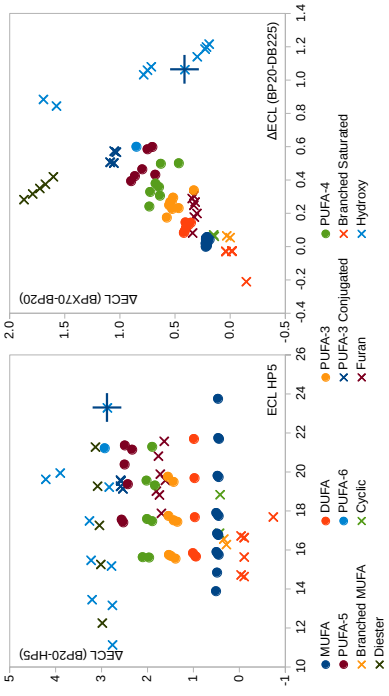

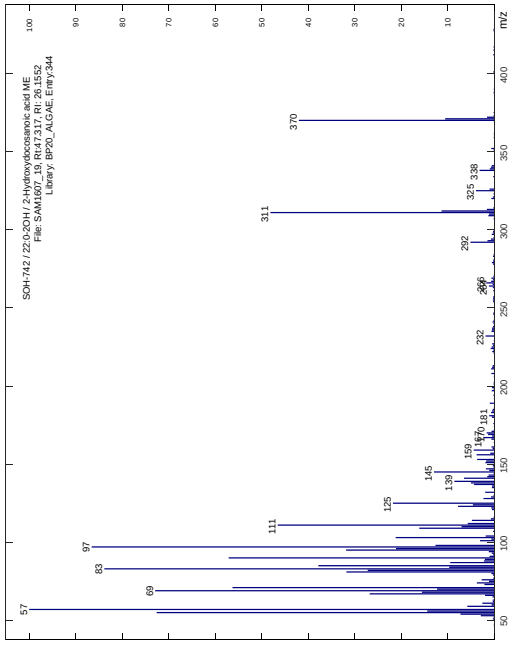

7.5.21 UNK-478 / Unknown / Unknown

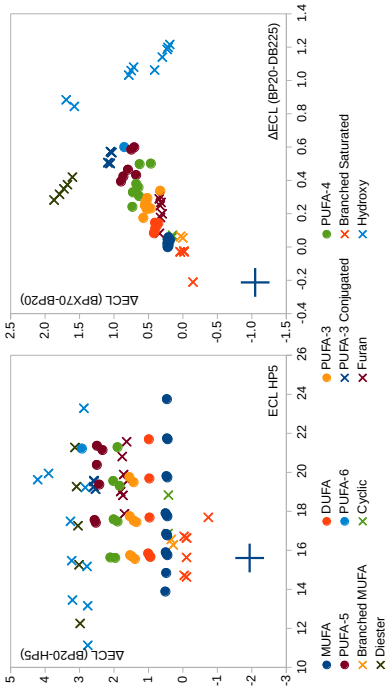

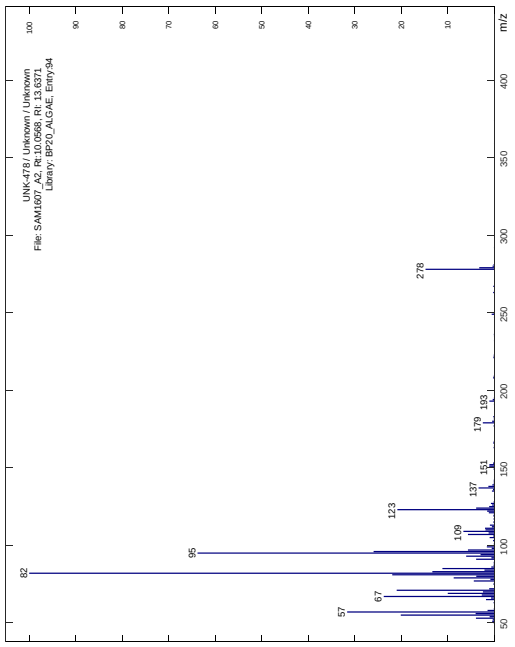

7.5.22 UNK-743 / Unknown / Unknown

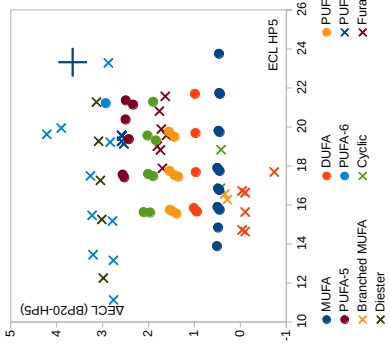

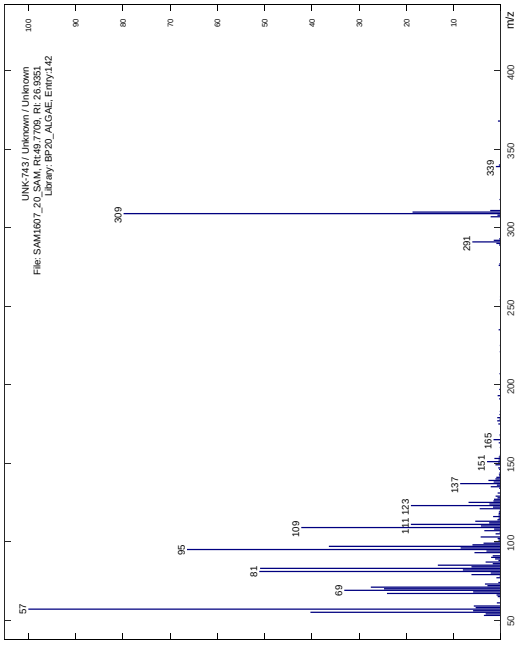

7.5.23 UNK-768 / Unknown / Unknown

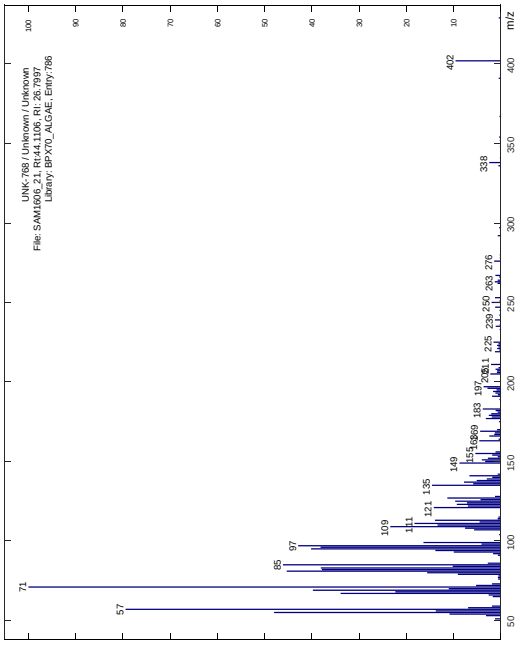

7.5.24 MOU-571 / 24:1 n-x / x-24:1

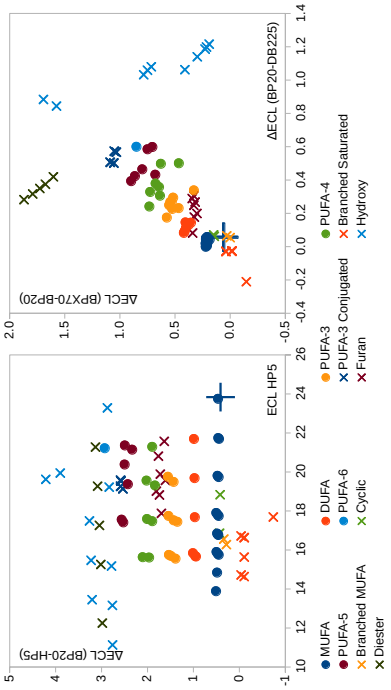

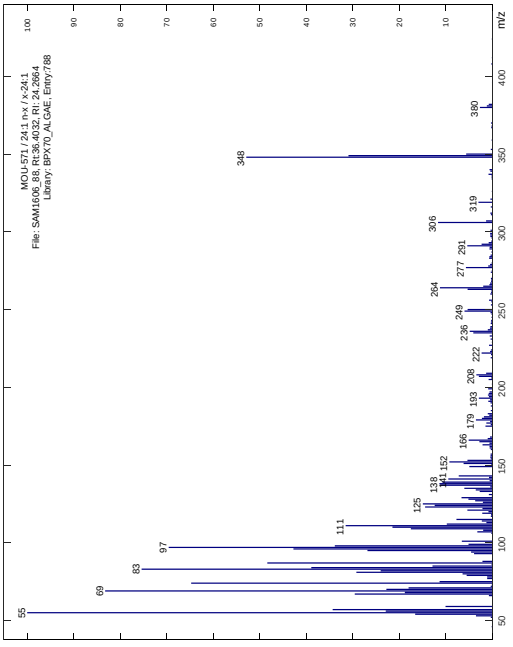

7.5.25 UNK-761 / Unknown / Unknown

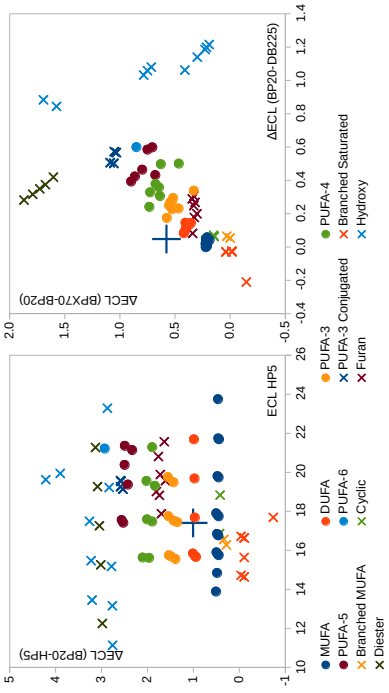

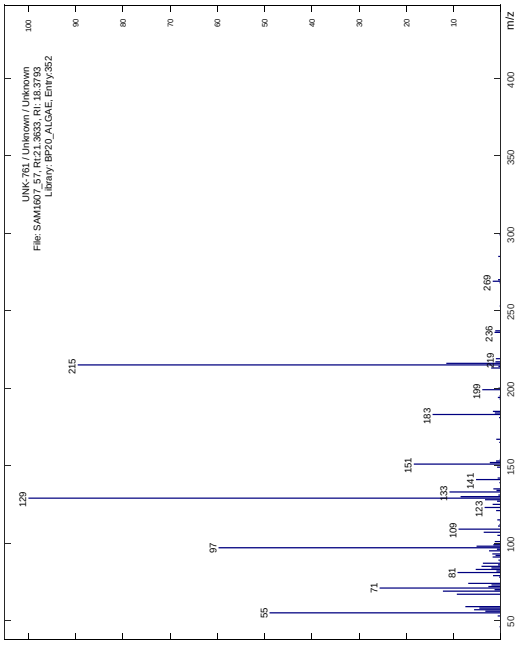

7.5.26 UNK-760 / Unknown / Unknown

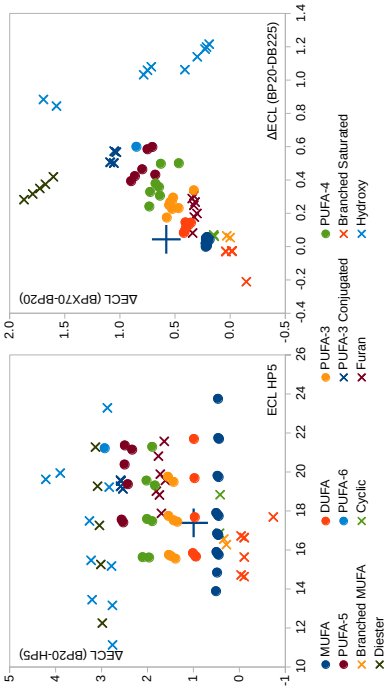

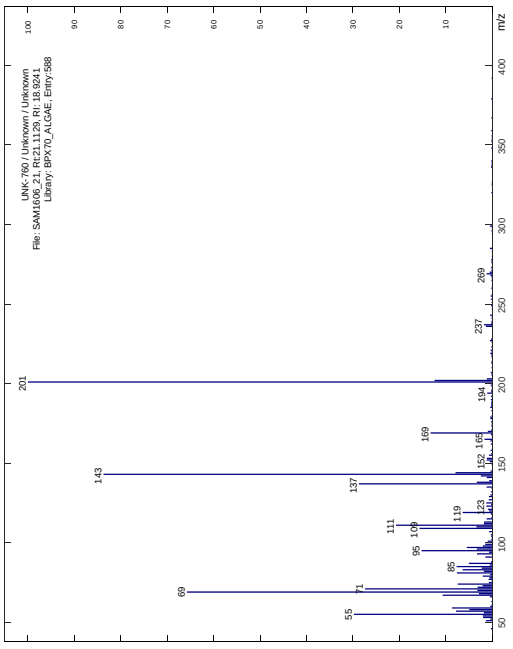

7.5.27 UNK-820 / Sterol Der. / Sterol derivative

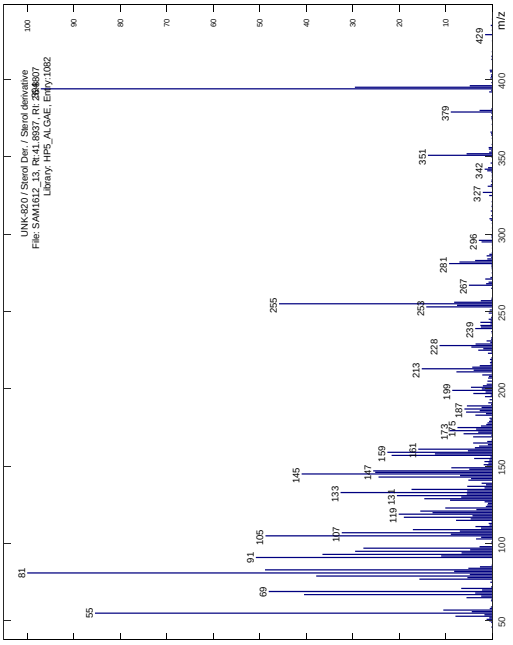

7.5.28 UNK-780 / Unknown / Unknown

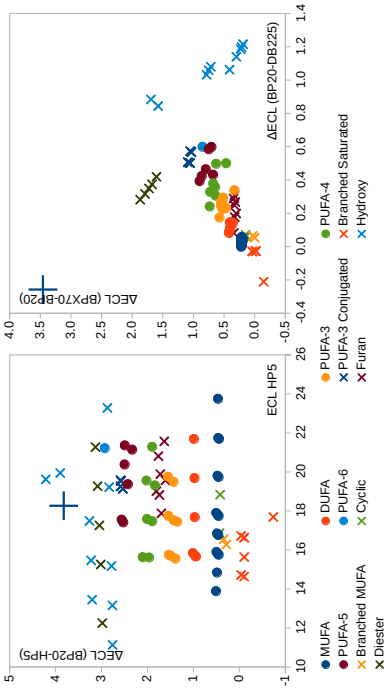

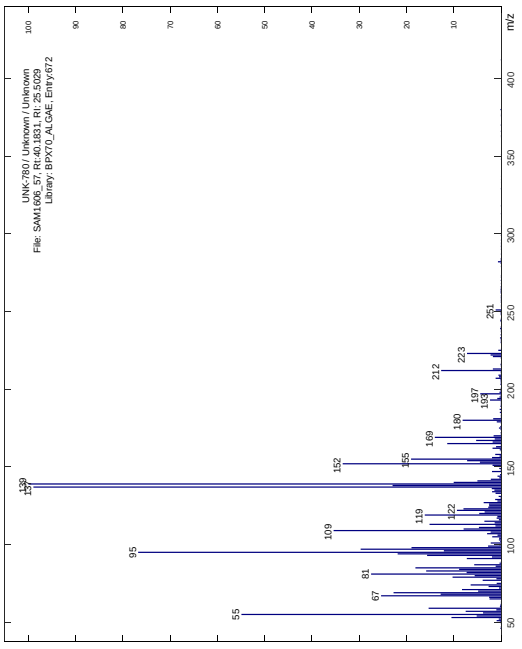

7.5.29 MOU-770 / 24:1 n-x / x-24:1

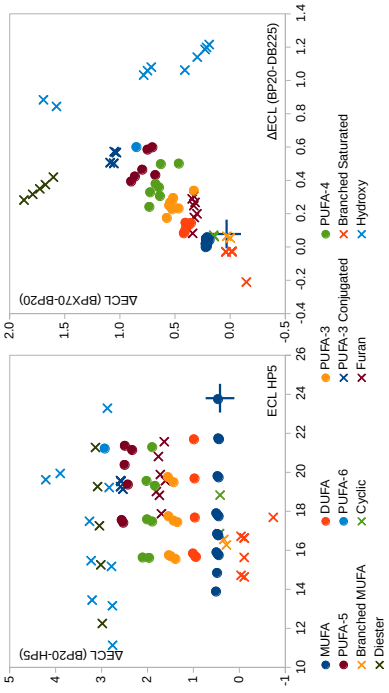

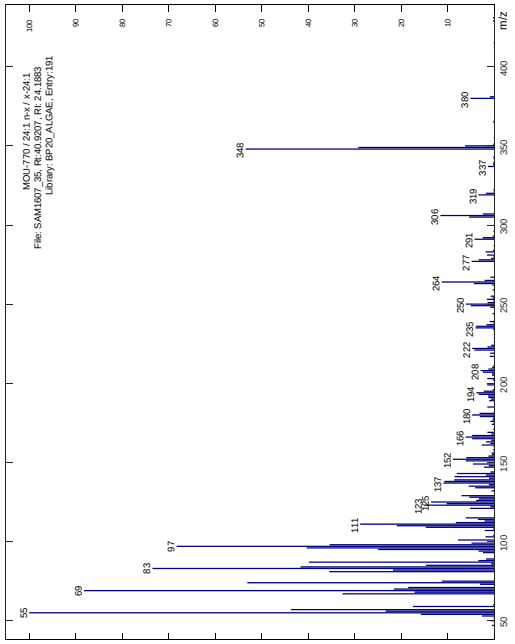

7.5.30 UNK-801 / Unknown / Unknown

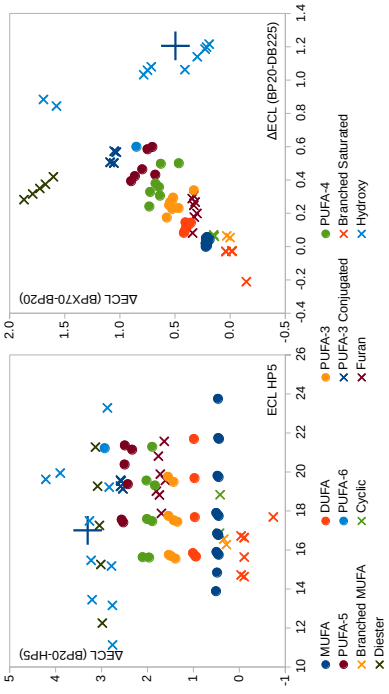

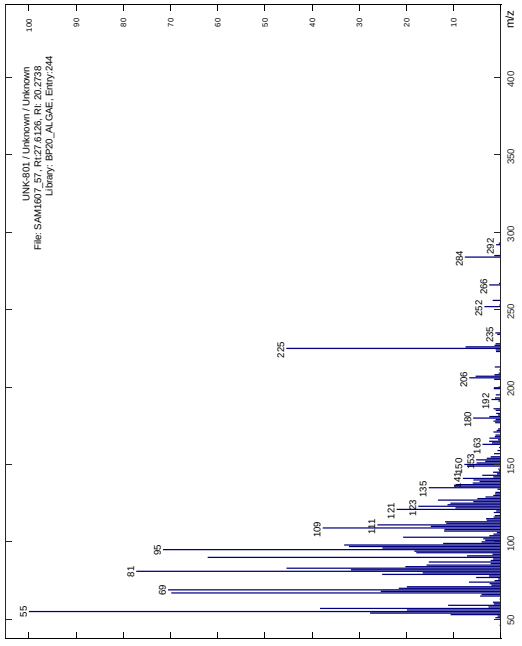

7.5.31 UNK-798 / Unknown / Unknown

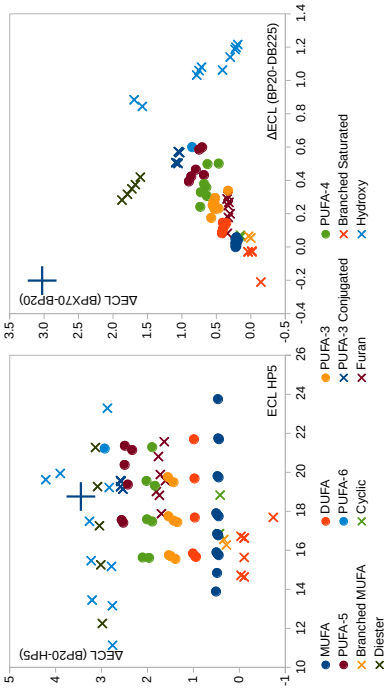

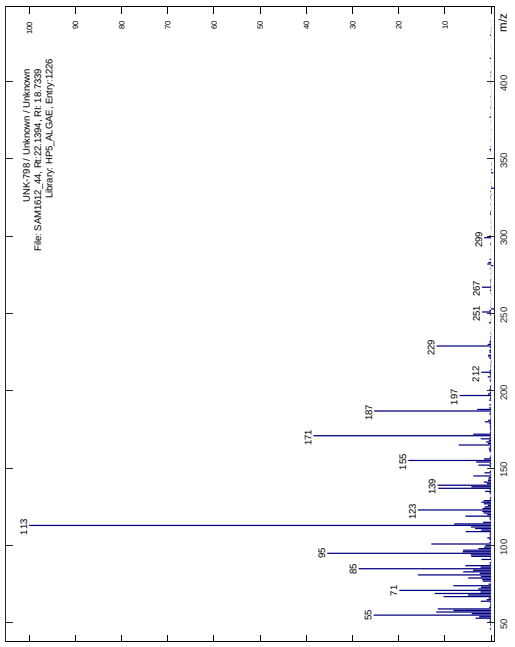

7.5.32 UNK-730 / Unknown / Unknown (alkene)

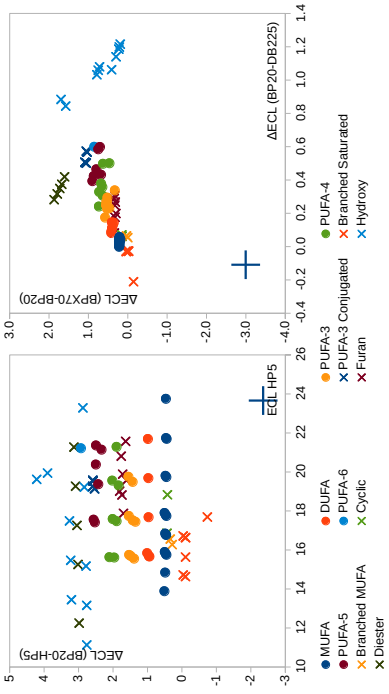

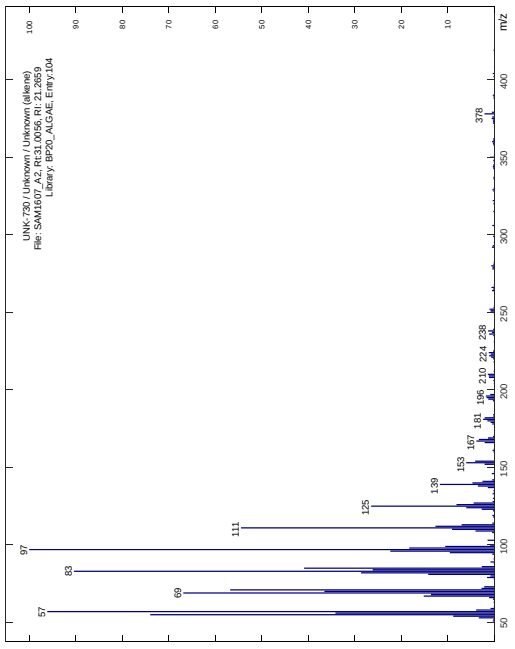

7.5.33 POU-583 / Unkn. FAME (PUFA) / Unknown FAME (PUFA)

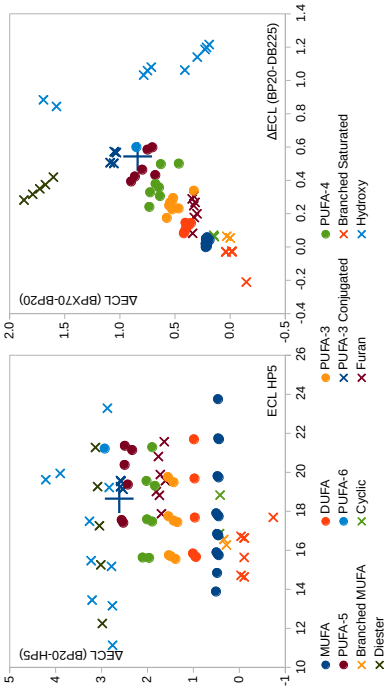

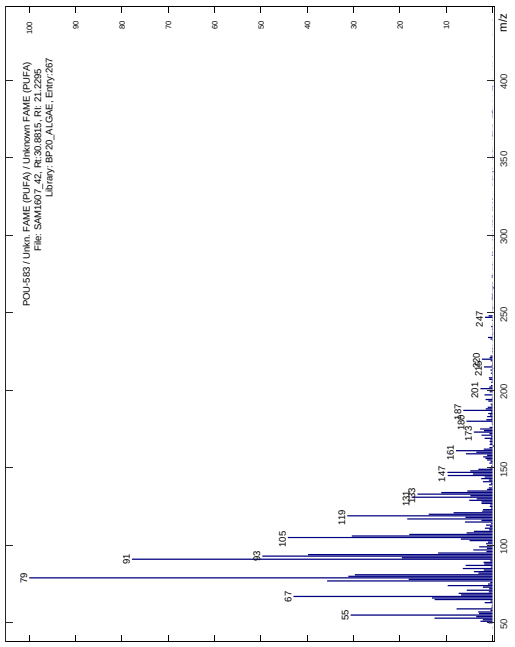

7.5.34 UNK-804 / Unknown / Unknown

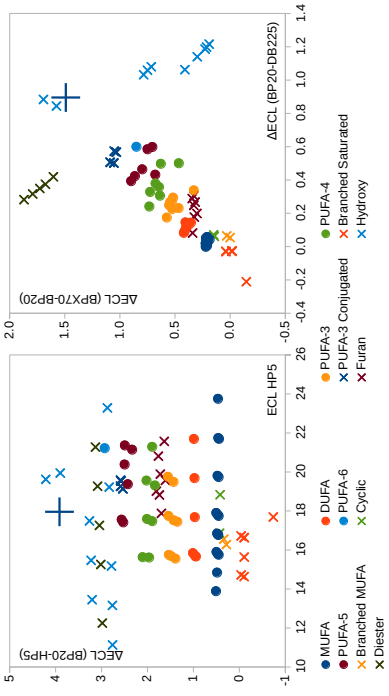

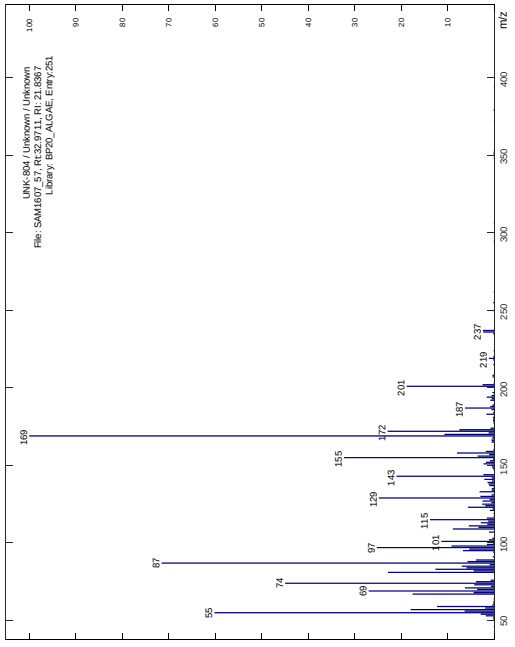

7.5.35 POU-069 / 21:5 n-3 / c6,c9,c12,c15,c18-21:5

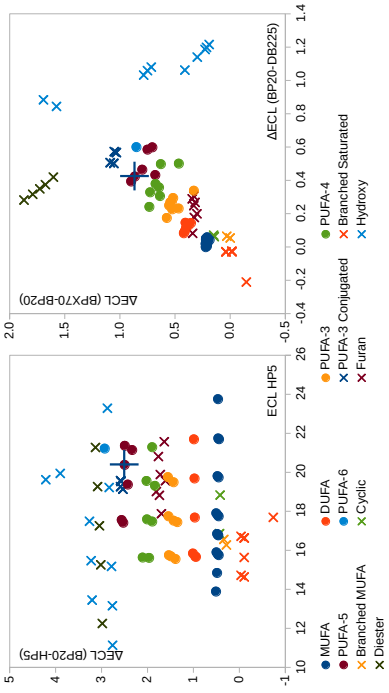

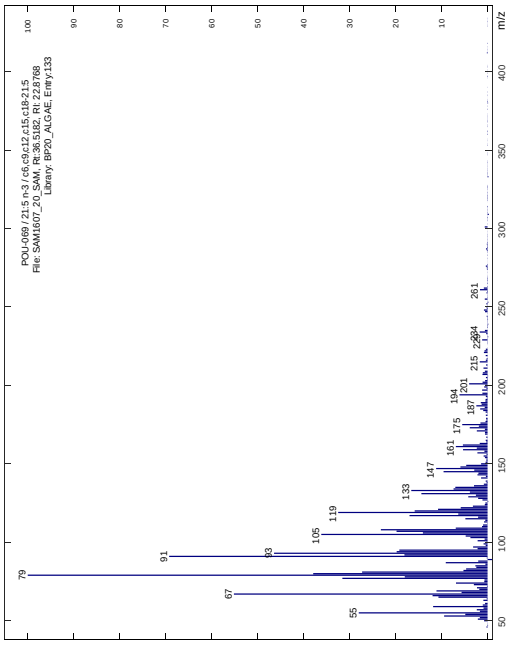

7.5.36 UNK-782 / Unknown / Unknown

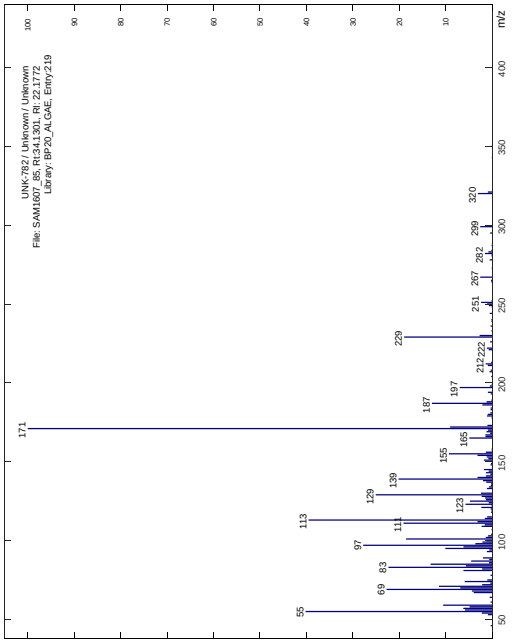

7.5.37 UNK-805 / Unknown / Unknown

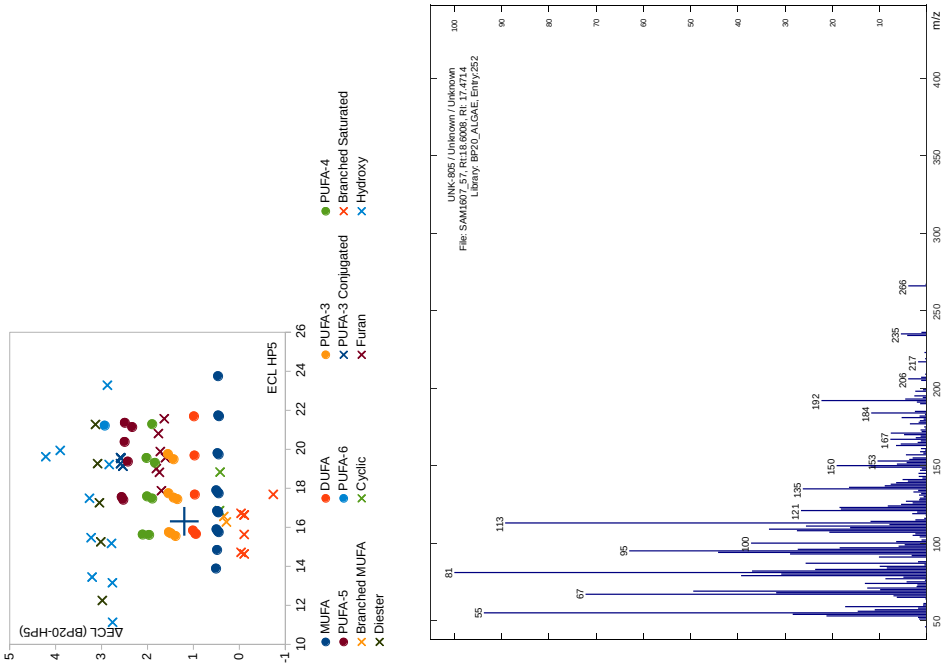

7.5.38 UNK-781 / Unknown / Unknown

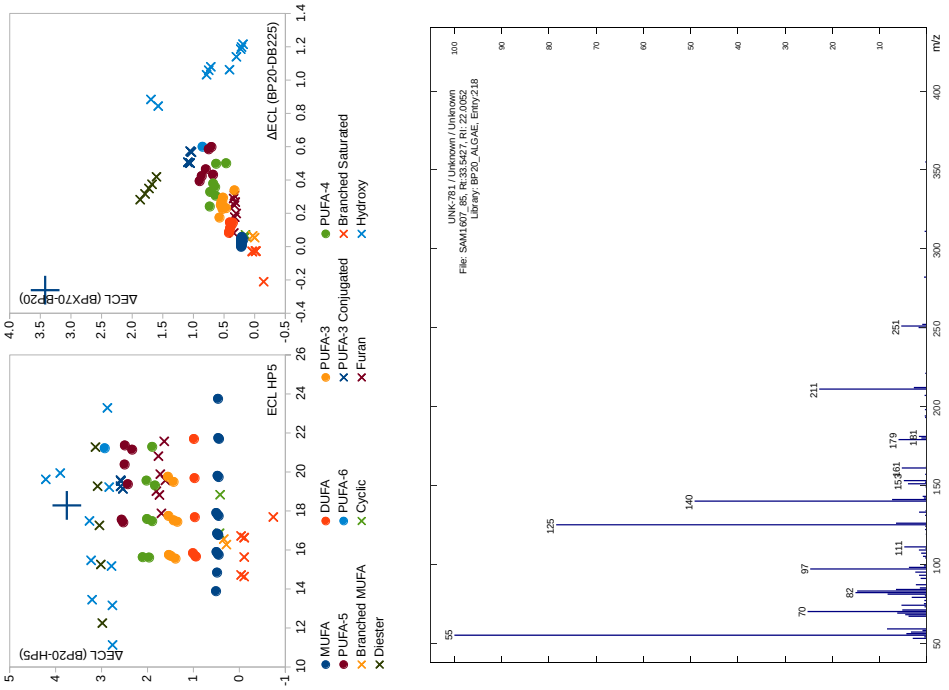

7.5.39 UNK-492 / Unkn. FAME / Unknown FAME

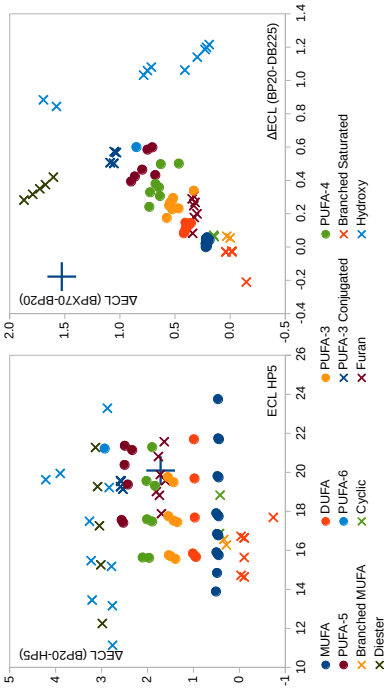

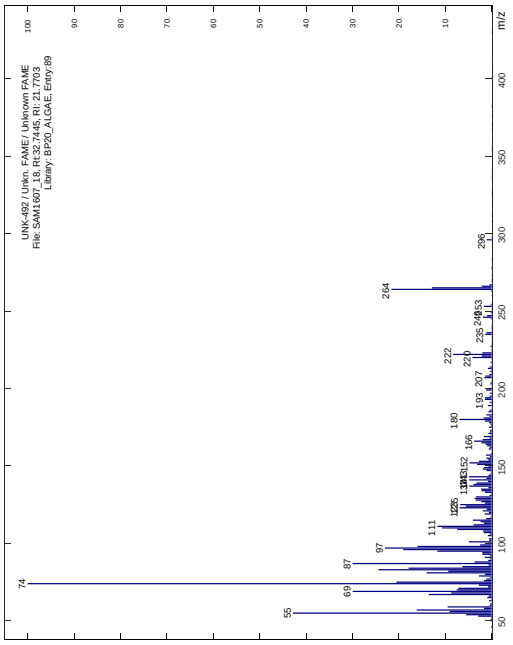

7.5.40 SOH-769 / 16:0-3OH / 3-Hydroxyhexadecanoic acid ME

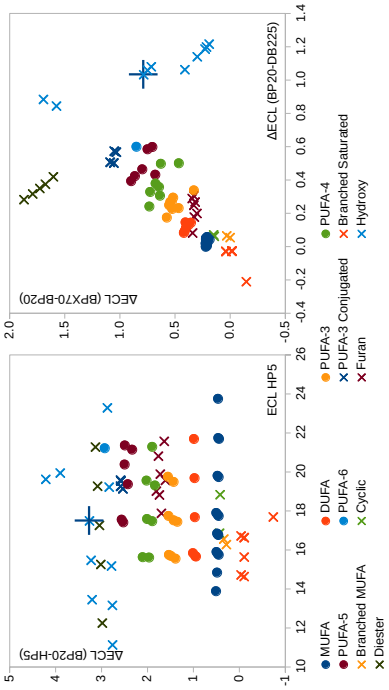

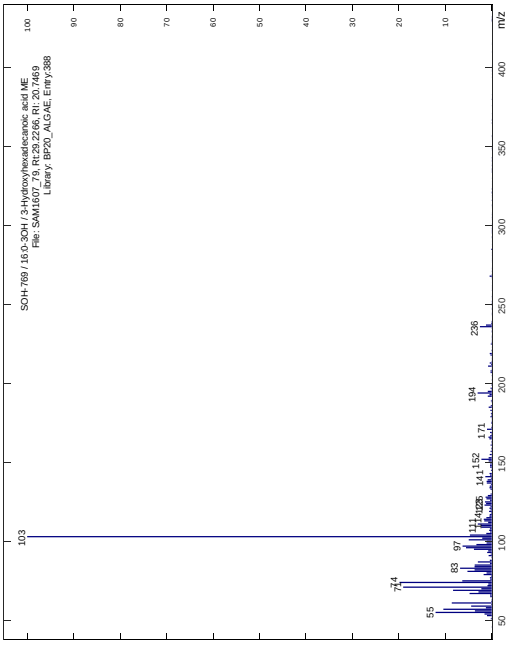

7.5.41 UNK-814 / Unknown / Unknown

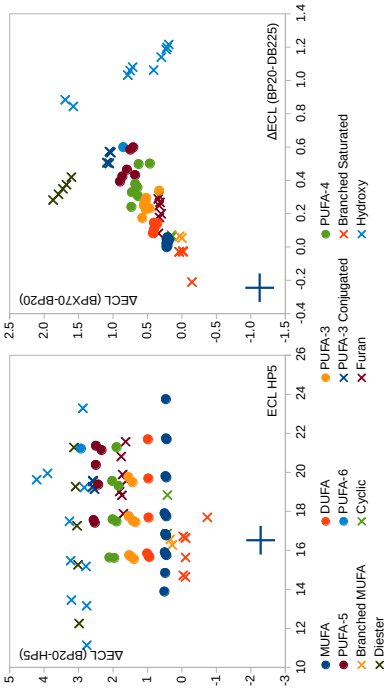

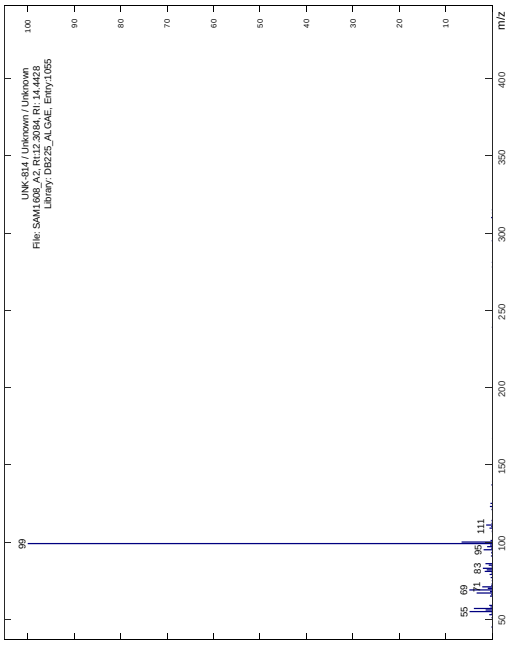

7.5.42 UNK-736 / Unknown / Unknown (br. alkane)

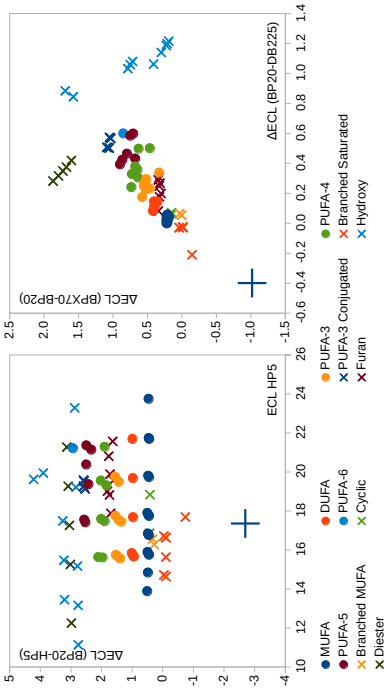

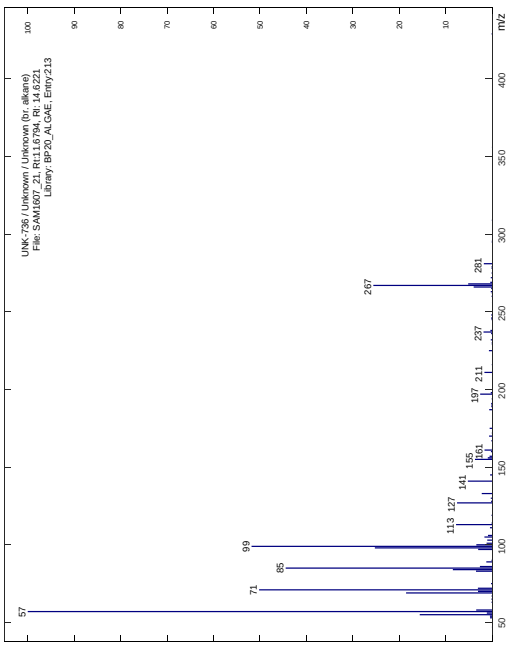

7.5.43 UNK-767 / Unknown / Unknown

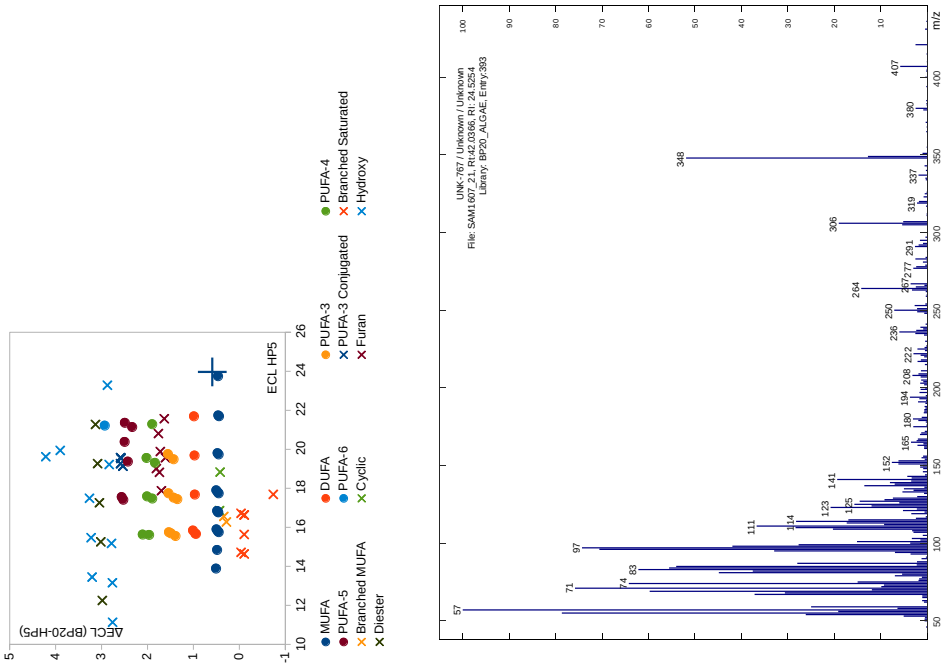

7.5.44 POU-245 / 20:4 NMI / c5,c11,c14,c17-20:4

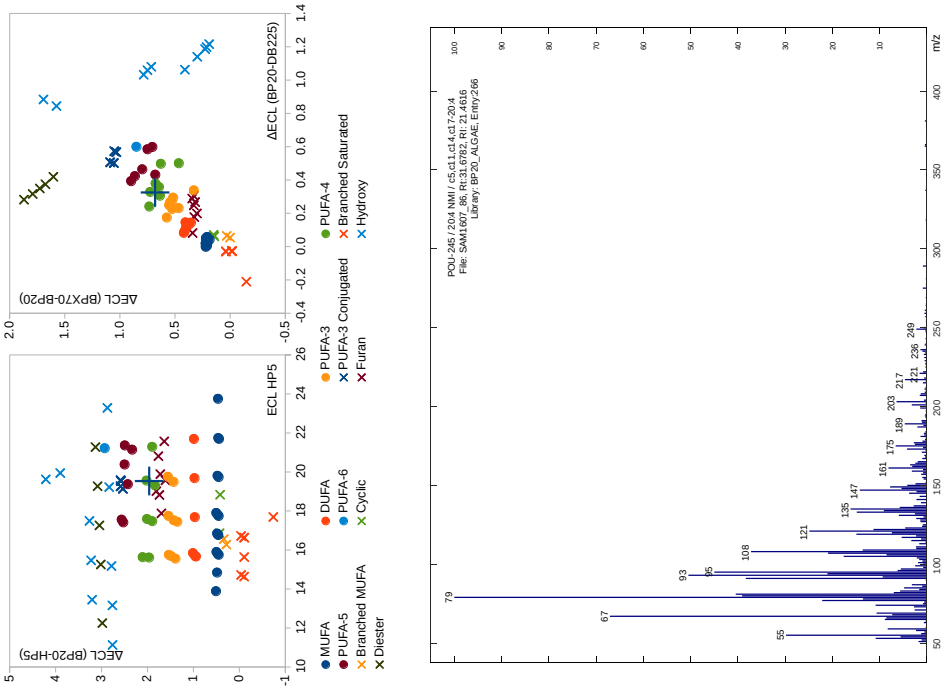

7.5.45 UNK-747 / Unknown / Unknown

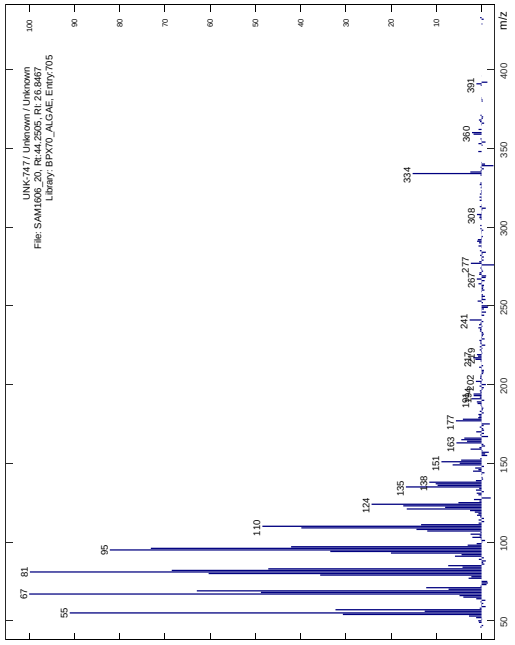

7.5.46 MOU-807 / 27:1 n-x / x-27:1

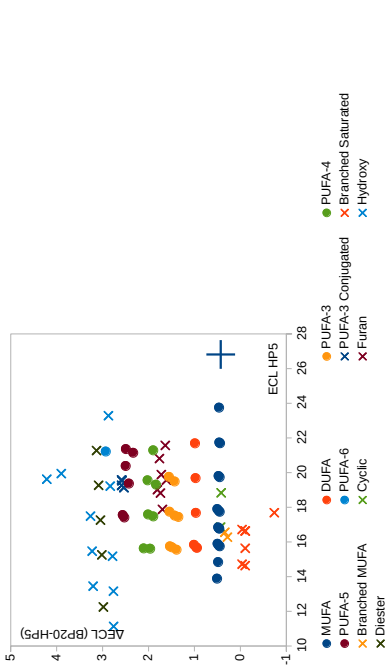

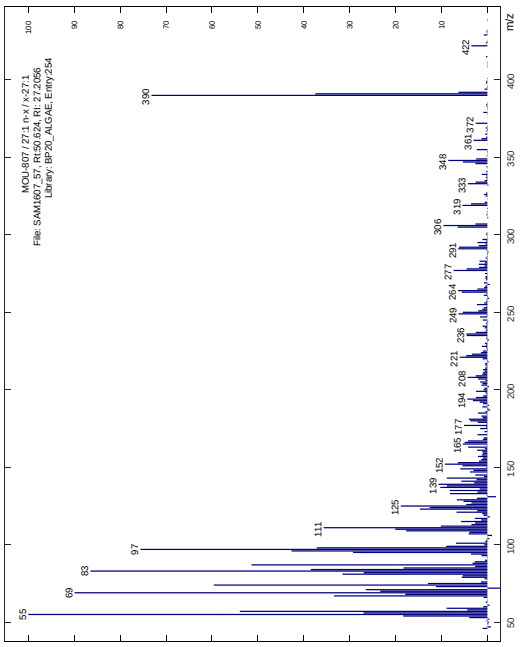

7.5.47 UNK-810 / Unknown / Unknown

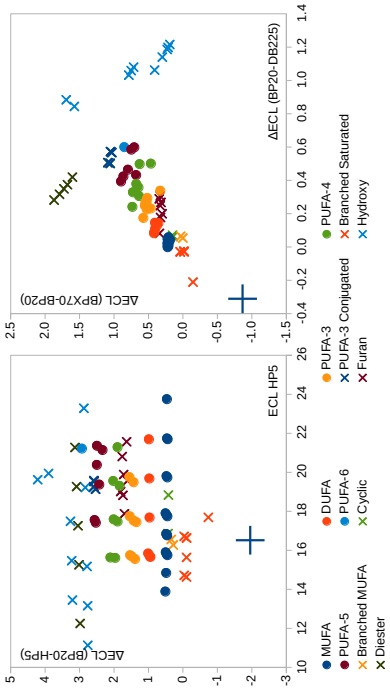

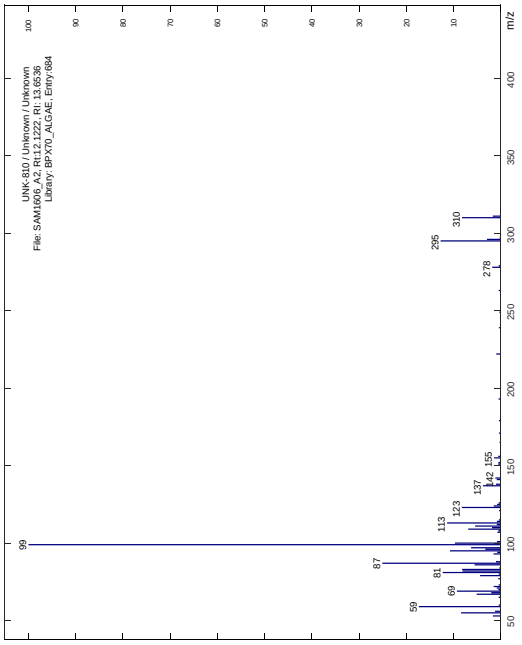

7.5.48 ALK-752 / Unknown / Unknown (br. alkane)

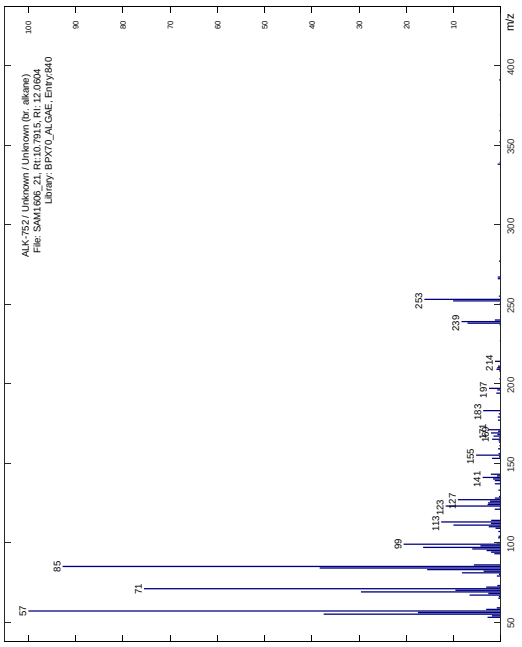

7.5.49 UNK-778 / Unknown / Unknown (PUFA)

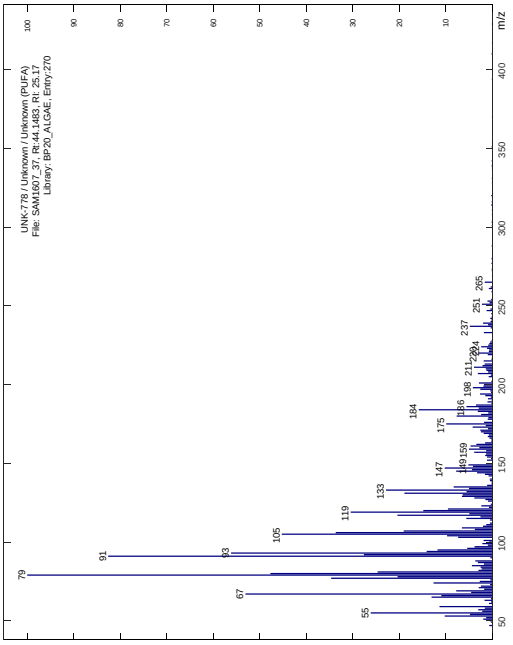

7.5.50 UNK-732 / Unknown / Unknown

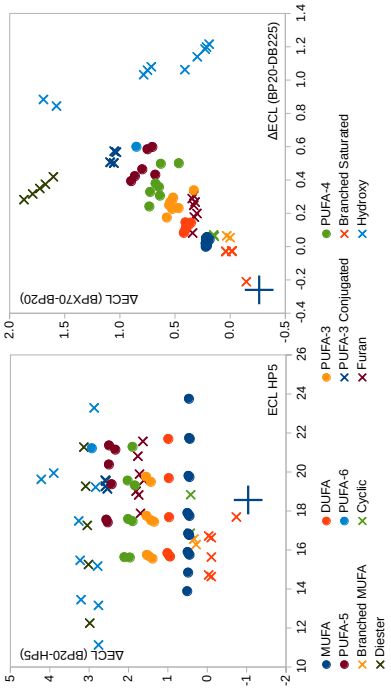

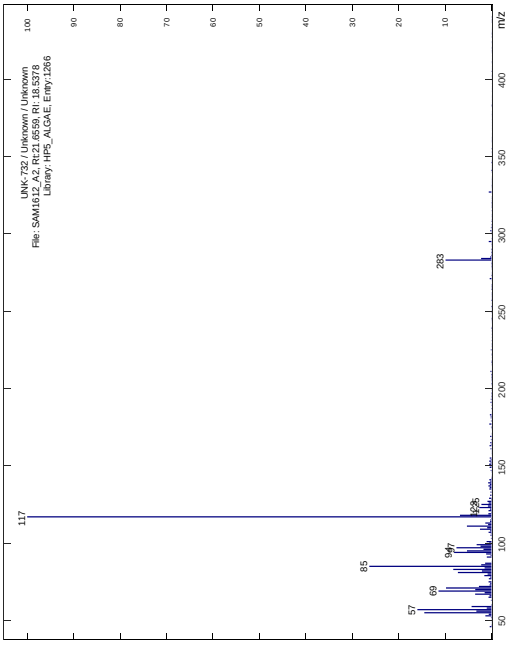

7.5.51 UNK-759 / Unknown / Unknown (br. alkane)

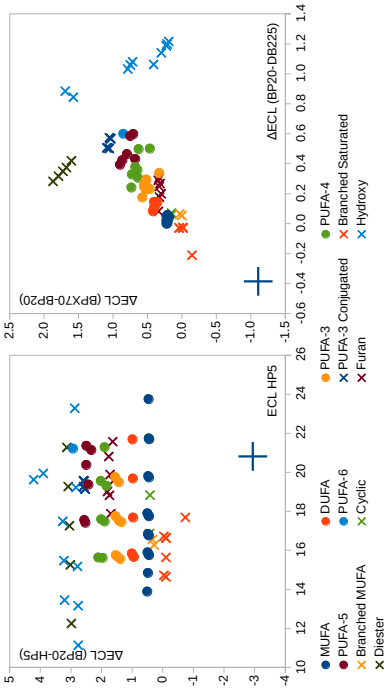

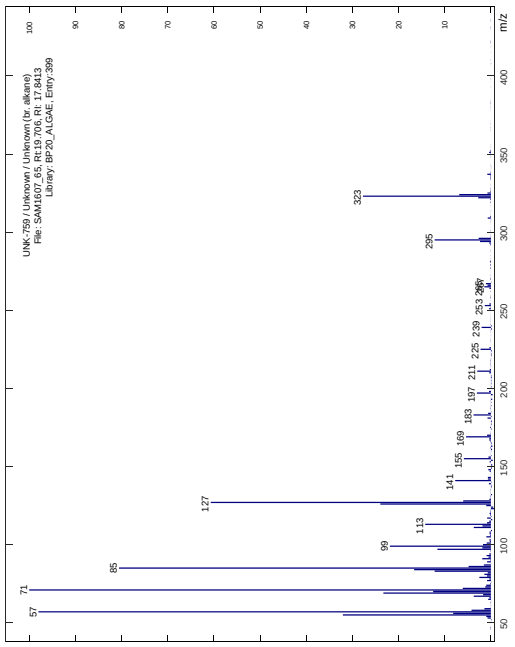

7.5.52 UNK-741 / Unknown / Unknown

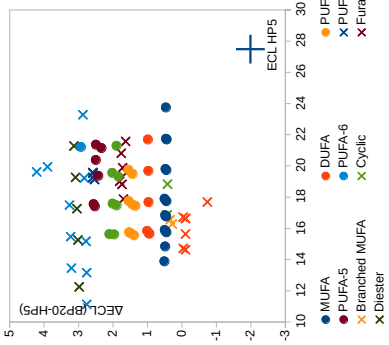

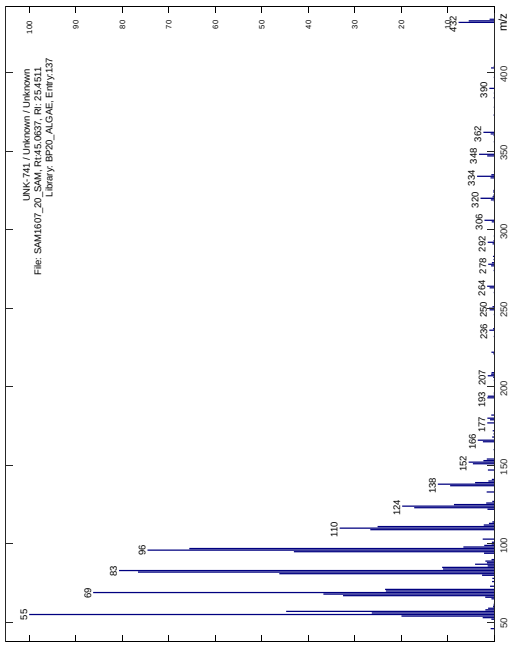

7.5.53 POU-318 / 24:6 n-3 / c6,c9,c12,c15,c18,c21-24:6

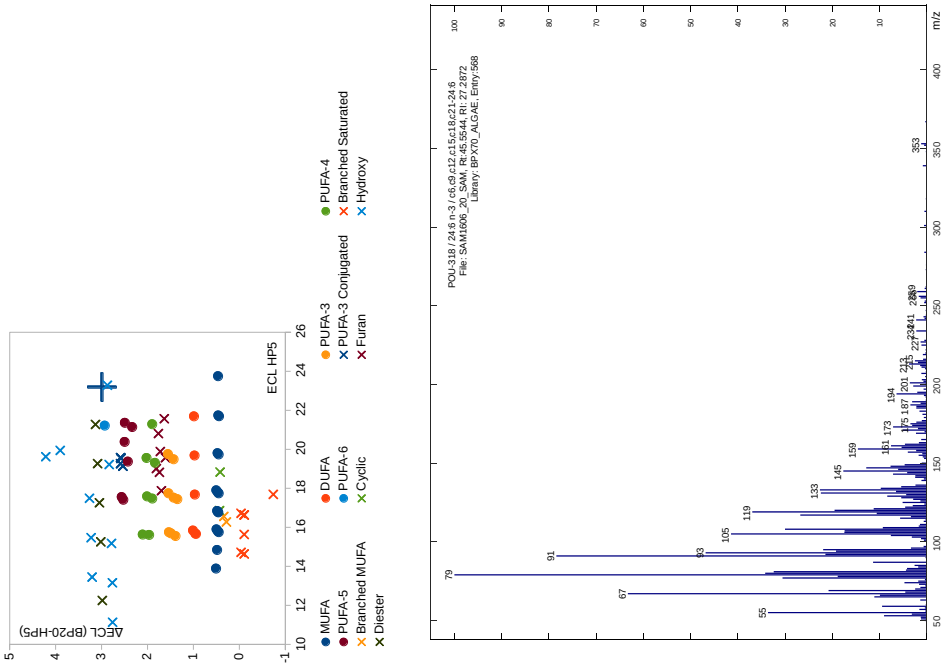

7.5.54 UNK-784 / Unknown / Unknown

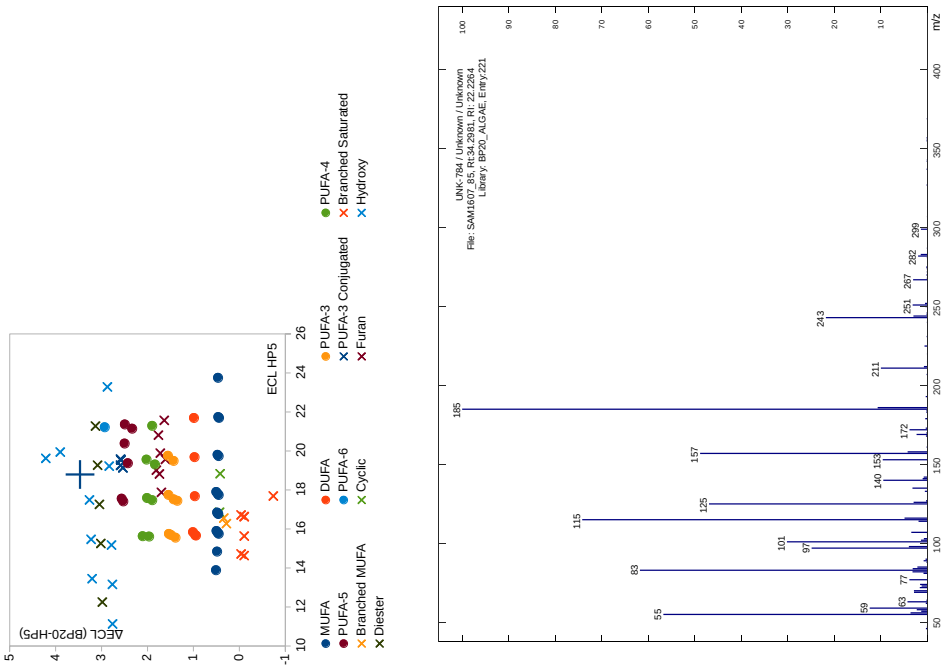

7.5.55 UNK-822 / Unknown / Unknown

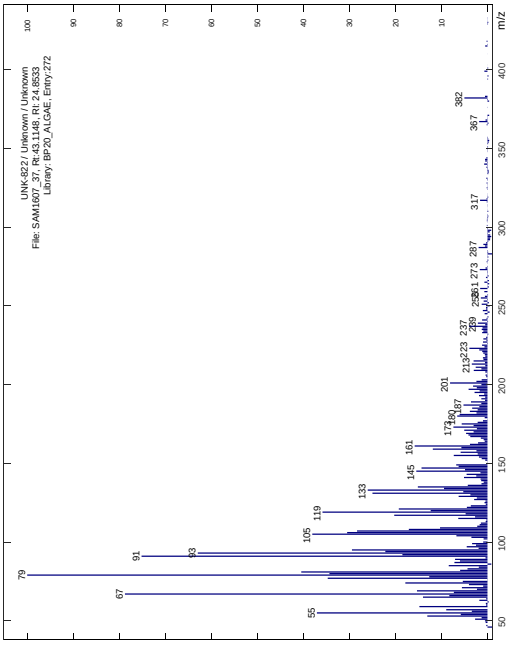

7.5.56 UNK-735 / Unknown / Unknown (br. alkane)

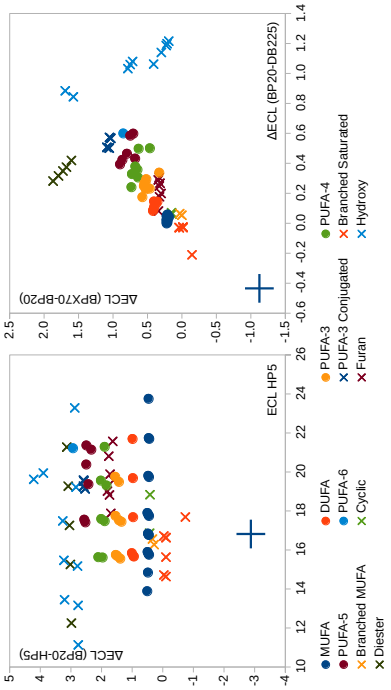

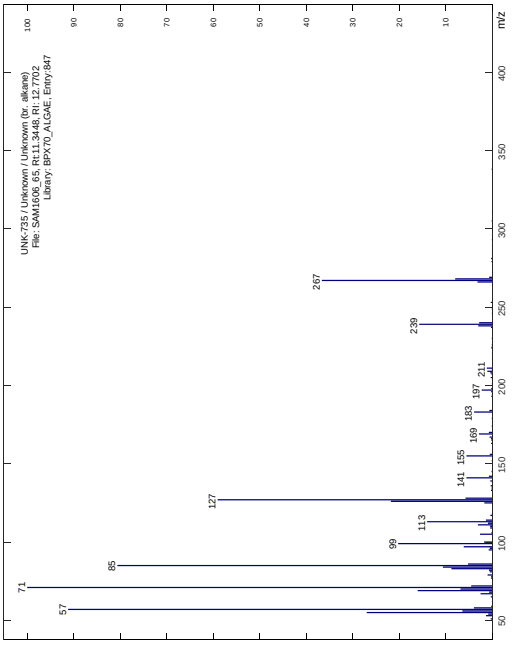

7.5.57 SAD-691 / 9:0 dME / Nonanedioic acid dME

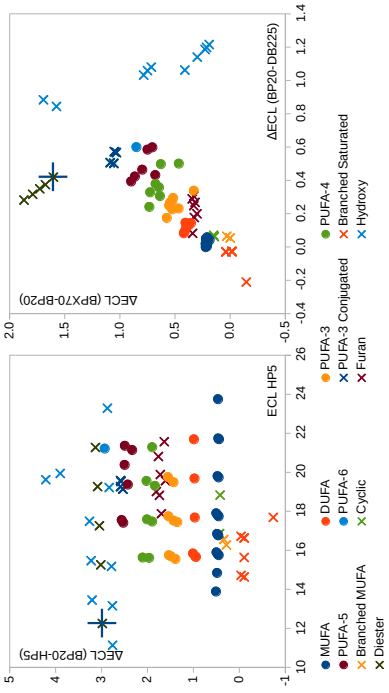

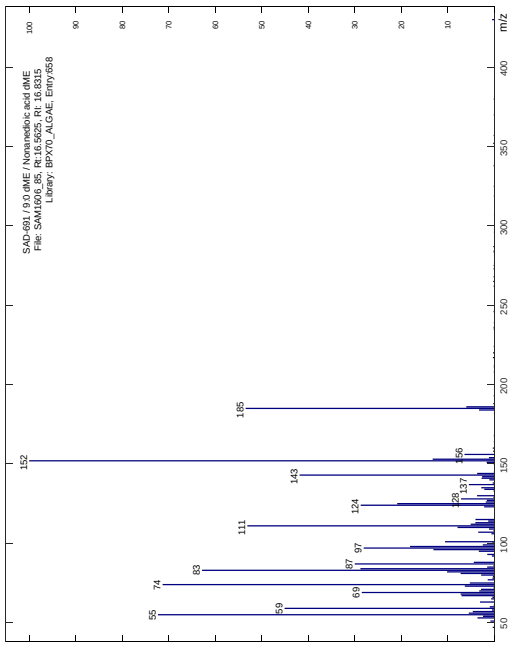

7.5.58 POU-751 / 24:5 n-6 / c6,c9,c12,c15,c18-24:5